# A SUSTAINABLE APPROACH FOR THERMOPLASTIC COMPOSITES WITH TAILORABLE CHARACTERISTICS BY THERMOKINETIC HYBRIDIZATION OF WASTE CELLULOSE AND VERMICULITE

by

**Gizem Semra Arıtürk**

Submitted to the Graduate School of Engineering and Natural Sciences
in partial fulfillment of the requirements for the degree of

**Doctor of Philosophy**

**SABANCI UNIVERSITY**

**July 2024**

# ABSTRACT

## A SUSTAINABLE APPROACH FOR THERMOPLASTIC COMPOSITES WITH TAILORABLE CHARACTERISTICS BY THERMOKINETIC HYBRIDIZATION OF WASTE CELLULOSE AND VERMICULITE

Gizem Semra ARITÜRK

Doctor of Philosophy, 2024

Material Science and Nano Engineering

Thesis Advisor: Prof. Dr. Yusuf Ziya MENCELOĞLU

Keywords: Hybridization, Polypropylene, Polylactic acid, Vermiculite, Cellulose, Upcycling, Sustainability

The ever-increasing demand for polymer-based high-performance materials with reduced environmental impact has driven research towards more sustainable and greener composite material designs. The fundamental approach in such designs is using either natural or recyclable material types that ensure a more sustainable product life cycle while providing an equivalent material response with respect to their non-green alternatives. Such demand can only be achieved with a correct material selection process targeted towards enhanced constituent interactions and effective manufacturing strategies. The implementation of these processes would allow the discovery of novel reinforcement agents adaptable to conventional thermoplastic polymers.

The main aim of this thesis is to present the outcomes of composite hybridization effort where multiple reinforcement phases are introduced to a biodegradable (PLA) and a recyclable (PP) polymer matrix. Considered reinforcement types were cellulose fibers which is a textile industry waste and vermiculite which is a naturally abundant clay. The rationale behind reinforcement selection relies on the fibrous morphology of WC and plate-like morphology of VC. The synergistic effect of both reinforcement types with significantly different properties are searched for when manufactured by a thermo-kinetic mixing followed by injection molding.

The thesis reveals the constitutive interactions between WC/VC and host matrices that lead to improved mechanical response along with ease of processing. The fundamental outcome of the PLA-base hybrid is the in-situ exfoliation of VC under high shear mixing which turns VC into nano-metric platelets that both ensure effective stress transfer between main reinforcement phase that is fibrous WC and micro-crack deflection in brittle PLA matrix. The findings indicated that the integration of WC and VC into PLA can enhance the Young's modulus by up to 127% and the flexural modulus by up to 137%, while maintaining the tensile strength at an optimal level.

From thereon, the thesis focuses on the results achieved when similar hybridization effort is applied to ductile PP polymer with significantly different mechanical response. Presented results revealed the presence of a serious WC entanglement which governs the overall mechanical response and the inability of VC to form the PP/VC fibrils in the presence of WC. However, the mechanical response of the obtained hybrid composites was even more improved due to inherent ductility of PP. When used in the presence of high fiber content (20WC10VC) such platelets contributed significantly to tensile strength by making PP more brittle and allowing for an effective stress transfer during WC cluster debonding events. The enhancements in the PP hybrid composite were 118% for Young's modulus and 115% for flexural modulus. Furthermore, the strength of PP was increased by the hybridization of WC and VC. The flexural strength and tensile strength exhibited increases of up to 42% and 56%, respectively.

The nature of this in-situ exfoliation is further evaluated where the effect of polarity difference between PLA and PP on VC interlayer region that contains crystalline water molecules. By focusing solely on VC composites arrives an important conclusion which is the formation of PP/VC fibril structures in non-polar PP matrix. Such fibrils are found to be formed of VC platelets uniformly distributed in PP fibrils occurred under extreme shear. Study proves that solely VC can enhance the Young's modulus of PP composites by up 110% Contrarily it has been explored that although the presence of crystalline water causes a better in-situ exfoliation, it causes water evaporation from polymer surface. The study has demonstrated that the addition of VC can significantly enhance the Young's modulus of PLA composites, with an increase of up to 147%. Presented results underlined the necessity of the hybrid approach.

Consequently, this thesis explores the impact of polymer type on the interaction with the fillers. It investigates the use of WC and VC in both PLA and PP composites, analyzing the resulting morphology and its influence on mechanical properties. By combining bio-based materials and natural fillers with innovative processing techniques, this research paves the way for the development of high-performance, eco-friendly composites. This thesis presents valuable insights into the potential of these green composites for various industrial applications requiring improved mechanical properties without compromising environmental responsibility.

# ÖZET

## ATIK SELÜLOZ VE VERMİKÜLİTİN TERMOKİNETİK HİBRİDİZASYONU İLE ÖZELLEŞTİRİLEBİLİR NİTELİKLERE SAHİP TERMOPLASTİK KOMPOZİTLER İÇİN SÜRDÜRÜLEBİLİR YAKLAŞIM

Gizem Semra ARITÜRK

Doktora Tezi, 2024

Malzeme Bilimi ve Nano Mühendisliği

Tez Danışmanı: Prof. Dr. Yusuf Ziya MENCELOĞLU

Anahtar Kelimeler: Hibridizasyon, Polipropilen, Polilaktik asit, Vermikülit, Selüloz, İleri Dönüşüm, Sürdürülebilirlik

Çevresel etkisi azaltılmış polimer bazlı yüksek performanslı malzemelere yönelik sürekli artan talep, araştırmaları daha sürdürülebilir ve daha yeşil kompozit malzeme tasarımlarına yönlendirmiştir. Bu tür tasarımlardaki temel yaklaşım, yeşil olmayan alternatiflerine göre eşdeğer malzeme tepkisi sağlarken daha sürdürülebilir bir ürün yaşam döngüsü sağlayan doğal veya geri dönüştürülebilir malzeme türlerinin kullanılmasıdır. Bu tür bir talep ancak gelişmiş bileşen etkileşimlerini ve etkili üretim stratejilerini hedefleyen doğru bir malzeme seçim süreci ile elde edilebilir. Bu süreçlerin uygulanması, geleneksel termoplastik polimerlere uyarlanabilen yeni takviye maddelerinin keşfedilmesine olanak sağlayacaktır.

Bu tezin temel amacı, biyolojik olarak parçalanabilen (PLA) ve geri dönüştürülebilir (PP) bir polimer matrise birden fazla takviye fazının eklendiği kompozit hibridizasyon çalışmasının sonuçlarını sunmaktır. Dikkate alınan takviye türleri, bir tekstil endüstrisi atığı olan selüloz lifleri (WC) ve doğal olarak bol miktarda bulunan bir kil olan genişletilmiş vermikülittir (VC). Takviye seçiminin ardındaki mantık, WC'nin lifli morfolojisine ve VC'nin plaka benzeri morfolojisine dayanmaktadır. Önemli ölçüde farklı

özelliklere sahip her iki takviye türünün sinerjik etkisi, yüksek kesmeli termo-kinetik karıştırma ve ardından enjeksiyon kalıplama ile üretildiğinde araştırılmaktadır.

Tez, WC/VC ve ana matrisler arasındaki, işleme kolaylığının yanı sıra gelişmiş mekanik tepkiye yol açan yapısal etkileşimleri ortaya koymaktadır. PLA bazlı hibridin temel sonucu, yüksek kesme karıştırması altında VC'nin yerinde pul pul dökülmesidir, bu da VC'yi hem lifli WC olan ana takviye fazı arasında etkili stres transferi hem de kırılgan PLA matrisinde mikro çatlak sapması sağlayan nano-metrik trombositlere dönüştürür. Bulgular, WC ve VC'nin PLA'ya entegrasyonunun Young modülünü %127'ye kadar ve eğilme modülünü %137'ye kadar artırabileceğini ve çekme mukavemetini optimum seviyede tutabileceğini göstermiştir.

Bundan sonra tez, benzer hibridizasyon çabası önemli ölçüde farklı mekanik tepkiye sahip sünek PP polimerine uygulandığında elde edilen sonuçlara odaklanmaktadır. Sunulan sonuçlar, genel mekanik tepkiyi ve VC'nin WC varlığında PP/VC fibrillerini oluşturma kabiliyetini yöneten ciddi bir WC dolanmasının varlığını ortaya koymuştur. Bununla birlikte, elde edilen hibrit kompozitlerin mekanik tepkisi, PP'nin doğal sünekliği nedeniyle daha da iyileştirilmiştir. Yüksek elyaf içeriği (20WC10VC) varlığında kullanıldığında, bu tür plakalar PP'yi daha kırılgan hale getirerek ve WC kümesi ayrışma olayları sırasında etkili bir stres aktarımına izin vererek çekme mukavemetine önemli ölçüde katkıda bulunmuştur. PP hibrit kompozitindeki artışlar Young modülü için %118 ve eğilme modülü için %115 olmuştur. Ayrıca, PP'nin mukavemeti WC ve VC'nin hibridizasyonu ile artırılmıştır. Eğilme mukavemeti ve çekme mukavemeti sırasıyla %42 ve %56'ya varan artışlar göstermiştir.

Bu in-situ eksfoliyasyonun doğası, PLA ve PP arasındaki polarite farkının kristal su molekülleri içeren VC ara katman bölgesi üzerindeki etkisiyle daha da değerlendirilmiştir. Yalnızca VC kompozitlerine odaklanarak, polar olmayan PP matrisinde PP/VC fibril yapılarının oluşumu gibi önemli bir sonuca varılmıştır. Bu fibrillerin, yüksek kesme altında meydana gelen PP fibrillerinde eşit olarak dağılmış VC plakalarından oluştuğu bulunmuştur. Çalışma, yalnızca VC'nin PP kompozitlerin Young modülünü %110'a kadar artırabileceğini kanıtlamaktadır. Aksine, kristal suyun varlığının daha iyi bir yerinde pul pul dökülmeye neden olmasına rağmen, polimer yüzeyinden su buharlaşmasına neden olduğu araştırılmıştır. Çalışma, VC ilavesinin PLA kompozitlerinin Young modülünü %147'ye varan bir artışla önemli ölçüde

artırabileceğini göstermiştir. Sunulan sonuçlar hibrit yaklaşımın gerekliliğinin altını çizmiştir.

Sonuç olarak, bu tez polimer türünün dolgu maddeleriyle etkileşim üzerindeki etkisini araştırmaktadır. Hem PLA hem de PP kompozitlerinde WC ve VC kullanımını araştırmakta, ortaya çıkan morfolojiyi ve mekanik özellikler üzerindeki etkisini analiz etmektedir. Biyo-bazlı malzemeleri ve doğal dolgu maddelerini yenilikçi işleme teknikleriyle birleştiren bu araştırma, yüksek performanslı, çevre dostu kompozitlerin geliştirilmesinin önünü açmaktadır. Bu tez, çevresel sorumluluktan ödün vermeden gelişmiş mekanik özellikler gerektiren çeşitli endüstriyel uygulamalar için bu yeşil kompozitlerin potansiyeline ilişkin değerli bilgiler sunmaktadır.

Dedicated to my mother and father…

## ACKNOWLEDGEMENTS

I would like to express my deepest gratitude to my advisor, Prof. Dr. Yusuf Ziya Menceloğlu, for guiding me throughout my Ph.D. journey with his invaluable knowledge and experience. This thesis would not have been possible without his support, encouragement, and guidance. I am deeply grateful for his contributions in developing my scientific thinking and inspiring my research efforts. I sincerely thank him for his patience and understanding through all challenges and for always being there to support me.

I extend my sincere appreciation to the esteemed members of the jury; Prof. Dr. Fevzi Çakmak Cebeci, Assoc. Prof. Dr. Burcu Saner Okan, Prof. Dr. Cengiz Kaya, and Assoc. Prof. Dr. Merve Senem Seven, for their time, expertise, and constructive input, which significantly enriched the quality of this work.

I would like to express my sincerest gratitude to Dr. Kaan Bilge for his invaluable support throughout the entire process, which has both accelerated and strengthened my work.

Special thanks go to my friends and flat mates, Sinem Elmas, Nargiz Aliyeva, Sina Khalilvandi Behrouzyar, Kuray Dericiler for their unwavering support, encouragement, and shared moments that provided much-needed balance during the demanding phases of this research.

I would also like to acknowledge the support of my colleagues; Atakan Koçanalı, Yeşim Yeniyurt Sepici, Nihan Birgün, Asu Ece Ateşpare, Saeed Salamat Gharamaleki, Ceren Yıldırım, Abdulrahman Al-Nadhari, Yağız Özbek, Orhun Şenol, Sercan Akgül, Buse Ataç Mostafa Mehdipour Aghbolagh and countless others who have contributed to the intellectual vibrancy of our academic community.

My heartfelt appreciation goes to the past and present members of the YZM Research group, particularly Çağla Girşken, Ogeday Rodop, Gökmen Şanlı, Gizem Kurtulmuş, Mine Aybike Ersin, Oğuz Alp Kurucu, İde Ezgi Önal, Rana Al-Nakib, Gülşah Yıldız whose collaboration and shared insights have played a pivotal role in the development of this research.

Furthermore, I would like to express my sincerest gratitude to Dr. Mustafa Sezer, Dr. Ceren Yargıcı Kovancı, Dr. Leila Poudeh for their invaluable support and understanding throughout the entire process.

Heartfelt gratitude is extended to my parents, Ata Arıtürk and Kadriye Arıtürk, for their unwavering encouragement, love, and belief in my abilities. Your support has been my anchor throughout this academic pursuit.

I would like to acknowledge the Sabanci University Faculty of Engineering and Natural Sciences Conference Travel Grant, for providing support to both of my international conference travels.

Finally, I would like to thank the Scientific and Technological Research Council of Turkey (TUBITAK) with project number 118C046 and ARÇELİK (BEKO) for supporting my research and industrial studies.

JULY Gizem Semra ARITÜRK

# TABLE OF CONTENTS

# ABBREVIATIONS

**2D** : 2-Dimensional
**C-NMR** : Carbon- nuclear magnetic resonance
**DMA** : Dynamic mechanical analysis
**DSC** : Differential scanning calorimetry
**DTGA** : Derivative thermogravimetric analysis
**FTIR** : Fourier transform infrared
**MAPP** : Maleic anhydride grafted polypropylene
**PLA** : Polylactic acid
**PP** : Polypropylene
**RPM** : Revolutions per minute
**SEM** : Scanning electron microscopy
**TGA** : Thermogravimetric analysis
**UTM** : Universal testing machine
**VC** : Vermiculite
**WC** : Waste cellulose
**WPC** : Wood polymer composites

## SYMBOLS

| | |
|---|---|
| **°C** | : Degree Celsius |
| **cm** | : Centimeter |
| **E, $E_{tens}$** | : Tensile modulus |
| **$E_{flex}$** | : Flexural modulus |
| **g** | : Gram |
| **G'** | : Storage modulus |
| **G''** | : Loss modulus |
| **h** | : Hour |
| **J** | : Joule |
| **L** | : Liter |
| **mbar** | : Millibar |
| **mg** | : Milligram |
| **min** | : Minute |
| **mm** | : Millimeter |
| **Mpa** | : Megapascal |
| **N** | : Newton |
| **nm** | : Nanometer |
| **Pa** | : Pascal |
| **rpm** | : Revolutions per minute |
| **s** | : Second |
| **Tc** | : Crystallization temperature |
| **Tg** | : Glass transition temperature |
| **Tm** | : Melting temperature |
| **w** | : Angular frequency |
| **wt.** | : Weight Fraction |
| **ΔHm** | : Heat of Fusion |
| **$\varepsilon_{yield}$** | : Elongation at yield |
| **η*** | : Complex viscosity |
| **θ** | : Theta |
| **µm** | : Micrometer |
| **$\sigma_{flex}$** | : Flexural Strength |

$\boldsymbol{\sigma}_{\mathbf{yield}}$ : Tensile Strength

$\chi$ : Degree of crystallinity

## LIST OF TABLES

## LIST OF FIGURES

# CHAPTER 1: State of Art

With plastic pollution and textile waste becoming a global crisis, there is an urgent need to turn to environmentally friendly and sustainable materials. In this context, upcycling has the potential to transform waste materials into valuable products. The developed composite material offers significant advantages in terms of sustainability, cost, and performance. Upcycling textile waste reduces the cost of the composite material, while hybridizing it with vermiculite significantly improves its mechanical properties in both PP and PLA matrices. Consequently, the composite material from the textile sector can be used in a wide range of plastics sectors.

In this study, the new composite material developed using cellulosic fiber obtained from textile wastes, PP, PLA and vermiculite is of great importance in terms of sustainability. This composite material, which offers many advantages such as reducing the amount of waste, optimizing the use of natural resources, reducing costs and improving mechanical properties, makes an important contribution to achieving sustainability goals in the textile and plastics sectors.

The upcycling of waste cellulosic fibers offers a more economical alternative to commercial compounds, reducing production costs. Furthermore, since cellulose can be obtained from domestic sources, it reduces our dependence on imports, thereby contributing to the national economy and saving foreign currency. It plays an important role in terms of utilizing the waste of industries that produce high amounts of waste in our country and contributing to the protection of natural resources. Reducing the use of plastics helps to prevent environmental pollution. Upcycling waste cellulose and integrating it into plastics provides numerous economic and environmental benefits. In addition to the aforementioned benefits, it is imperative to acknowledge the detrimental effects of not utilizing waste cellulose. If waste cellulose is not employed, it must be disposed of in some manner. The disposal of waste cellulose necessitates both transportation and incineration processes, both of which are costly and detrimental to the environment. However, by integrating waste cellulosic fibers into plastics, the need for these disposal processes is eliminated. Consequently, the costs and environmental damage associated with both transportation and incineration are also eliminated. The fibrous structure of cellulose also enhances the mechanical properties of the material. Consequently, the resulting products are more durable and robust. The utilization of cellulose offers a multitude of benefits, both economic and environmental. Cellulose can be utilized in a multitude of sectors, including automotive parts, electronic devices, construction materials, packaging materials, furniture, and textiles.

In conclusion, the upcycling of waste cellulose and its integration into plastics represents a cost-effective and domestically sourced raw material solution, effectively addresses the issue of waste management, reduces environmental pollution, and enhances the durability and strength of products.

Vermiculite is a clay mineral with a sliced structure like mica, which is abundant in nature. Since its formation takes place underground, its structure mostly depends on the geological characteristics of the region where it is formed [1]. Vermiculite is composed of regular, end-to-end layers of silicate minerals called "phyllosilicate". Phyllosilicate can consist of octahedral structures composed of oxygen atoms surrounding aluminum or magnesium atoms in the center or tetrahedral structures composed of oxygen atoms surrounding silicon atoms in the center [1], [2] Vermiculite, which has a 2:1 phyllosilicate structure, consists of layers of 2 layers of tetrahedral and 1 layer of octahedral structures. At the interface between these layers there are cation ions surrounded by water molecules. Unlike other clays, vermiculite has a unique property. Thanks to its layered structure, vermiculite has the ability to swell or, in other words, exfoliate thanks to the various processes it undergoes. When thermal, chemical or microwave processes are applied, vermiculite can increase to 20-30 times its original size. It swells and takes on a curved, accordion-like (worm-like) shape. This swelling process occurs as a result of the evaporation of water molecules between the layers [1] . Expanded vermiculite has many characteristics compared to vermiculite of the original size. These include its porous structure, low thermal conductivity and resistance to high temperatures. It is also light, cheap and non-toxic. It can be used as a filler in many materials thanks to its resistance to thermal degradation and its insulating properties. In addition, vermiculite plays an important role in the removal of unwanted species from the environment as it has high ion exchange performance [1], [3] . Vermiculite is a filler that can be used in many areas because it has unique properties such as special two-dimensional layer structure, cation exchange capacity and active surface. Thanks to its thermal stability, thermal expansion and environmentally friendly properties, it can be used in areas such as oil adsorption, water treatment or heat and sound insulation [1], [4], [5] . It can be added into many kinds of polymers such as thermoplastics, thermosets or elastomers and the resulting product can be classified as thermoplastic, thermoset, elastomer-based composites in various forms such as film, sheet, foam or gel [1] . As a filler in the polymer matrix, vermiculite can impart many important properties to petroleum-based materials such as polyolefins, such as ecological sustainability, heat and sound insulation, oil and water absorbency, flame retardancy and gas barrier [6] Vermiculite not only functionalizes the polymers to which it is bonded, but also significantly improves their mechanical and thermal properties.

In essence, the thesis philosophy seeks to bridge the gap between achieving high-performance in materials and minimizing the environmental footprint associated with their development and use. This is achieved by exploring the potential of bio-based polymers and natural fillers to create environmentally benign composites. However, the focus of this research extends beyond the mere replacement of traditional materials. It delves into the concept of hybridization, investigating the combined effects of different natural fillers, such as waste cellulose (WC) and vermiculite (VC). This approach aligns with the principle of eco-friendly reinforcement. The research investigates the potential of readily available and renewable resources with the aim of achieving durable materials without compromising environmental responsibility. Green composite development and hybridization strategies are employed to pave the way for a new generation of eco-friendly composites with superior properties for various industrial applications.

This dissertation comprises five interconnected chapters, each offering significant findings on their respective topics. The initial chapter presents a comprehensive review of the current state of the art, outlining the challenges and motivations that underpin the study's originality.

The second chapter highlights the importance of developing sustainable materials as alternatives to petroleum-based polymers. By using waste cellulosic textile fibers and vermiculite, the study promotes the utilization of renewable resources, contributing to reduced environmental impact and lower greenhouse gas emissions. The research introduces a high shear mixing process at 5000 rpm to blend PLA, WC, and VC without the need for any chemical modifications or compatibilizers. This novel process ensures efficient mixing and uniform dispersion of the fillers within the PLA matrix, contributing to the enhanced properties of the composites. Hybrid composites show significant improvements in mechanical properties. This makes the material suitable for applications requiring improved mechanical strength, such as in the automotive, electronics, and household appliance industries. The study demonstrates that hybrid composites are more readily processable than neat PLA at high temperatures (200°C). The successful development of these hybrid composites opens up possibilities for their use in various industries that traditionally rely on petroleum-based polymers. The improved mechanical and thermal properties, combined with the eco-friendly nature of the materials, make them a promising alternative for sustainable product development. The upcycling of textile waste creates opportunities to utilize these materials in high-value products. By incorporating vermiculite without modification, we have demonstrated the ability to load high amounts of this mineral into the polymer matrix. The use of bio-based polymers further emphasizes the environmentally friendly approach of this study. In conclusion, this study is significant as it addresses the dual challenges of sustainability and performance in material science. By developing hybrid composites with superior properties from renewable resources, it provides a pathway towards greener and more efficient materials for various applications.

The third chapter explores hybrid composites of polypropylene (PP) strengthened with waste cellulose (WC) fibers and expanded vermiculite (VC). The aim is to develop stronger, stiffer, and thermally durable composites. Polypropylene (PP) is commonly used due to its favorable properties and recyclability. This research focuses on using waste cellulose fibers and vermiculite to enhance PP composites. Previous studies have shown that both cellulose fibers and vermiculite improve mechanical properties, and hybrid formulations could offer synergistic benefits. By mixing WC and VC with PP via high shear thermokinetic mixing, the research evaluates the mechanical and thermal properties of these composites. The study introduces a hybrid reinforcement approach that leverages the strengths of both fibrous (cellulose) and particulate (vermiculite) materials. This synergy not only enhances the mechanical and thermal properties but also mitigates issues such as fiber entanglement and poor wettability that are common with high fiber content. The research provides valuable insights into the interactions between natural fibers and mineral particles within a polymer matrix. It expands the understanding of how these materials can be optimally combined to achieve superior composite properties. By utilizing waste materials and enhancing them for practical industrial applications, the research not only addresses environmental sustainability but also pushes the boundaries of material science and engineering. This positions the study as a critical contribution to the field, offering practical solutions to contemporary challenges in material development and application.

The fourth chapter investigates the integration of expanded vermiculite (VC) into polylactic acid (PLA) and polypropylene (PP) matrices to create enhanced thermoplastic composites through efficient dispersion and integration of the VC platelets into the polymer matrices. The study utilizes high shear thermokinetic mixing to incorporate 30 wt. % VC into these polymers without using compatibilizers or ex situ modification strategies. This chapter demonstrates the morphological changes and associated mechanical property improvements achieved by melt blending. High shear mixing facilitated effective dispersion of VC in both PLA and PP matrices, resulting in homogeneous composite mixtures. As distinct morphological changes VC underwent in situ exfoliation in the PLA matrix, forming micrometer-sized platelets. In contrast, in the PP matrix, PP-VC fibrillated, enhancing tensile and bending strength. The study underscores the potential of VC to significantly enhance the mechanical properties of PLA and PP composites, offering a cost-effective approach to producing superior thermoplastic materials. The study achieves complete fibrillation of PP- VC in PP and in situ exfoliation in PLA. This innovative approach not only simplifies the production process but also enhances the tensile and bending modulus of the composites substantially. These findings have significant implications for industries reliant on strong, durable materials. The ability to enhance the properties of PLA and PP through efficient VC integration opens new avenues for applications in automotive, construction, and consumer goods. Furthermore, the study contributes to the broader understanding of how morphological adaptations at the microstructural level can influence the macroscopic properties of composite materials.

The final chapter offers a general conclusion to the studies. This thesis addresses a critical gap in literature by demonstrating the potential of upcycled cellulose fibers and vermiculite as sustainable reinforcements for high-performance composites. By overcoming challenges associated with natural filler incorporation and highlighting the environmental benefits, this work paves the way for the development of a new generation of eco-friendly supplements and compounds. These sustainable alternatives have the potential to replace synthetic additives currently used in various industrial applications, achieving maximum performance without compromising environmental responsibility. This research provides a robust foundation for future studies investigating the optimization and large-scale production of these green composites, with the ultimate goal of contributing to a more sustainable future. A summary diagram delineating the scope of the thesis is provided in Figure 1.

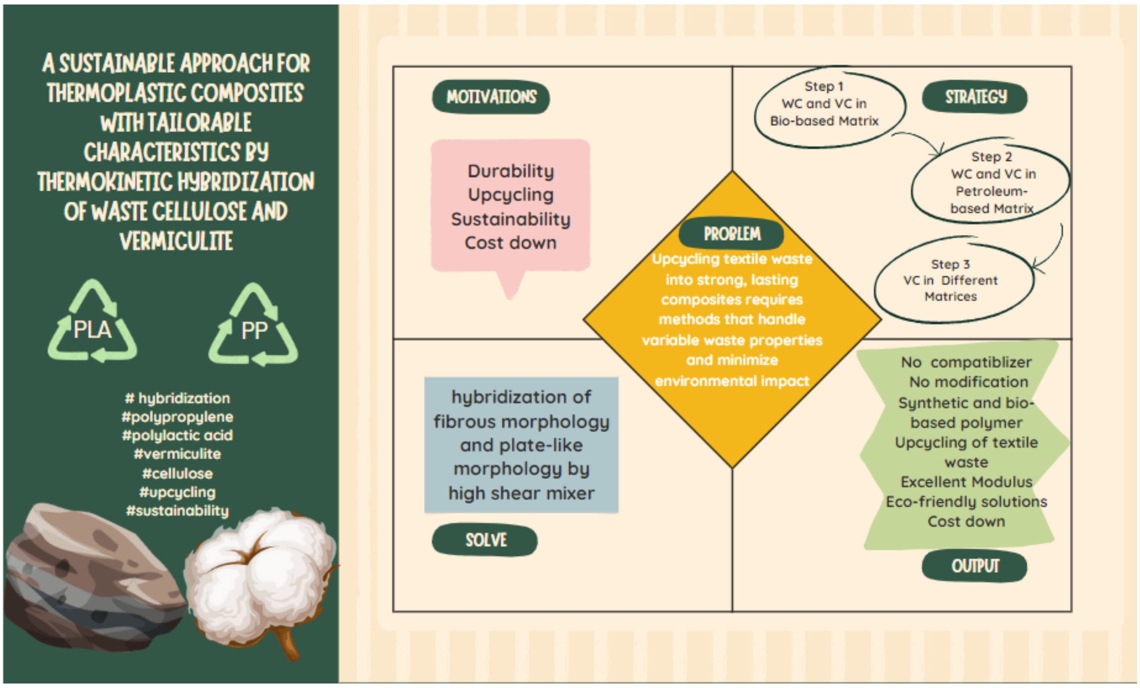

**Figure 1** Summary diagram of the thesis

# CHAPTER 2: Hybrid Green Composites of PLA Incorporated with Upcycled Waste Cellulose and Vermiculite

## 2.1 Abstract

The work aims to utilize a hybridization method where vermiculite and waste cellulose fibers are embedded inside bio-based PLA to manufacture green composites with superior characteristic properties such as improved thermal conductivity, enhanced processability, and increased mechanical strength in the resulting green composites. The potential of polymeric composites for emerging greener material development is very high. Originating from this point, this article reports the experimental findings on a hybrid composite reinforcement strategy where two types of renewable materials are employed as co-reinforcement agents in a biodegradable polylactic acid (PLA) matrix. Green composite sample manufacturing was performed via high shear mixing (5000rpm). Composite samples containing waste cellulose fibers (WC), (average diameter: 15 μm) and vermiculite platelets (VC), (average size: 1.4mm) as inclusions and a low crystallinity thermoplastic PLA matrix are targeted. Two-phase composites having 10, 20,30 wt. % WC, 30 wt.% VC, and hybrid composites having 15VC-15WC wt. % and 7.5VC-22.5WC wt. % are manufactured. Composite samples are then tested for their thermal, rheological, and mechanical responses. Thermal analysis suggests that thermal conductivity is improved by 68 % for PLA30VC samples and in hybrid composites, thermal conductivity is regulated by WC, while crystallinity is regulated by VC. Rheological measurements suggest both filler materials contribute to the processability of PLA, and hybrid composites are more readily processable than neat PLA at 200°C. While the tensile strength remains the same in all composites, a 137% increase in E modulus and 127% increase in flexural modulus is achieved with hybrid composites. The damage modes and contribution of both inclusion types to macro and micro fracture mechanisms are discussed in detail. Overall, results suggested that a stronger, easily processable, and thermally more conductive yet stable superior material alternative could only be achieved by the synergistic use of WC fibers and VC platelets.

## 2.2 Introduction

Environmental concerns such as increasing global warming, greenhouse gas emissions, and carbon footprint along with the reduction of petroleum resources throughout the world drive attention to the usage of environmentally friendly renewable resources [7], [8]. To reduce the negative ecological effect of polymeric materials and protect the environment, more green materials such as biopolymers are encouraged to be used instead of petroleum-based [9], [10]. Having low environmental impact and low carbon footprint performance due to their unique properties such as abundant availability, sustainability, renewability, eco-friendliness, and lightweight, biopolymer materials are receiving significant attention to develop efficient bio-composites [11]–[13]. The incorporation of VC and WC into the PLA matrix not only enables the development of a green and cost-effective composite but also enhances the value of agricultural waste for the production of biodegradable polymer-based composites, minimizing both cost and environmental impact [14], [15]. They are seriously considered as a potential alternative to petroleum-based plastics [16]–[19]. Among these biopolymers, PLA is the most currently used biopolymer since it is biobased, biocompatible, and recyclable linear aliphatic thermoplastic polyester and it can be obtained from renewable plant-based resources [20]. It is a promising biopolymer due to its eco-friendliness and its less need for energy during production compared to petroleum products [21], however, it has some shortcomings in terms of production and performance [22]. It causes difficulties during processing and has some poor mechanical properties such as low toughness, brittleness, low heat resistance, and moderate tensile properties [23]. Enhancing the mechanical and thermal properties of PLA can be achieved by incorporating nanofillers, allowing the customization of various characteristics based on the needs of the end user [24]. To manage these drawbacks of PLA, the addition of plasticizers, polymer blends, and natural or synthetic fibers is considered [25].

Traditional synthetic fibers such as glass and carbon fibers or some polymeric fibers offer better reinforcement due to higher stiffness and impact resistance for PLA than natural fibers [26], [27], but they cause loss from biodegradability [28]. Therefore, the use of biobased natural fillers along with biobased polymers may overcome the problem of biodegradability while providing sufficient mechanical performance. Natural fillers have many advantages compared to synthetic fillers, such as low weight, low cost, high stiffness, renewable nature, and being recyclable and biodegradable [29], [30]. Among them, cellulose fibers are the most used ones due to their abundance in nature, good mechanical properties, low cost, and lightweight properties [31]–[33]. Cellulose is a polysaccharide having a continuous, long, and strong filament structure, due to its hydroxyl groups and their ability to make hydrogen bonding, which provides enhanced tensile and flexural strengths as well as rigidity [34], [35]. The pronounced polar characteristics of cellulose pose a challenge to its dispersion in non-polar media, presenting a major obstacle in the production of cellulose-reinforced composites. The abundant hydroxyl groups on cellulose surfaces tend to create hydrogen bonds, leading to microfibril aggregation and subsequently diminishing the reinforcing effects on non-polar polymers. Surface modification serves to enhance cellulose dispersibility in non-polar polymers by reducing its inherent polarity [36]. However, our previous studies support that cellulose improves processability by using a custom-made mixer and properties of PLA such as its brittleness, poor heat resistance, and melt elasticity without compromising its superior stiffness and strength [37], [38].

Another type of natural fillers are clays such as vermiculite which have layered structure silicates [39] that are negatively charged so the polymer matrices can interact more readily and form more rigid and strong structures which improves mechanical properties [40]. Its exfoliated platelet form, having a high aspect ratio, provides very high stiffness and tensile strength [41], [42]. Moreover, vermiculite has a lower density than other natural clays such as talc, and provide lightweight property [43], [44]. According to literature, several studies show that incorporation of vermiculite in PLA matrix improves mechanical properties such as increasing tensile strength, tensile modulus, and impact strength with increasing vermiculite content [45], [46].

Besides the mechanical properties, the thermal and rheological characteristics of PLA can be altered by the incorporation of these fillers. Due to its inherent drawbacks such as low thermal stability and low melt strength, linear PLA chains result in sagging, and necking which limits its processing. However, cellulose fibers are good rheological modifiers that surround themselves between polymer chains, provide high stability, lower viscosity, and ease the processing of PLA [47]. Both fillers also contribute to improving the thermal properties of PLA for instance, flame retardancy [48], [49]. Moreover, cellulose fibers and vermiculite have a significant effect on improving the thermal conductivity of polymer matrix [50], [51]. Enhanced thermal conductivity of polymers is advantageous for electronic devices that produce high energy density and create a large amount of excess heat which may harm the device and need to be released outside to protect the device and its lifetime [52].

This study aims to encourage the use of biopolymers with enhanced mechanical properties for industries such as automotive, house appliances, and electronics that require improved mechanical properties for their products and benefit from petroleum-based polymers. Due to their high contribution to greenhouse gas emissions and carbon footprint, an alternative to petroleum-based polymers is being considered. In this scope, hybrid green composites of PLA were produced via the incorporation of waste cellulose (WC) and vermiculite (VC) as natural reinforcing agents at different loading levels. High shear mixing at 5000 rpm is utilized as a significant novelty; PLA, cellulose, and vermiculite were processed easily without the necessity for any modification or compatibilizer. PLA/WC and PLA/VC blends were compounded to be able to obtain fully biobased and durable polymeric compounds with improved mechanical and thermal properties. Results showed that a synergistic ratio between vermiculite and waste cellulose was found at 7.5 wt.% vermiculite and 22.5 wt.% waste cellulose loaded formulation (PLA7.5VC22.5WC) having superior mechanical performance such as better mechanical properties of young's modulus, tensile strength, elongation at break, flexural strength, and flexural modulus values. Therefore, this study suggests that the hybrid use of waste cellulose and vermiculite in PLA matrix forms promising biopolymers and an alternative to petroleum-based polymers due to their improved mechanical properties and eco-friendly nature.

### 2.3 Materials and Method

Waste cellulosic cotton fibers derived from the textile industry were supplied by Zorlu Linen Textile, Istanbul, Turkey. The average diameter of these fibers was measured as 15-20 micrometers. Detailed characterizations (FTIR and C-NMR) are given in Figure 2 and Figure 3 respectively. As shown in Table 1 superfine vermiculite with an average particle size of 1.4 mm was purchased from Serakulit, Canakkale, Turkey. Vermiculite consists of 39.2% $SiO_2$, 16.2% $Al_2O_3$, 15.4% MgO, 15.0% $Fe_2O_3$, 5.6% $K_2O$, 4.8% CaO, and trace amounts of other compounds (provided in the material data sheet). An injection grade of PLA (Total Corbion, Luminy L130) with a melt flow rate of 23g/10min (210°C/2.16kg) was purchased from Kumru Kimya, Istanbul, Turkey.

**Table 1** Sieve analysis result of vermiculite

| Size (mm) | Abundance (%) |
|---|---|
| 1.4 | 46.3 |
| 1.0 | 35.0 |
| 0.7 | 12.5 |
| 0.5 | 4.3 |
| <0.5 | 1.9 |

All materials were used as they were received. Firstly, all the additives and polymers were mixed physically at different ratios. Formulations were prepared by a custom-made thermokinetic mixer, Gelimat GI (Draiswerke). Thermokinetic mixing is the most convenient method to handle natural fiber like cellulose. It has higher shear and lower retention time than the conventional melt blending method like extrusion. With the help of the high shaft speed of the mixer, formulations were prepared in less than a minute. At around 5000 rpm, the temperature of the mixing chamber reaches 190 ° C. At this stage, the polymer melts and forms a homogeneous mixture with waste cellulose and vermiculite.

After the polymeric composite produced with a thermokinetic mixer is taken from the mixer's chamber, it is waited for cooling and then it is turned into granules with the help of a crusher. Test samples are molded by using an Xplore 12 mL micro-injection molding machine (XPlore, Sittard, Holland) with a pressure of 12 bar to perform the relevant mechanical and thermal tests.

Within the scope of the project, different formulations consisting of 10%, 20%, and 30% waste cellulose by mass were prepared. Since the 30% waste cellulose composite is the most durable mechanically, vermiculite was added by keeping the additive ratio constant at 30%. The contents of the composites and their both weight and volume ratios are represented in Table 2. Volume ratios were calculated by using densities of PLA, WC, and VC. The densities of WC, VC, and PLA were measured with a pycnometer as 1.5 g/ml, 1.7g/ml, and 1.2 g/ml respectively.

**Table 2** Formulation table a) weight fraction b) volume fraction.

| **a) Sample Name** | **Content (Weight %)** | | |
|---|---|---|---|
| | **PLA** | **Waste Cellulose** | **Vermiculite** |
| **Neat PLA** | 100 | 0 | 0 |
| **PLA_10WC** | 90 | 10 | 0 |
| **PLA_20WC** | 80 | 20 | 0 |
| **PLA_30WC** | 70 | 30 | 0 |
| **PLA_7.5VC-22.5WC** | 70 | 22.5 | 7.5 |
| **PLA_15VC-15WC** | 70 | 15 | 15 |
| **PLA_30VC** | 70 | 0 | 30 |

| **b) Sample Name** | **Content (Volume %)** | | |
|---|---|---|---|
| | **PLA** | **Waste Cellulose** | **Vermiculite** |
| **Neat PLA** | 100 | 0 | 0 |
| **PLA _10WC** | 92 | 8 | 0 |
| **PLA_20WC** | 83 | 17 | 0 |
| **PLA_30WC** | 74 | 26 | 0 |
| **PLA_7.5VC-22.5WC** | 75 | 6 | 19 |
| **PLA_15VC-15WC** | 76 | 13 | 11 |
| **PLA_30VC** | 77 | 0 | 23 |

Thermal analysis and crystallinity degree of polymer composite samples were conducted by Differential Scanning Calorimetry (DSC) method using DSC 3 + 700 (Mettler Toledo, Columbus, OH, USA) under the nitrogen atmosphere from at the rate of 10 °C/min 25 °C to 230 °C. STARe software (Mettler Toledo, Columbus, OH, USA) was used in order to obtain the melting enthalpy ($\Delta H_m$), melting temperature ($T_m$), and glass transition temperatures ($T_g$). Melting enthalpies of first melting scans were used to evaluate the crystallinity degree of polymer in the composites according to the method of Zhang et al. [53] $T_g$, $T_m$, melting enthalpies and crystallinity degrees were represented in Table 4.

$$\text{Crystallinity } (\chi)\ \% = \frac{\Delta H}{\Delta H^{*}} * \frac{1}{\Phi\ PLA} \qquad (1)$$

$\Delta H$ is the integral of the heat flow after the baseline subtraction, and $\Delta H^*$ is the melting enthalpy of a 100% crystalline PLA, which can be found in the literature to be 93 $Jg^{-1}$. $\Phi_{PLA}$ represents the weight fraction of PLA in the green composites [53].

Thermal analyses were completed with TA Q 500 TGA by using Universal Analysis 2000 software. Analyzes were carried out at a heating rate of 20°C per minute from room temperature to 950°C under the nitrogen atmosphere.

The conductivity of the specimens was measured at room temperature with a thermal constant analyzer, TPS 2500 S with Kapton insulated sensors.

Mettler Toledo DMA 1 was used to determine Dynamic Mechanical Properties (DMA) from 25°C to 125°C with a 3K/min ramp rate and in single cantilever mode at a frequency of 1.00Hz

Rheological analyses, frequency sweep, and viscosity sweep were carried out by MCR 702 TwinDrive Rheometer (Anton Paar, Graz, Austria).

In order to carry out the morphological studies, fracture surfaces of both 3-point bending and UTM test specimens were coated 3 times with a thin layer of gold-platinum. Surface topography and morphology were analyzed by using Leo Supra 35VP Field Emission Scanning Electron Microscope (FESEM, Carl Zeiss AG, Jena, Germany). Fractographic inspections were carried out in Insight Laboratories, TR.

Tensile and 3-point bending tests were performed to obtain mechanical properties by using a 5982 Static Universal Test Machine (UTM, Instron, Norwood, MA, USA) with a rate of 2.0mm/min and 5 kN load cell for ISO 527-2 and ISO 178 standards.

## 2.4 Results and Discussion

### 2.4.1 Structural Analysis of Waste Cellulosic Fibers

The cellulosic cotton fibers were analyzed using Thermo Scientific Fourier transform infrared spectroscopy (FTIR) across a spectrum from $4000-400$ cm$-1$, employing a resolution of 4 cm$-1$ and 16 scans for comprehensive characterization. In the FTIR analysis, Figure 2, a broad peak observed in the range of 3500-3000 $cm^{-1}$ is attributed to the presence of hydroxyl groups in the cellulose structure. A characteristic β-glycosidic linkage band is observed at 893 $cm^{-1}$. Notably, the absence of the characteristic band observed at 1730 $cm^{-1}$ in hemicellulose suggests the absence of hemicellulose in the structure. The peak observed at 1636 $cm^{-1}$ is attributed to water absorption by the fibers. Additionally, distinctive features include the absorption band at 1427 $cm^{-1}$, corresponding to the symmetrical stretching of $CH_2$, and the bending vibrations of C-H and C-O at 1370 $cm^{-1}$ and 1317 $cm^{-1}$, respectively. Furthermore, the stretching vibration at 1027 $cm^{-1}$ is indicative of the polysaccharide structure in cellulose. Peaks at 2900 $cm^{-1}$, and 1370 $cm^{-1}$ represent stretching and deformation vibrations of the C-H unit. These detailed observations provide valuable insights into the chemical composition and structural characteristics of the analyzed sample.

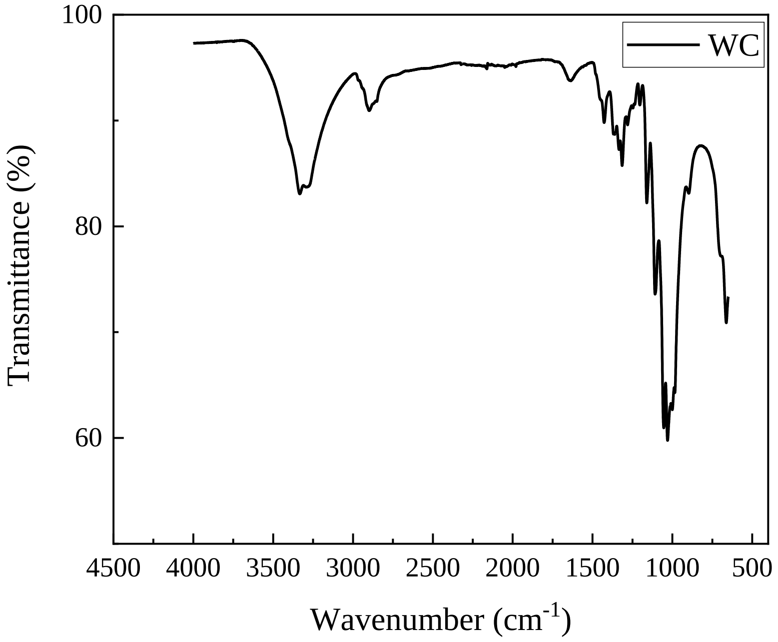

**Figure 2** FTIR spectrum of Waste Cellulose

Based on the data obtained from the Carbon-13 nuclear magnetic resonance (C-NMR) spectrum of cellulose, specific carbon atoms exhibit distinct chemical shifts. In the C-NMR spectrum of cellulose (Figure 3), the resonance at 110-107 ppm is attributed to C1, while the glycosidic bond carbon, C4, displays shifts at 90-91 ppm. Additionally, C6 is observed at 64 ppm. The resonance of the ring carbons C2, C3, and C5 exhibits chemical shifts in the range of 79-74 ppm.

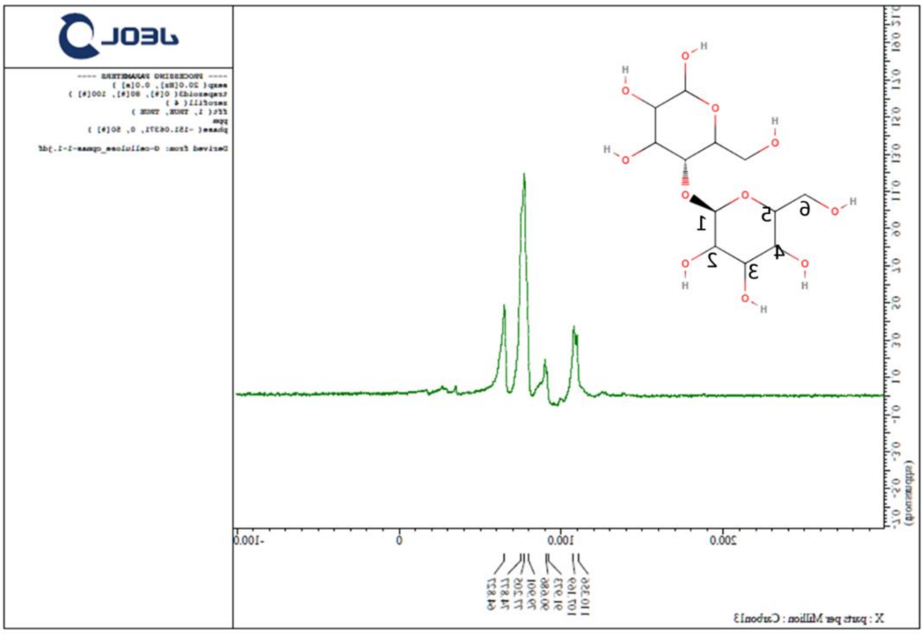

**Figure 3** C-NMR spectra of waste cellulose

### 2.4.2 Thermal Characterization Results

The thermal characterizations of neat PLA and PLA-based composites were evaluated by observing the results of TGA and DTGA, as presented in Figure 4 and Table 3, TGA curve of VC is given in Figure 5. All the materials start to decompose at above 236° C. It can be seen that the degradations of PLA and composites are a single-step process with a maximum degradation of around 264 °C observed in neat PLA.

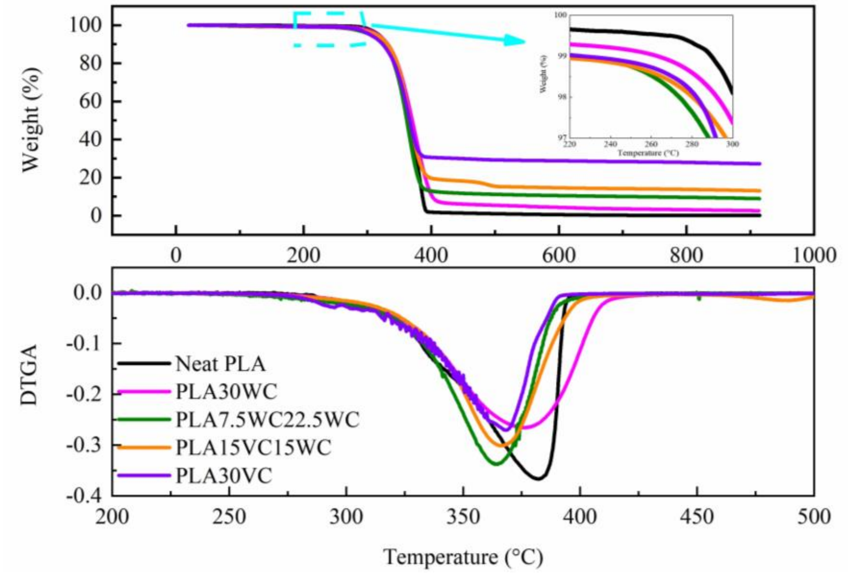

**Figure 4** TGA thermograms of neat PLA and PLA hybrid composites with 30% filler content. Weight change vs temperature at the top and derivative of weight change at the bottom. Neat PLA (black), PLA30WC (magenta), PLA7.5VC22.5WC (green), PLA15VC15WC (orange), PLA30VC (purple)

Furthermore, the addition of WC and VC, either separately or combined, decreases the onset degradation temperature of the material by up to 10%. It is also worth noting that waste cellulose (WC) containing composites thermally degrade completely without almost any char formation. On the contrary, in vermiculite (VC) containing composites, the addition of this mineral filler increases residue at elevated temperatures.

**Table 3** Onset-Offset temperature and % residue of PLA and hybrid composite.

| **Name** | **$T_{onset}$** | **$T_{offset}$** | **Residue @ 950 °C** |
|---|---|---|---|
| | **°C** | **°C** | **%** |
| **Neat PLA** | 264 | 408 | 0.1 |
| **PLA_30WC** | 237 | 437 | 2.6 |
| **PLA_7.5VC-22.5WC** | 236 | 416 | 8.9 |
| **PLA_15VC-15WC** | 244 | 417 | 13 |
| **PLA_30VC** | 247 | 408 | 27.2 |

Figure 5 shows that up to 200 °C, the physical absorption of water has been observed. In the temperature range from 200 to 500 °C, the dissociation of hydroxyl groups has occurred. Above 500 °C, mass loss has been observed due to the degradation of organic molecules or impurities. At higher temperatures, only inorganic residues (91.6%) such as metal oxides remain in the structure.

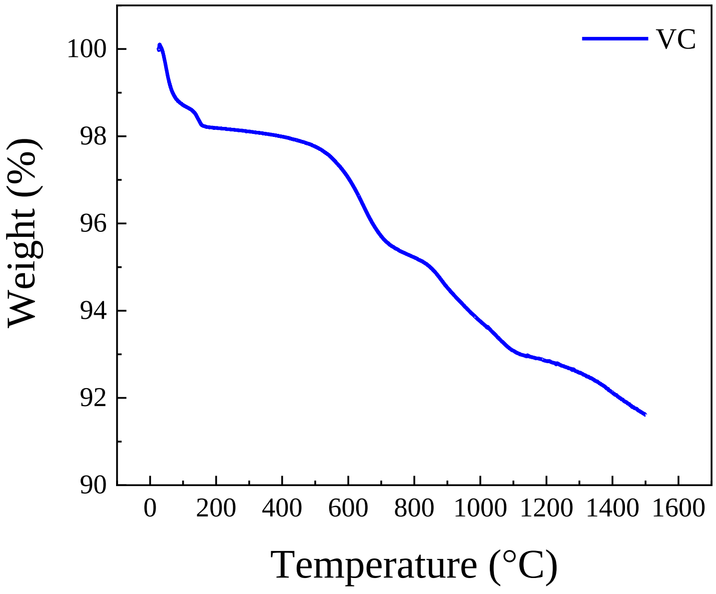

**Figure 5** TGA thermograms of vermiculite

Thermal properties such as glass transition temperature, melting enthalpy, and crystallinity of samples are investigated by considering DSC measurements (Figure 6). At around 100 °C neat PLA undergoes a cold crystallization. [54], [55] With varied weight fractions of cellulose fibers there is no appreciable change in the glass transition temperature of the PLA, Table 4. Vermiculite bundles, on the other hand, constrain molecular motions and raise Tg slightly. [56] When the glass transition temperatures of the 30% filled composites are examined, about a 4°C increase is observed compared to the composite containing only cellulose. It is observed that Tg does not change significantly in the produced composites. Thus, it is predicted that environmentally friendly composites can be used alternatively in the application areas of neat PLA.

**Table 4** Thermal properties of Neat PLA and PLA hybrid composites.

| **Name** | **Glass Transition Temperature, Tg (°C)** | **Melting Temperature, Tm (°C)** | **Melting Enthalpy, ΔH (g/J)** | **Crystallinity, (χ) %** |
|---|---|---|---|---|
| **Neat PLA** | 58.9 | 174.2 | 6.1 | 6.6 |
| **PLA_10WC** | 61.6 | 175.2 | 21.5 | 25.7 |
| **PLA_20WC** | 64.4 | 178.5 | 19.7 | 26.4 |
| **PLA_30WC** | 60.9 | 176.7 | 17.5 | 26.8 |
| **PLA_7.5VC-22.5WC** | 64.5 | 177.5 | 12.8 | 19.6 |
| **PLA_15VC-15WC** | 63.6 | 175.3 | 16.7 | 25.7 |
| **PLA_30VC** | 63.2 | 174.0 | 22.8 | 35.1 |

The addition of 10% by mass of cellulose increases the enthalpy of the composite from 6.1% to 21.5%. However, enthalpy begins to decrease with increasing cellulose loading. The enthalpy decreasing with the cellulose content might be considered as the cellulose fibers make hydrogen bonds with hydroxyl groups of PLA, inhibiting the formation of polymer crystals [57]. PLA crystallinity is expected to increase with the addition of reinforcements made of cellulosic materials [58].

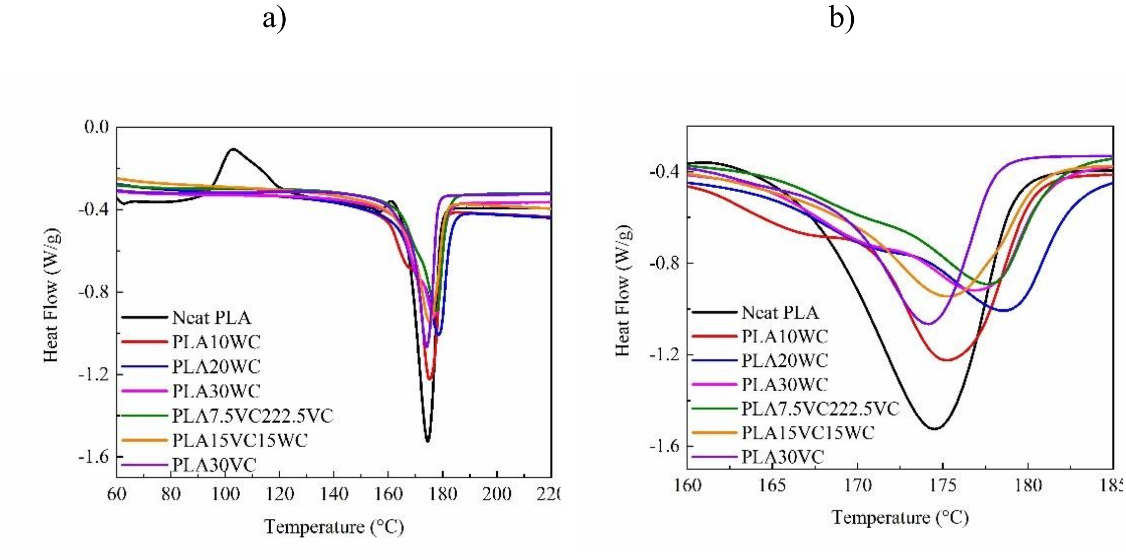

**Figure 6** DSC thermograms for a) Neat PLA and composites and b) Closer view; Neat PLA (black), PLA10WC (red), PLA20WC (blue), PLA30WC (magenta), PLA7.5VC22.5WC (green), PLA15VC15WC (orange), PLA30VC (purple).

As can be clearly seen in Table 4, neat PLA has a crystallinity of 6.6%, while the crystallinity improves drastically to 25.7% with 10% by weight cellulose addition. Cellulose fibers on the other hand support a heterogeneous nucleation mechanism, which lowers the free energy barrier and accelerates crystallization [59]. An increase in the WC ratio seems to be ineffective in measuring sample crystallinity. On the other hand, the same phenomenon is not observed in samples containing VC crystallinity increases with respect to VC amount, reaching up to 35.1 % crystallinity for PLA30VC. The highest number of crystalline regions however formed in PLA30VC samples which suggests that VC particles increase PLA crystallinity by complex nucleation mechanisms. Clay nanoparticles have been reported to influence the nucleation and crystal growth rates of PLA-based composites [60]. In nanocomposites with an intercalated morphology, the clay acts as an effective nucleating agent due to the incompatibility between the polymer matrix and the inorganic clay, leading to an increase in bulk crystallization rates. Dispersed nanosized clay particles might act as nucleating agents in PLA nanocomposites, enhancing nucleation and enabling crystallization [61]. This leads to the formation of smaller spherulites, and higher degrees of crystallization compared to exfoliation [62]. These findings imply that vermiculite speeds up the crystallization of polymer matrix, possibly due to its nucleation agent impact [63]. Crystallization enthalpies rise with the addition of clay and as the clay loading rises. PLA30VC with a melting enthalpy of 22.8 g/J has the maximum value. The sample having less amount of VC, PLA7.5VC722.5WC, has the lowest melting enthalpy out of hybrid composites. The increase in composite enthalpy with increasing vermiculite content suggests that the inorganic layers are well dispersed in the matrix as intercalated or exfoliated [64]. In the case of the combination of WC and VC, it can be interpreted that the crystallinity is regulated by VC.

### 2.4.3 Thermal Conductivity Results

Thermal properties of Neat PLA and PLA hybrid composites such as thermal conductivity, diffusivity, and effusivity are investigated according to their filler content. Table 5 shows that the thermal conductivity of the PLA hybrid composites increases concerning the Neat PLA with increasing filler content. This increase is clearly observable for samples PLA10WC, PLA20WC, and PLA30WC where the waste cellulose (WC) content is increased compared to neat PLA. This behavior of PLA-cellulose composites can be explained by the morphology and chain alignment of the samples. Since in semi-crystalline polymer crystalline domains are aligned and amorphous domains are randomly twisted and entangled chains, the lack of periodicity in the amorphous domains localizes the vibrational modes, thereby suppressing the thermal conductivity. Therefore, increasing the chain alignment is expected to enhance the thermal conductivity of polymers [65]. As opposed to Table 4, where crystallinity increases with WC addition independent of its amount, thermal conductivity, on the other hand, increases depending on WC amount for PLA10WC, PLA20WC, and PLA30WC samples. So, the aligned fibrous structure of the cellulose fibers enhances the thermal conductivity of PLA-WC composites [66]. In addition to thermal conductivity values, thermal diffusivity, representing the speed of propagation of heat during changes of temperature over time, and thermal effusivity, representing the material's ability to exchange heat with the environment, which are the parameters dependent on thermal conductivity also show an increasing trend upon increasing WC content [67].

The thermal conductivity values of PLA30WC, PLA7.5VC22.5WC, PLA15VC15WC, and PLA30VC show that 30% filler content provides the highest thermal conductivity. However, changing the content of these samples with increasing or decreasing WC/VC ratio modifies the thermal diffusivity and effusivity values. Among these samples, the increasing vermiculite content does not show a significant effect on conductivity and moreover, the expanded layered structure of vermiculite decreases the speed of propagation of heat in the sample and decreases the thermal diffusivity values [68]. However thermal effusivity values experience an increase with the increase in vermiculite values. This behavior may result from the stored thermal energy in vermiculite-incorporated composites due to their poor thermal diffusivity. The material tends to converge its steady state by liberating the stored excessive heat energy via dissipating it to its surroundings which is defined as the increase in thermal effusivity.

**Table 5** Thermal conductivity properties of Neat PLA and PLA hybrid composites.

| Name | Temperature °C | Thermal Conductivity W/mK | Thermal Diffusivity mm2/s | Thermal Effusivity - | Thermal Conductivity (%) |
|---|---|---|---|---|---|
| **Neat PLA** | 21.8 | 0.21 | 0.14 | 555.6 | 0.0 |
| **PLA_10WC** | 21.8 | 0.25 | 0.19 | 582.5 | 21.6 |
| **PLA_20WC** | 22.4 | 0.29 | 0.22 | 610.2 | 39.7 |
| **PLA_30WC** | 24.2 | 0.34 | 0.29 | 636.3 | 64.5 |
| **PLA_7.5VC-22.5WC** | 24.0 | 0.34 | 0.30 | 616.1 | 61.9 |
| **PLA_15VC-15WC** | 24.0 | 0.33 | 0.26 | 654.9 | 59.9 |
| **PLA_30VC** | 24.0 | 0.35 | 0.26 | 685.1 | 68.0 |

When the effect of both fillers on thermal conductivity is considered, the effect of vermiculite on the increase in thermal conductivity is more pronounced. The highest thermal conductivity value is obtained with PLA30VC. However, their hybrid usage in the samples PLA7.5VC22.5WC and PLA15VC15WC shows that when both fillers are used together, thermal conductivity is dominated by WC since PLA7.5VC22.5WC have higher WC content and higher thermal conductivity improvement (61%) compared to neat PLA. This behavior can also be attributed to the chain alignment property of WC fibers.

### 2.4.4 DMA results

Storage modulus and damping factor of all samples are investigated by DMA with a temperature range between room temperature to 120 ° C. DMA results of injection molded samples are represented in

Table 6 and Figure 7.

Tan delta (damping factor) can be interpreted as a compatibility criterion. There are 3 main conditions to fulfill to be mentioned ‘compatibility’. First, a shift in the maxima through the higher T, second, a decrease in peak intensity, third, peak broadening [69]. For all composites, 2 of these are fulfilled except PLA7.5VC22.5WC. Almost all maximum damping factor temperatures remain unchanged, which is around 65°C. Figure 7a shows that the maximum value of the damping factor decreased considering Neat PLA and broader transitions are observed for all samples rather than PLA7.5VC22.5WC.

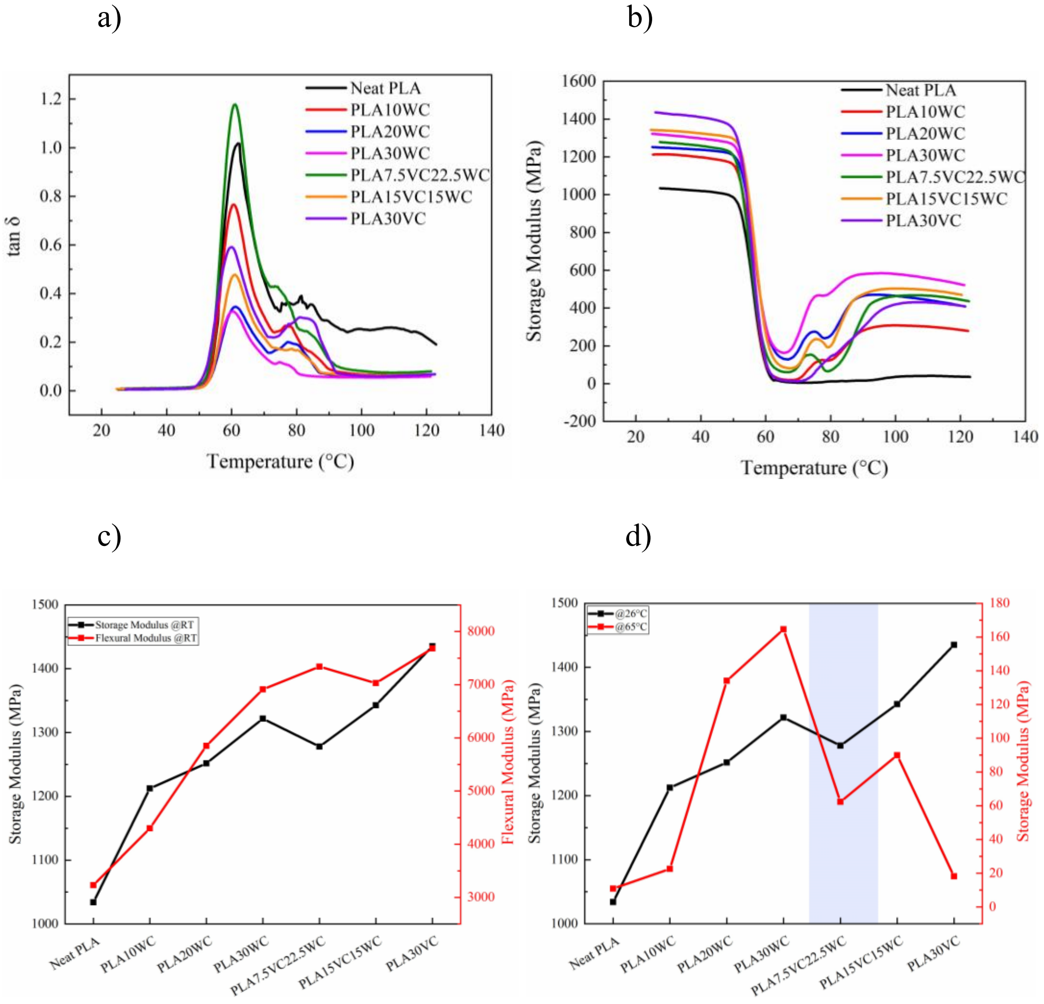

**Figure 7** DMA results of hybrid composites a) Damping factor b) Storage Modulus c) Storage Modulus vs. Flexural modulus at room temperature d) Storage modulus at 26°C and 65°C.

Storage modulus data show that in both glassy and rubbery regions all composites have a higher modulus of neat PLA (Figure 7b and Table 6). Transition from the glassy state to the rubbery state the storage modulus of all samples decreased drastically as expected. However, increasing cellulose loading results in increasing storage modulus for both glassy and rubbery regions. Cellulose restricts chain motions and improves modulus. Neat PLA has 11 MPa of storage modulus at 65°C. PLA10WC, PLA20WC, and PLA30WC lead to enormous improvements such as 108%, 1136%, and 1417%, respectively, of storage modulus for the rubbery state. These composites might be a candidate for solving the low heat resistance of PLA which is one of the major drawbacks of PLA.

In Figure 7c, the correlation between flexural modulus and storage modulus at room temperature has been proven. The same trend is observed for all datasets Figure 7d and

Table 6 show that flexural modulus storage modulus improved for both room temperature and elevated temperatures (at 65 °C). Instead of Neat PLA, these produced hybrids and upcycled products can be preferred as greener, cheaper, and more resistant to heat alternatives.

**Table 6** Flexural modulus and storage modulus at glassy (26°C) and rubbery (65°C) regions.

| Names | Flexural Modulus MPa | Improvement % | Storage Modulus MPa | |
|---|---|---|---|---|
| | Room Temperature | | 26°C | 65°C |
| **Neat PLA** | 3230 | - | 1034 | 11 |
| **PLA_10WC** | 4300 | 33 | 1213 | 23 |
| **PLA_20WC** | 5850 | 81 | 1252 | 134 |
| **PLA_30WC** | 6910 | 114 | 1322 | 165 |
| **PLA_7.5VC-22.5WC** | 7340 | 127 | 1278 | 62 |
| **PLA_15VC-15WC** | 7030 | 118 | 1343 | 90 |
| **PLA_30VC** | 7680 | 138 | 1435 | 18 |

### 2.4.5 Rheology Results

All samples investigated demonstrate a typical increase in storage (G’) and loss moduli (G’’) with respect to angular frequency. However, composites’ rheological behavior changes upon filler addition. In general, the G’ of the composites are higher than their loss modulus (Figure 8 a, c). This demonstrates that samples are in elastic character and degrade elastically. Both G’ and G’’ of composites are higher than neat PLA at low frequencies, except PLA30VC, implying that fillers are distributed uniformly within the polymeric matrix. G’ and G’’ of PLA30VC composite is lower than neat PLA, particularly at higher frequencies, indicating that 30 wt. % VC reinforcement in fact reduces the elastic character. On the other hand, the addition of 10, 15, 20, 22.5, and 30 wt.% cellulose gradually increases G' and G'' implying that further entanglement is introduced into the polymeric matrix. Here, there's a slight deviation from the order, in the case of PLA7.5VC22.5WC, which we observe throughout the whole rheology measurements (Figure 8Figure 7-a to -f, green). This is probably due to the competition between the contributing and impeding traits introduced by the fillers WC and VC, respectively. Here, WC dominates the overall rheological characteristics as the increasing trend of G' and G'' curves are similar, and the amount of VC introduced determines the overall G' and G'' values within the specified angular frequency range.

The evaluation of G' with respect to temperature reveals that all the composites' G' increases with filler addition (Figure 8Figure 7-b). Moreover, G' values of composites containing 30, 20, and 15 wt.% WC are drastically higher than composites containing low or no amount of WC. Hence, the incorporation of WC decreases the overall mobility of the composites more distinctly than VC. Storage moduli of all composites are higher than neat PLA at processing temperature (200 °C). Therefore, fillers aggravate shaping as higher energy barriers should be overcome to distort them. Looking at the loss moduli (Figure 8Figure 7-d), all the composites and neat PLA exhibit plastic behavior ($\tan\delta = G''/G' > 1$). The same trend is observed in storage moduli; since VC does not melt within the temperature range, it reduces the interaction between WC and PLA resulting in lower viscosity [70].

Analyzing the complex viscosity from the angular frequency perspective (Figure 8-e), all PLA composites within the dataset reveal a shear-thinning behavior. In addition to that, a Newtonian plateau is not observed in composites (except neat PLA). As shear thinning is an important factor for processability [71], we can conclude that both filler materials contribute to the processability of PLA. Moreover, from the slopes of the curves, it is evident that composites containing 10, 20, 22.5, and 30 wt.% of cellulose demonstrate similar shear thinning trends while their complex viscosity values differ concerning cellulose amount. However, there is a slight deviation from the cellulose amount correlation as in the case of storage moduli. Another proof that there is competition between the acting forces on polymer matrices, entanglements introduced by WC, and the obstacles introduced by VC. Nevertheless, at the processing temperature, only PLA7.5VC22.5WC composite exhibits elastic polymeric melt behavior.

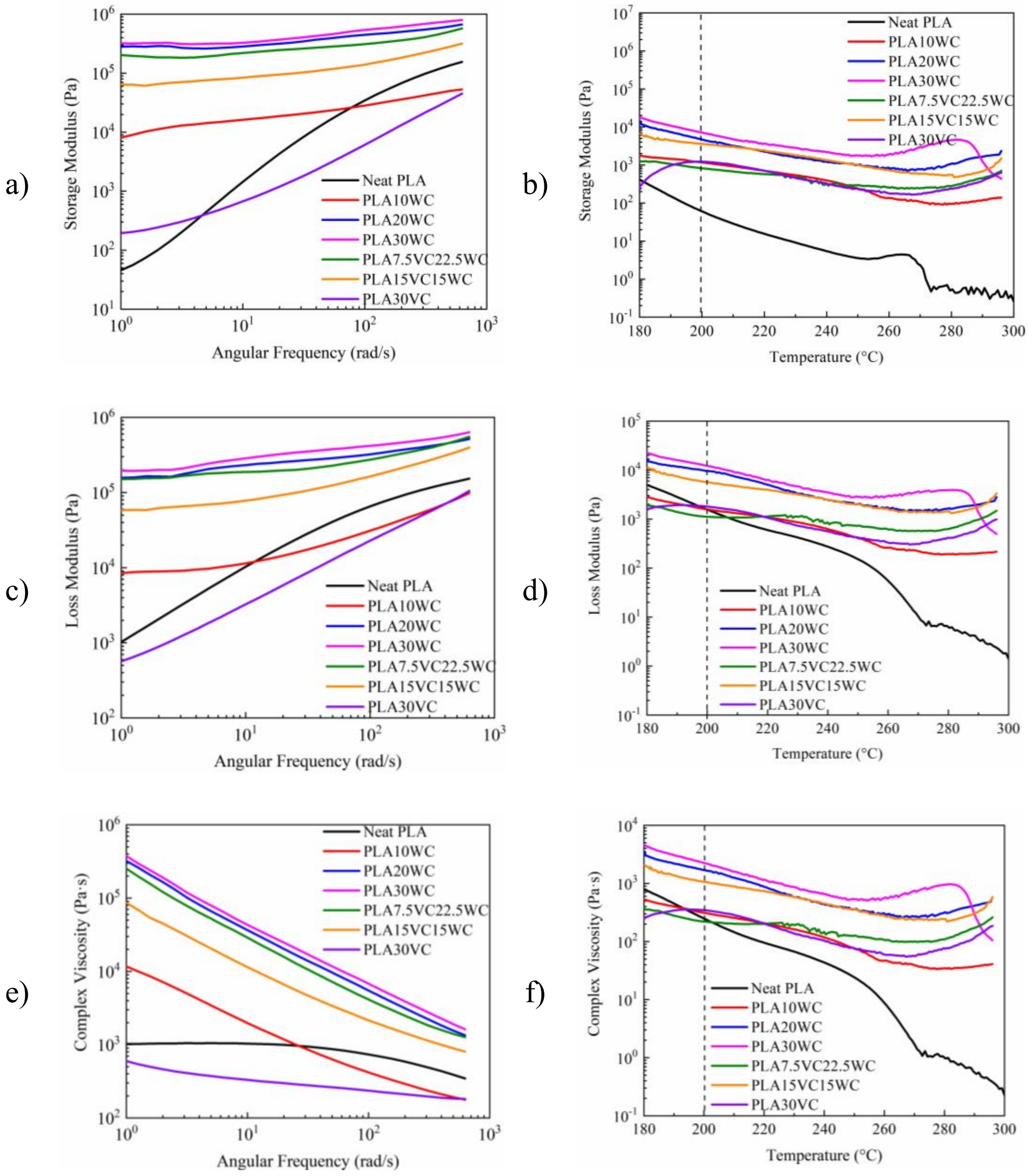

**Figure 8** Viscoelastic behavior of PLA-WC-VC samples. Storage, loss modulus, and complex viscosities with respect to angular frequency, (a, c, e, respectively) and with respect to temperature (b, d, f, respectively).

Investigating the temperature profiles of viscoelastic properties of the samples, one can easily notice that both G', G'', and melt viscosities decrease as the temperature increases. Complex viscosities of PLA30WC, PLA20WC, and PLA15VC15WC are always observed significantly higher than the neat PLA within the temperature range scanned (Figure 8-f). This, again, means that these samples are more readily processable than neat PLA, particularly within the compounding process temperature (200 °C).

Starting from the initial temperature (180 °C), the melt viscosity of neat PLA is greater than PLA30VC, PLA15VC15WC, and PLA7.5VC22.5WC up to 190 °C. In this region, both fillers in this ternary system act as a lubricating agent to PLA [72]. As the system's temperature reaches 190-205 °C, we observe a transition in the viscosity behavior of PLA10WC and PLA30VC PLA7.5VC22.5WC compared to neat PLA. Above 195 °C, PLA10WC and PLA30VC become more viscous than neat PLA. Similarly, above 200 °C PLA7.5VC22.5WC becomes more viscous than neat PLA. Other samples never undergo such a transition. In these regions, we may talk about two competing mechanisms of extension between cellulose and vermiculite. In the case of cellulose, at high temperatures, the disentanglement in polymer chains enables more flow, resulting in less viscosity [73]. Conversely, vermiculite acts as an obstacle to flow, thus increasing the viscosity. Here, it is important to note that the expansion of vermiculite starts after 300 °C. The counteracting effects cancel each other at temperatures where their complex viscosity curves intersect with neat PLA’s.

### 2.4.6 Mechanical testing and hybrid strengthening mechanism by co-use of WC and VC

The effect of the hybrid reinforcing strategy on the mechanical response of the PLA matrix is evaluated by tension and 3-point bending tests assisted with fractographic analysis for identification of failure modes. Tensile test results suggested that all the samples behave elastically under applied tensile loading. Except for neat PLA and PLA7.5VC22.5WC sample cases, stress-strain curves shown in Figure 8a contained a mid-failure event changing the stiffness of the samples which suggests that the damage progression mechanisms in hybrid composites are to be examined.

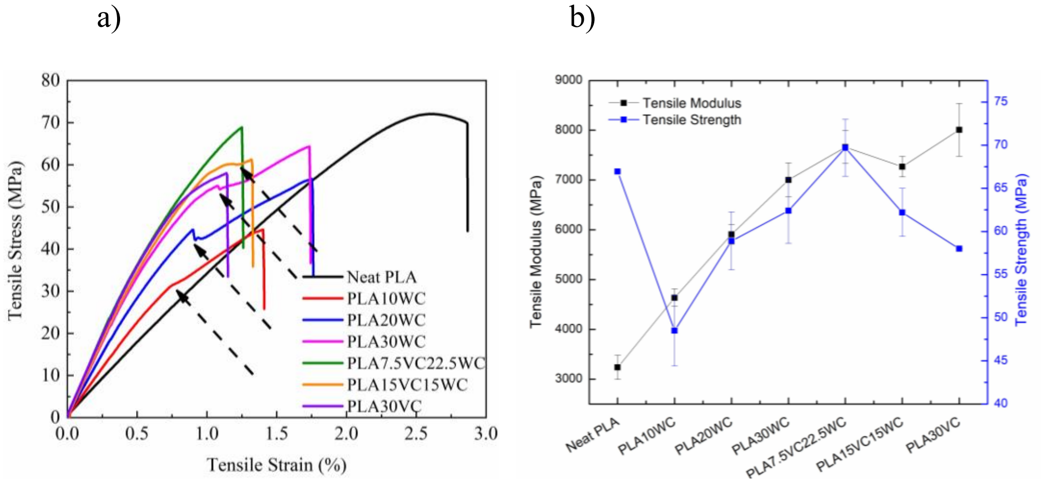

**Figure 9** a) Tensile stress-strain curves of PLA and composites (arrows indicating the mid-failure events) b) Tensile modulus and tensile strength of PLA and PLA composite.

An initial comparison was made between the samples containing only WC as a reinforcement phase (namely PLA10WC, PLA20WC, and PLA30WC). The nature of the stress-strain curves suggested that the E value increases and tensile strength remains almost the same as the amount of WC increases (Table 7 and Figure 9b). For such samples, the yielding event has caused a stress drop after specific stress and strain values hereby named as 'In-situ failure events' (Figure 9a). The nature of this event has been investigated on the fracture surfaces of failed specimens under tensile loading (Figure 10a-b-c). When examined at the presented scale, the presence of shear failure zones causing ridges during brittle fracture [74], [75] is observed in the fracture surface PLA10WC and PLA20WC.  In the case of PLA30WC, the fracture surface (Figure 10c) contains a lot more damage marks (more surface roughness) suggesting more damage progression events before the final fracture.

**Table 7** Tensile test results of Neat PLA and PLA composites

| **Name** | **Tensile Strength (MPa)** | **Young's Modulus (MPa)** | **Improvement %** | **Strain at break (%)** |
|---|---|---|---|---|
| **Neat PLA** | 66.9 (±0.1) | 3236 (±30) | | 2.5(±0.0) |
| **PLA_10WC** | 48.5 (±4.1) | 4635 (±176) | 43 | 1.5 (±0.3) |
| **PLA_20WC** | 58.9 (±3.4) | 5908 (±199) | 83 | 1.6 (±0.1) |
| **PLA_30WC** | 62.4 (±3.8) | 7002 (±342) | 116 | 1.6 (±0.1) |
| **PLA_7.5VC-22.5WC** | 69.7 (±3.3) | 7661 (±330) | 137 | 1.3 (±0.1) |
| **PLA_15VC-15WC** | 62.2 (±2.8) | 7267 (±207) | 125 | 1.3 (±0.1) |
| **PLA_30VC** | 58.0 (±0.2) | 8008 (±531) | 147 | 1.1 (±0.1) |

In the case of PLA10WC (Figure 10a), different from PLA30WC, the fracture surface was less rough with periodic brittle cracking events (underlined in blue lines) separated with a major transverse cracking plateau (dashed red arrows).  The comparison of these surfaces underlined the 2 in-situ failure events namely PLA micro-cracking and WC/PLA fiber/matrix debonding events are present in all samples. The presence of such events is identified as the cause of strength reduction on WC reinforced samples by causing premature failure.

**Table 8** In-situ failure results of Neat PLA and PLA composites

| **Name** | **In-situ failure stress (MPa)** | **In-situ failure strain (MPa)** |
|---|---|---|
| **Neat PLA** | - | - |
| **PLA_10WC** | 31.3 | 0.7 |
| **PLA_20WC** | 44.5 | 0.9 |
| **PLA_30WC** | 54.8 | 1.1 |
| **PLA_7.5VC-22.5WC** | - | - |
| **PLA_15VC-15WC** | 59.7 | 1.1 |
| **PLA_30VC** | - | - |

Contrarily, when only VC is considered as the sole filler (PLA30VC), homogenized PLA cracking events which are mostly transversely aligned (Figure 10f) suggest a more brittle failure progression. Young's modulus and flexural modulus values (Figure 11) were measured underlining the fact that an effective dispersion of VC platelets is achieved.

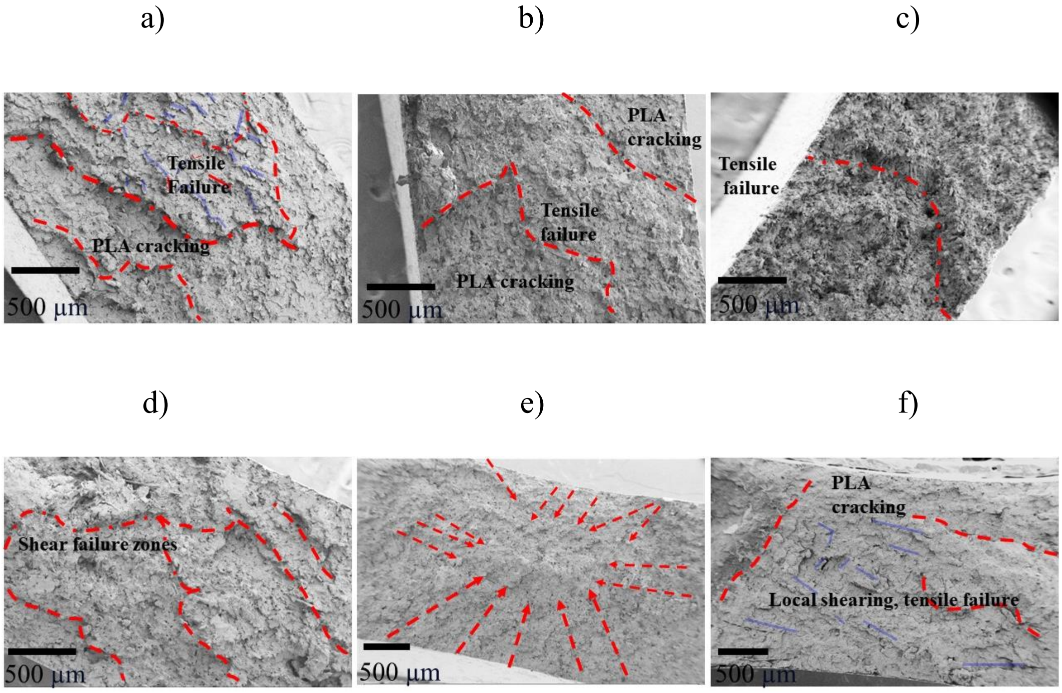

**Figure 10** Tensile fracture surfaces of a) PLA10WC, b) PLA20WC, c) PLA30WC, d) PLA15VC15WC, e) PLA7.5VC22.5WC, f) PLA30VC.

The measured tensile strength of PLA30VC samples is higher than any in-situ failure strength identified in WC-reinforced cases which suggests that VC-PLA matrix reactions are more favorable than WC-PLA interactions in terms of failure. When both WC and VC are used together inside the PLA matrix, the stress-strain curves suggest that, in the PLA15VC15WC case, the occurrence of in-situ failure events cannot be avoided. This fact is shown in fracture surfaces (Figure 10d) where shear zones due to fiber debonding and PLA micro-cracking events are observed. On the other hand, for PLA7.5VC22.5WC samples with the highest tensile strength, any types of pre-mature failures were avoided thanks to VC platelets reflecting the transverse PLA cracking that intensifies with the debonding of main load carrier WC fibers. Compared to previous studies on cellulose-based PLA composites, the improvements reported in Young's modulus of hybrid formulation observed in the current study are significantly greater (137%) without any significant strength loss than those observed in similar works in literature [7], [58], [76]

.

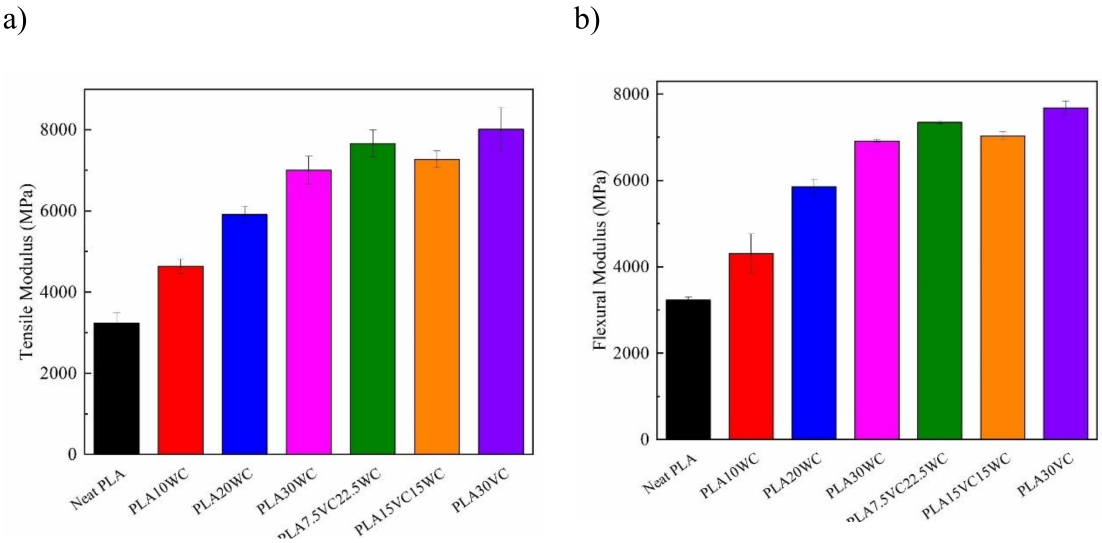

**Figure 11 a)** Young’s modulus b) Flexural Modulus

## 2.5 Conclusion

The Current study demonstrates that hybrid composites of biopolymer, PLA, are successfully produced via upcycled cellulose and vermiculite. These green hybrid composites provide stiff, strong, thermally conductive, and environmentally friendly alternatives to commercial petroleum-based polymeric composites. In general, no obvious change is observed in the thermal stabilities of the composites when VC and WC fillers are added. Comparing the thermal decomposition properties of the samples, composites with only cellulose incorporated as filler, and the onset temperature of thermal degradation of PLA decreases slightly (up to 10%), independent of WC amount. Although the overall onset degradation temperature drops slightly in VC-incorporated composites, the onset temperature increases with respect to VC amount. It is also observed, from the DSC results, that there's no significant change in the Tg value of the polymer, implying that the processability of PLA is not affected by the incorporation of fillers. It is also worth noting that the slight increments in the Tg values are regulated by the VC amount. In all composites (binary or ternary) the highest thermal conductivities are observed when only VC is added (68%, PLA30VC). However, in hybrid composites where WC is added, WC governs the thermal conductivity. DMA results shows that compared to neat PLA modulus of the composites are improved for both glassy and rubbery region. Moreover, storage moduli of all composites are higher than neat PLA at processing temperature (200 °C), implying that fillers aggravate shaping. Overall, all the composites are in elastic character and degrade elastically (G''>G'). In rheology measurements from both the angular frequency and temperature perspective, there is a deviation from the filler amount order in PLA7.5VC22.5WC composite, and this deviation is attributed to the competition between the acting forces of fillers to the PLA matrix. The incorporation of WC introduces disentanglements at high temperatures which decreases the overall viscosity of the composites, while the incorporation of VC introduces obstacles to the polymeric matrix, thus increasing viscosity. The synergistic effect observed in PLA7.5VC22.5WC is attributed to the composite's rheological properties at processing temperature (200 °C) where only PLA7.5VC22.5WC composite exhibits elastic polymeric melt behavior. Similar synergy is observed in mechanical results as well, all the composites except PLA7.5VC22.5WC break before the ultimate tensile stress (UTS) point. This implies that in the synergistic composition of PLA7.5VC22.5WC, we do not observe de-bonding and no in-situ failure break. In general, the filler WC is responsible for de-bonding events that cause strength reduction, while VC generates brittle fractures. But where the hybrid filler strategy is concerned, PLA7.5VC22.5WC demonstrates the highest tensile strength. In this particular composite, VC platelets introducing transverse cracking in the PLA matrix are observed to intensify with the debonding of the main filler (WC).

# CHAPTER 3: A sustainable strengthening/stiffening approach for injection molded polypropylene matrix thermoplastic composites

## 3.1 Abstract

Hybrid interaction/co-working mechanisms of waste cellulose (WC) fibers and expanded vermiculite (VC) in polypropylene (PP) resulted in stronger, stiffer, and thermally durable composites with ease of processing. Fibrous WC and particulate VC inclusions were mixed with the PP matrix via high shear thermokinetic mixer under 4000 rpm. Thermal and mechanical characterization efforts assisted with fractographic investigations are performed on 5 sample sets such as i) two-phase WC fibrous PP composites and ii) three-phase WC-VC hybrid composites. Results suggested that as the main reinforcement agent WC is able to increase the axial stiffness of PP (1.7 GPa) up to 4GPa (30WC) as the weight fraction increases with a reduction in ductility. However, a strength threshold due to WC cluster entanglement leaving partially un-wet clusters of WC and limited crystallization volume for PP at high WC weight fractions is noted. In-situ formed VC platelets placed between WC fibers are proven to provide PP crystallization loci to increase the axial stiffness (4.1GPa) and brittleness. When used with 10WC, they contributed to lacking stress transfer between randomly aligned WC fibers. More strikingly, in the 20WC10VC case the inherent problem of WC cluster entanglement and consequently caused polymer shear failure significantly improved the tensile strength of the samples (45MPa).

## 3.2 Introduction

There exists an accelerating demand for stronger and lighter thermoplastic composites with a strong emphasis on environmental concerns [77]–[79]. This demand is mainly driven by recyclability[80] , ease of processing[81], and low energy consumption during their entire life cycle[82]. One promising approach to fulfill this demand is offered using natural fibers[83] either in the continuous form [84] to compete with conventional composite structures[85], [86] or in the discontinuous form [87], [88] that are readily adaptable to conventional [89] and emerging polymer processing techniques[90]. Among various thermoplastics, polypropylene (PP) is the most common petroleum-based polymer product used in various industries such as construction, transportation, and household appliances due to its attractive properties such as being lightweight and having high strength, high stiffness, and hardness[91], [92]. Hence the composites of PP with organic cellulose fibers[93], [94] and/or inorganic clay particles[95] occupy a great place in industrial, technical, and scientific applications.

The linear filament structure of cellulose along with its long and strong molecular chains provide enhanced tensile and flexural strengths as well as rigidity[96]. Also, hydroxyl groups and their tendency to form hydrogen bonding play a key role in the reinforcing nature of cellulose fibers[35]. On the other hand, mica-type layered silica particles such as vermiculite platelets play an important role in strengthening the polymers[97]. Especially expanded vermiculite, forming a layered platelet structure with a high aspect ratio, enables better intercalation with the matrix or forming fibrils that provide very high stiffness and strength[41], [45]. Recent studies show that either individual or hybrid use of these fillers contributes to the improvement of the mechanical properties of the polymer matrix. For instance, Joseph et al.[98] studied the dynamic mechanical properties of PP composites containing sisal fiber with a high cellulose content. They observed that the addition of sisal fiber to neat polypropylene increased the storage modulus along with the mechanical strength and modulus which were found to increase with fiber loading. Different cellulose fiber types with increasing cellulose content in the PP matrix with and without MAPP as a coupling agent are studied by Borja et al.[99]. Results reveal that increasing the amount of fiber improves the tensile strength and modulus values. Also, Bataille et al. introduce cellulose fibers into the PP matrix and obtain enhanced elastic modulus values up to a threshold content of 30 phr, while endangering the yield stress values which decrease with increasing cellulose content[100]. A similar threshold challenge is observed in the study of Risnasari et al.[101] who use cellulose fibers in the PP matrix which is either neat or modified with MA. While tensile modulus values improve with increasing cellulose content and the coupling agent addition, the tensile strength values slightly decrease with increasing cellulose content. On the other hand, Gomes et al. studied the PP/vermiculite blends in different ratios investigating the mechanical properties of the compounds, and observed an increasing trend in tensile strength and modulus values [95]. Li et al. also used organic vermiculite in wood–plastic composites (WPC) and obtained improved mechanical properties as higher flexural and tensile properties due to homogeneous dispersion and strong interfacial interaction in the WPC suggesting enormous potential applications as WPC-based engineering materials[102]. Another study conducted by Zhang et al. preparation of polypropylene/organo-vermiculite nanocomposites revealed that the addition of vermiculite in the PP matrix even in lower amounts (1%) the tensile and flexural strength of these nanocomposites however, higher amounts of vermiculite does not show better performance due to the change in its crystal structure[103]. Vermiculite incorporation into the PP and PLA matrix is studied by Arıtürk et al. suggesting that vermiculite improves the tensile and flexural properties of PP due to the fibrillation of vermiculite in the PP matrix and acting as a reinforcing agent[104]. Hybrid formulations of these fillers arouse interest due to synergistic effects between them, ecological concerns, and contribution to ease of processing. Arıtürk et al. use cellulose and vermiculite in PLA matrix to obtain hybrid green composites of PLA with improved tensile properties with easily processable compounds[105]. Also, Mustapha et al. studied the co-incorporation of cellulose and clay into the PP matrix which results in an improvement in tensile strength. This is attributed to good dispersion and enhanced efficiency of the stress transfer mechanism between the silica and the cellulose within the PP matrix resulting from the prevention of entanglement of discontinuous cellulose fibers via clay addition[106].

This study comprises the preparation of hybrid composites of PP via the incorporation of waste cellulose (WC) and vermiculite (VC) as natural reinforcing agents at different loading levels to fulfill the expectation for mechanically improved, easily processable, hybrid green composite polymeric materials. In this scope, using discontinuous fiber reinforcements may be limited due to fiber entanglement which may deteriorate the mechanical performance. However, with a hybrid approach, we are able to manufacture hybrid PP composites that are manufacturable by injection molding, more crystallization, and better resistance against shear deformation during failure without suffering from inherent fiber entanglement causing insufficient polymer/fiber wetting.

## 3.3 Materials and experimental

### 3.3.1 Materials

Waste cellulosic fibers derived from the textile industry were supplied by Zorlu Linen Textile, Istanbul, Turkey. Superfine vermiculite with a reported average particle size of 1.4 mm was purchased from Serakulit, Canakkale, Turkey. Homopolymer PP (Borealis HE125MO) with a melt flow rate of 12 g/10min (230°C/2.16kg) was purchased from Efa Kaucuk, Kocaeli, Turkey.

As employed (as purchased) morphologies of fibrous WC and platelet expanded V in Figure 12. The average width of WC fibers is 20 um they have varying individual diameters, and several sheet-like WCs may be entangled /rolled to form larger fibers. Such morphological variabilities of industrial waste-based fibrils are expected and noted for further interpretation of the in-situ behavior of WC in PP.

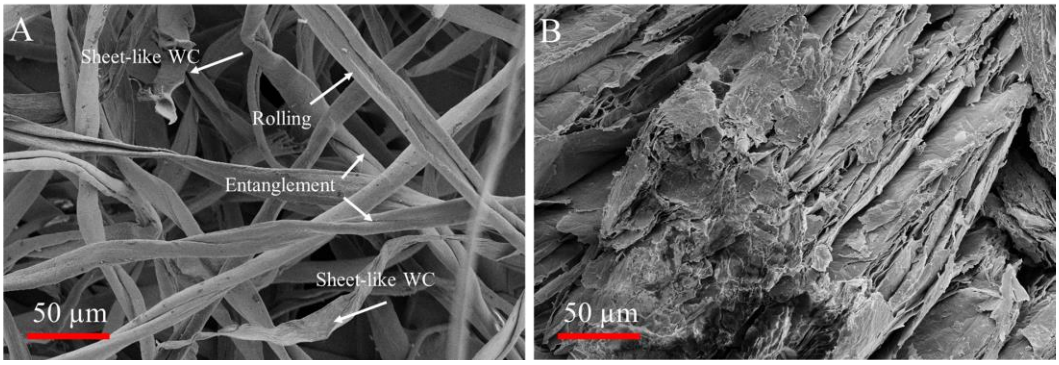

**Figure 12** As used morphologies of a) waste cellulose, WC b) expanded vermiculite, VC.

As employed (as purchased) expanded VC consists of nano-metrically stacked platelets situated in significantly larger (as sold) VC particles (Figure 12b). It is then hard to predict the in-situ particle size and geometry of VC particles which are known to go through significant morphological changes depending on the co-processed polymer type[104].

### 3.3.2 High Shear Mixing

Thermokinetic mixer Gelimat GI (Draiswerke), Sabanci University, was used to prepare the composite samples containing PP, WC, and VC in varying weight ratios reported in Table 9. PP, WC, and VC were melt blended at around 4000 RPM.

**Table 9** Weight contents of formulations.

| Sample Name | Waste Cellulose | Vermiculite | Polypropylene |
|---|---|---|---|
| | | Weight % | |
| **PP** | 0 | 0 | 100 |
| **10WC** | 10 | 0 | 90 |
| **20WC** | 20 | 0 | 80 |
| **30WC** | 30 | 0 | 70 |
| **20WC10VC** | 20 | 10 | 70 |
| **10WC10VC** | 10 | 10 | 80 |

After being removed from the mixing chamber of the thermokinetic mixer, the polymeric composite is allowed to cool before being crushed into granules. In order to perform the material performance tests, test samples are molded using an XPlore 12 mL micro-injection molding machine (XPlore, Stittard, Holland). Injection molded composites and their weight ratios are represented in Table 9. Example views from manufactured composite samples are shown in Figure 13 .

**Figure 13** Injection molded samples from left to right 10WC, 20WC, 30WC, 20WC10VC, and 10WC10VC.

## 3.4 Material Characterization

### 3.4.1 Thermogravimetric analysis

Thermo-gravimetric analyses of the samples were completed with TA Q 500 TGA using Universal Analysis 2000 software. Analyses were conducted under a nitrogen atmosphere at a heating rate of 20°C per minute from ambient temperature to 950°C.

### 3.4.2 Differential Scanning Calorimetry

Thermal analysis and the degree of crystallinity of polymer composite samples were performed using Differential Scanning Calorimetry (DSC) method with DSC 3 + 700 (Mettler Toledo, Columbus, OH, USA) Mettler Toledo under a nitrogen environment from 25 °C to 260 °C at a rate of 10 °C/min.

The melting enthalpies (Hm), melting temperatures (Tm), and crystallization temperatures (Tc) were calculated using the STARe software (Mettler Toledo, Columbus, OH, USA). The melting enthalpies were utilized to assess the degree of polymer crystallinity in the composites. Table 10 shows Tm, melting enthalpies, and crystallinity degrees.

$$\text{Crystallinity } (\chi)\ \% = \frac{\Delta H}{\Delta H^*} * \frac{1}{\Phi\ PP} \qquad (1)$$

ΔH is the integral of the heat flow after the baseline subtraction, and ΔH* is the melting enthalpy of a 100% crystalline PP, which can be found in the literature to be 207 $J.g^{-1}$ [107] Φ PP represents the weight fraction of PP in the composites.

### 3.4.3 Mechanical Testing

Tensile tests were performed to obtain mechanical properties by using a 5982 Static Universal Test Machine in Sabancı University (UTM, Instron, Norwood, MA, USA) with a rate of 2.0 mm/min and 5 kN load cell according to ISO 527-2 standards.

### 3.4.4 Electron Microscopy

The fracture surfaces of both the 3-point bending and UTM test specimens were coated three times with a thin layer of gold-platinum in order to perform the morphological examinations. Surface topography and failure morphologies were analyzed by using Leo Supra 35VP Field Emission Scanning Electron Microscope, Sabanci University. (FESEM, Carl Zeiss AG, Jena, Germany). Specimens were coated with a thin layer of gold-platinum. Fractographic analysis of the samples was performed in Insight Technology Development, TR.

### 3.4.5 Rheology

Rheological assessments, including frequency sweeps were performed using the MCR 702 TwinDrive Rheometer from Anton Paar in Graz, Austria. The complex viscosity of the samples was determined under a consistent shear strain of 10% at a frequency of 1 Hz at 170°C.

## 3.5 Results and Discussion

### 3.5.1 Thermogravimetric Analysis

Manufactured samples via high-shear mixing were initially introduced to TGA to check the obtained reinforcement weight fractions in the PP matrix as depicted in Figure 14. Measured residues after applied temperature scan suggested that obtained wt.% of WC were 9-18-32 (weight loss after T1) respectively for samples 10WC, 20WC, and 30WC (Figure 14-a). As evident from the DTGA analyses (Figure 14-b), as in the PPWC samples, there were 2 steps of degradation for all formulations. This phenomenon proves that cellulose is responsible for two-step degradation. As expected, PPWC cases had no residue at 950°C due to their organic content whereas incorporation of VC resulted in increasing the residue amount at the same temperature.

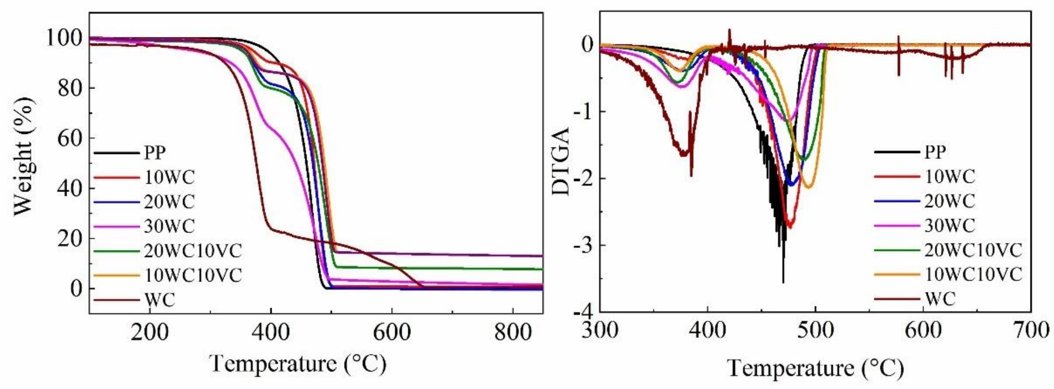
a) b)

**Figure 14** a) TGA measurements and b) measurements DTGA performed to manufactured PP composites.

The thermal resistance was preserved when the amount of cellulose was reduced, and V was added in order to facilitate the production process. The thermal decomposition temperature range can be considered as the T1 onset and T2 offset, it has been observed that the thermal durability of the hybrid composites is improved by 20.9 % and 27.6 % for 20WC10VC and 10WC10VC, respectively, and has higher thermal resistance compared to 30WC. Moreover, as portrayed in Figure 14a, for the 30WC sample there exists a shift in weight % vs. temperature plots more towards pure WC curve indicating possible non-wet WC fiber possibly in the WC-clusters that will be discussed thoroughly in fractographic analysis.

### 3.5.2 Constituent interactions (DSC) and monitoring

The increase in cellulose content made the melt processing more challenging, hence hybrid states were created by reducing the WC percentage and reinforcing with VC. These hybrid states were analyzed for their thermal properties such as crystallization percentage and melting-cooling behaviors using Differential Scanning Calorimetry (DSC). Table 10 shows that varied weight fractions of WC or VC additions did not contribute any notable change in the melting transition temperature of PP. Thus, it can be deduced that incorporation of VC into PP does not influence the processing of neat PP and PPWC composites so hybrid composites can be used alternatively in the application areas of neat PPWC composites.

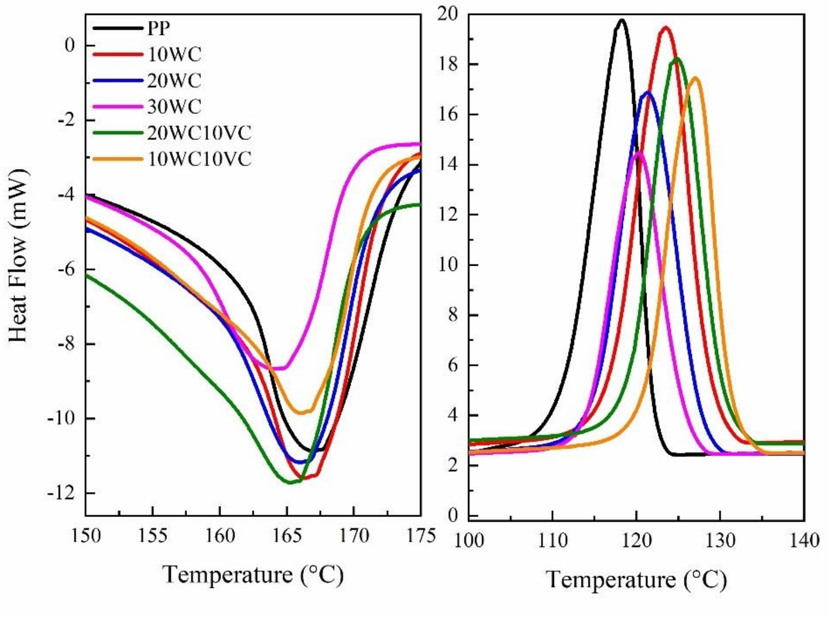

**Figure 15** DSC measurements of manufactured PP composites.

As shown in Figure 15 when 10% cellulose is added, the crystallization temperature of neat PP was increased by 7°C. Typically, an increase in cellulose content would lead to a higher crystallization temperature. However, unexpectedly, the crystallization temperature (Tc) decreased instead. In fact, for the 30WC condition, it approached that of neat PP. This phenomenon can be attributed to the increased entanglement with the higher cellulose content which consequently resulted in insufficient interactions between WC and polymer. That behavior limits the available volume for PP to crystallize around WC. When VC is added to the formulation, the observed increase in crystallization temperature can be attributed to VC reducing the existing entanglement, thereby creating available spaces for crystallization.

While the addition of WC reduces Tc, the addition of VC increases Tc, meaning that hybrid formulations are more prone to crystallization.

We can deduce that the increase in cellulose content has had a favorable effect by looking at the crystallinity percentages[105]. Neat PP has a crystallinity of 45.8%, but 10WC, 20WC, and 30WC have enhanced to 52.8%, 53.9%, and 55.7%, respectively.

Reducing the cellulose content and adding VC resulted in higher crystallization percentages. In WC-V hybrid composites, the highest crystallinity values reached were 59.2% and 57.2% for 20WC10VC and 10WC10VC, respectively.

**Table 10** Melting characteristic and crystallinity % of samples.

| **Sample Name** | **Melting Temperature, Tm (°C)** | **Crystallization Temperature Tc (°C)** | **Melting Enthalpy, ΔH (g/J)** | **Crystallinity, % (χ)** |
|---|---|---|---|---|
| **PP** | 166.9 | 118.0 | 94.9 | 45.8 |
| **10WC** | 166.3 | 123.7 | 98.4 | 52.8 |
| **20WC** | 165.9 | 121.2 | 89.3 | 53.9 |
| **30WC** | 163.9 | 120.1 | 80.7 | 55.7 |
| **20WC10VC** | 165.2 | 125.0 | 85.7 | 59.2 |
| **10WC10VC** | 166.0 | 127.0 | 82.9 | 57.2 |

An important governing factor in the crystallization of PP around WC and VC is the in-situ size of such inclusions. Due to their relatively high aspect ratio, WC-PP crystallization is limited with the surface of WC fibers ( Figure 16a) (highlighted as yellow regions). This behavior is highlighted as trans-crystallization[108] and is frequently mentioned in the literature. It is apparent from Figure 16b (a transverse fracture region on WC) this region had significantly different properties than the bulk WC fibers. A comparison of Figure 16c and Figure 16d shows that VC-PP crystallization rather affects the whole volume of PP since high shear effectively turns large VC particulates into well-distributed VC platelets in the bulk of the PP matrix.

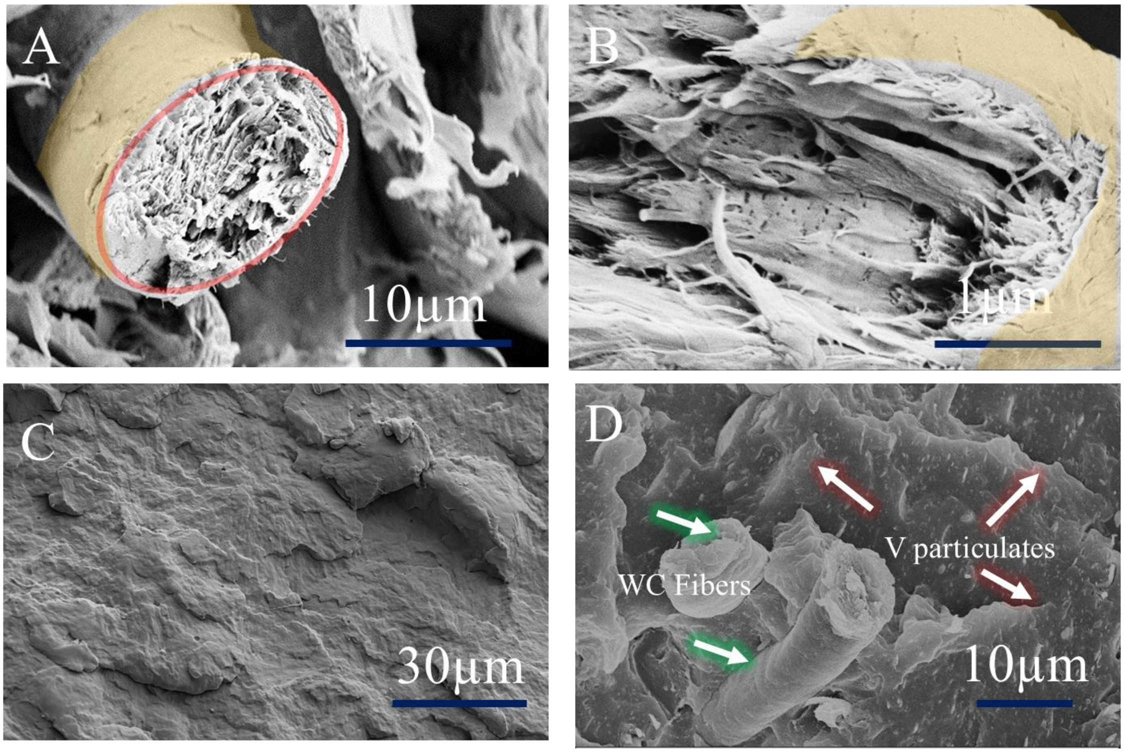

**Figure 16** a) A perpendicularly aligned WC fiber on tensile fracture surfaces with hierarchical microstructure b) A transversely aligned WC fiber with progressive failure over its thickness (yellow regions show PP/WC interaction regions) c) Neat PP morphology d) A view from tensile fracture surfaces of hybrid composites.

### 3.5.3 Rheology measurements

A rheological analysis was conducted by performing a frequency sweep at 170°C to investigate the frequency dependence of complex viscosity of both PP and the manufactured composites. As shown in Figure 17, it is evident that the lowest complex viscosity across all frequency ranges belongs to neat PP. With increasing cellulose content in the polymer matrix, the complex viscosity also increases, leading to enhanced flow resistance. This situation has led to issues during the manufacturing process of composites.

Previous studies have reported a correlation between the incorporation of fiber into polymer matrices and the flow of the composites. Higher fiber contents obstacle the flow and result in increasing complex viscosity [109]–[111].

When observing the 20WC10VC and 10WC10VC hybrids, it can be seen that they exhibit a trend similar to that of 20WC. Consequently, by incorporating clay instead of cellulose, it can be inferred that we attained the same complex viscosity trend with composites having lower additive ratios, thereby facilitating the process.

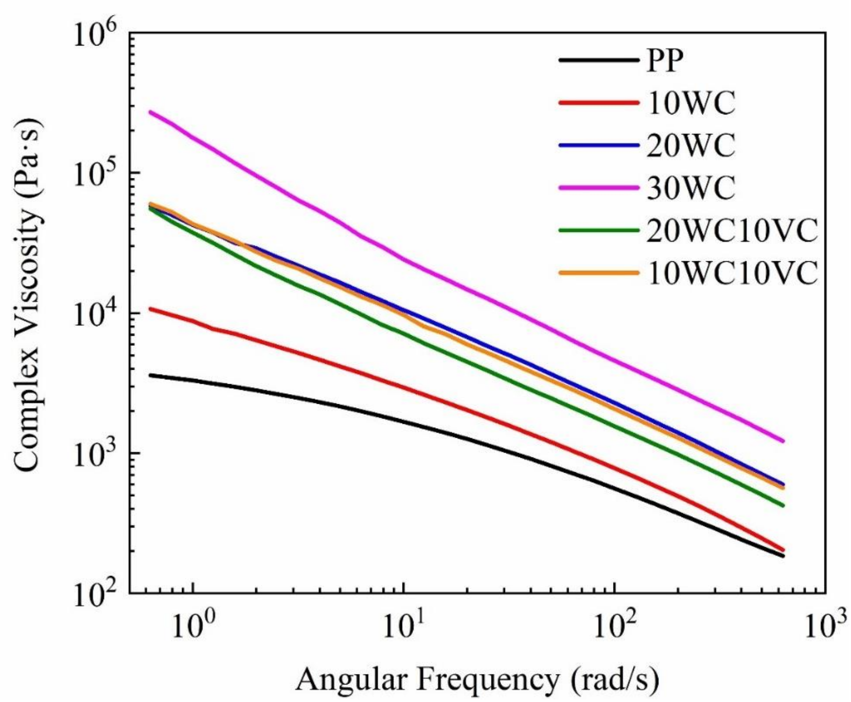

**Figure 17** Angular frequency vs. complex viscosity plot for manufactured PP composites

### 3.5.4 Mechanical Test Results and Fractography

Obtained stress-strain curves from uniaxial tension tests applied to investigated hybrid composites with varying reinforcements are portrayed in Figure 18. Note that the strain at failure for neat PP cases goes up to 600% and part of its stress-strain curve is portrayed. The highly ductile behavior of the PP matrix is of crucial importance to note in determining the deformation behavior of composite samples.

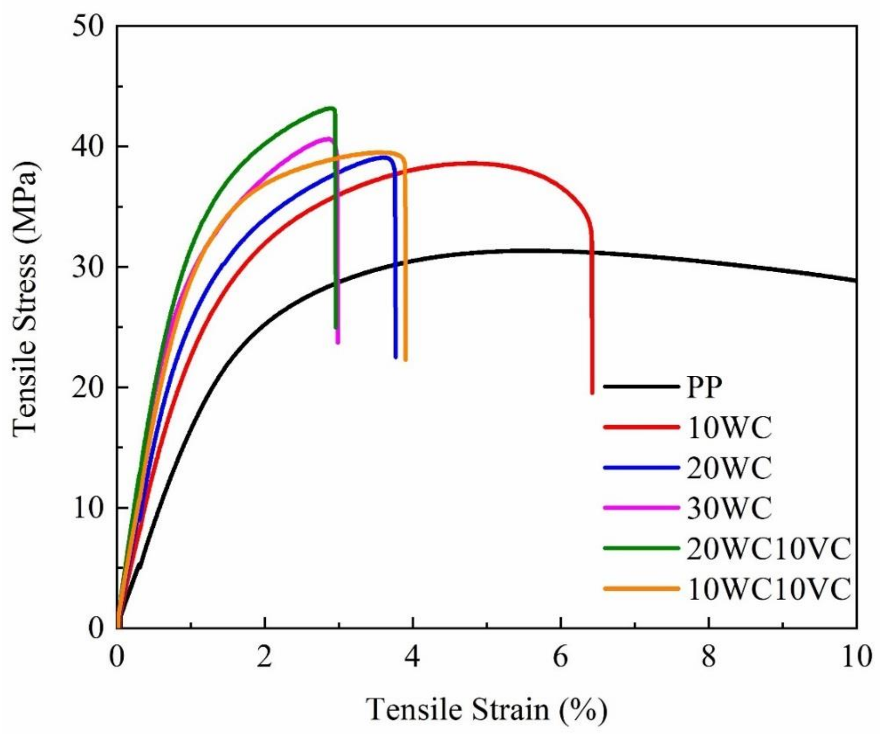

**Figure 18 Tensile Stress vs. tensile strain plot for manufactured PP composites.**

In the case of 10WC strain at failure (εmax) values decreased to 6.3% with a rather increasing slope after the yielding stress which signals the contribution of WC to the plastic deformation of the samples which will later on be revealed. This behavior was investigated with the comparison of neat PP and 10WC fracture surfaces (Figure 19). A region of interest with a large (entangled cluster) and a small (single fiber) WC debonding event (marked by a red circle) was portrayed in Figure 20a. When PP morphologies near such debonding events were investigated it is certain that there was no change in matrix morphology due to local WC debonding even for the large debonding area. This observation suggested two important conclusions such as i) The interaction between PP and WC was not favorable and debonding did not cause any shear deformation if WC is not heavily entangled ii) the yielding of samples occurred due to fiber debonding and individual PP yielding. When the overall fracture surface of the sample (Figure 19a) was investigated such independent behavior was portrayed as locally un-reinforced PP (schematically represented with red dots) and reinforced PP regions (differentiable with fiber debonding and failure marks).

**Table 11** Tensile test results of PP composites

| Name | Tensile Strength (σmax) (MPa) | Improv-ement % | Young's Modulus (MPa) | Improvement % | Strain at break (%) |
|---|---|---|---|---|---|
| **PP** | 28.7 (±6.8) | | 1880 (±51) | | 560.0 (± 10.0) |
| **10WC** | 38.2 (±0.3) | 33 | 2774 (±25) | 48 | 6.3 (±0.5) |
| **20WC** | 40.2 (±1.6) | 40 | 3402 (±277) | 81 | 4.0 (±0.3) |
| **30WC** | 40.5 (±1.2) | 41 | 3998 (±288) | 113 | 3.1 (±0.3) |
| **20WC10VC** | 44.7 (±0.7) | 56 | 4098 (±197) | 118 | 3.2 (±0.3) |
| **10WC10VC** | 39.5 (±0.3) | 38 | 3816 (±189) | 103 | 3.6 (±0.2) |

**Table 12** Flexural test results of PP composites

| Name | Flexural Strength (MPa) | Improvement % | Flexural Modulus (MPa) | Improvement % |
|---|---|---|---|---|
| **PP** | 46.9 (±0.5) | | 1690 (±28) | |
| **10WC** | 53.3 (±2.1) | 14 | 2310 (±167) | 37 |
| **20WC** | 59.3 (±0.3) | 26 | 3040 (±16) | 80 |
| **30WC** | 57.0 (±4.0) | 22 | 3520 (± 229) | 108 |
| **20WC10VC** | 66.6 (±0.8) | 42 | 3630 (±25) | 115 |
| **10WC10VC** | 61.2 (±0.3) | 30 | 3390 (±34) | 101 |

As the WC amount was increased to 20 wt.%, Young's modulus (E) of composites was also increased up to 3.4 GPa and 3.0 GPa for flexural modulus (Table 12) with a decrease in εmax (4.0%) and a relatively slight increase in σmax (40.2 MPa) (Table 11). This behavior in stress-strain signaled an increased WC entanglement with increasing WC content. Large-scale fractographs (Figure 19b) suggested that such entanglement caused a 3D block failure which initiates, propagates in the PP matrix (smaller when compared to 10WC), and ends up with the separation of large blocks of PP-WC clusters rather than individual WC failure. An example region with such clustering is portrayed in Figure

20b with marks of matrix shear deformation around WC which suggested that entangled WC cluster -PP debonding and shear deformation of PP during such debonding played an important role in the strength evolution of 20WC samples.

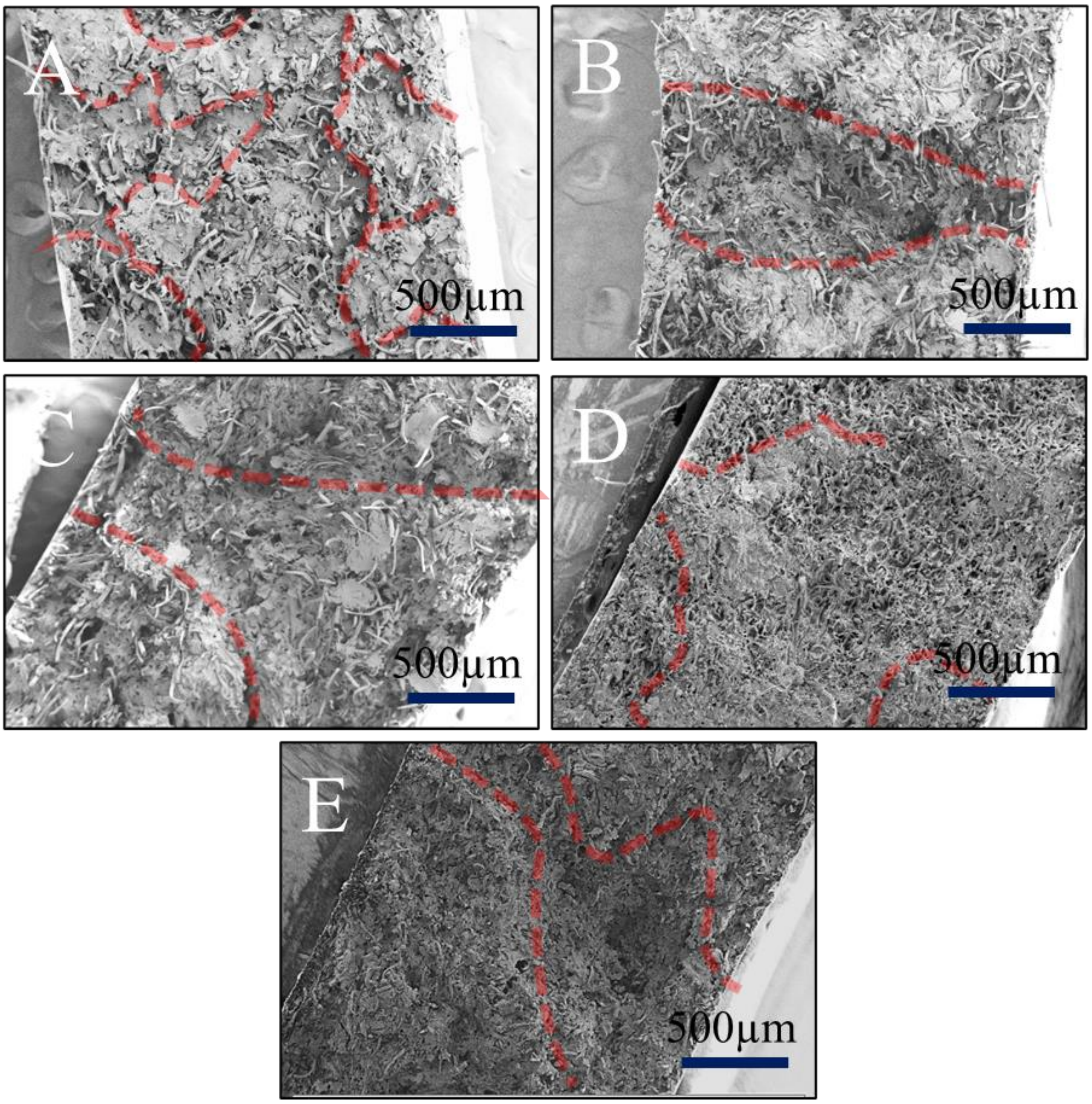

**Figure 19** Large-scale tensile fractographs of a)10WC b)20WC c)30WC d)10WC10VC e)20WC10VC (dotted regions correspond to distinguishable ridges on failure surfaces)

This behavior was further underlined in the case of 30 WC where no increase in σmax, a further decrease in εmax, and an increase in E values are noted when compared to 20WC. A similar block failure event was discovered in the middle of tensile test specimens (Figure 19c). When combined with observations in 20WC it can then be suggested that increasing the amount of WC is a limited strengthening approach for PP composites due to the presence of WC clusters with rather random orientation which may remain un-interacted with the polymer during processing (see TGA analysis).

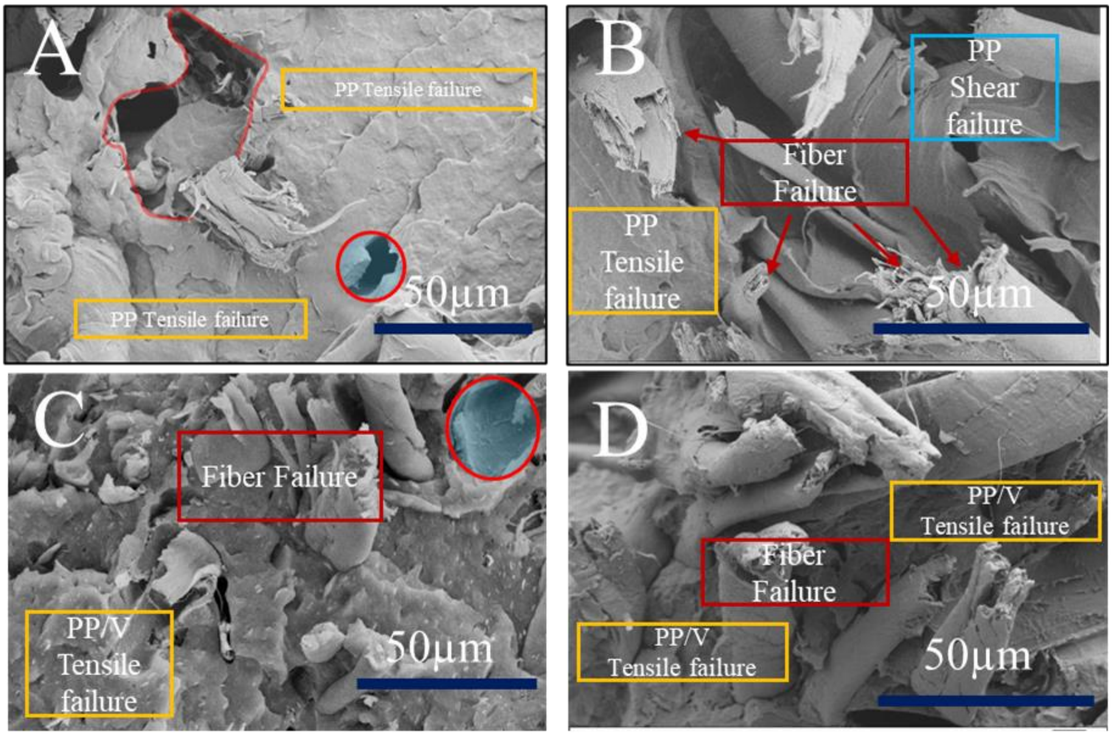

**Figure 20a)** A fiber (small) and cluster (large) debonding region in 10WC b) A fiber entanglement region in 20WC with PP shear failure around fiber interfaces c) A fiber failure region in 10WC10VC d) A fiber entanglement region in 20WC10VC with lack of PP shear fail.

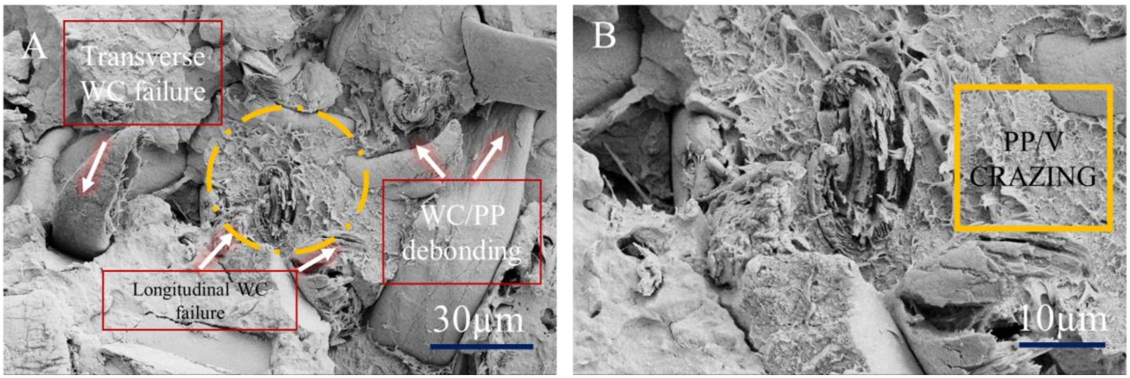

**Figure 21** a) View from a WC cluster region on tensile fracture surfaces in 20WC10VC with distinct WC failure modes. b) Zoomed in view of the yellow dotted circle in a) for identification of PP/VC crazing event on the region encircling a single WC parallelly aligned

In this context, 20WC10VC exemplified the effective reinforcement effect achieved with 20WC and observed the toughening effect in 10WC10VC with vermiculite platelets. The noted average E value of this case was 4.1 GPa which is comparable with 30WC when measurement errors were considered. The main superiority of 20WC10VC was its tensile strength (44.7 MPa). Large-scale fracture surfaces of 20WC (Figure 19b) and 20WC10VC (Figure 19e) were quite similar with block failure in the middle of the specimen due to local fiber entanglement. However, when investigated on a closer view (Figure 20d) it can be seen that it is due to that brittle PP nature that it cannot go through the shear deformation underlined in  Figure 20b which explains the further reduction in εmax for hybrid composites. The source of strength in this case was then improved tensile strength of PP-VC regions enabling high crack resistance to fiber-related failures like individual debonding and cluster debonding.

In order to provide solid proof of the hybrid toughening approach an important region of interest on the fracture surfaces of 20WC10VC was portrayed in Figure 21a. In this specific region, a single WC fiber fracture parallelly aligned to applied loading was captured (encircled in a yellow dotted circle). On the left-hand side, an example of a transversely fractured WC can be seen whereas on the right-hand side, a largely debonded WC fiber was observable. Most importantly, in this specific region, longitudinal PP/VC failure occurred at a relatively high-stress level causing crazing on the V-reinforced PP region surrounding the fiber fracture event (Figure 21b). This observation underlines the capability of reinforced PP/VC matrix in stress transfer during WC-related failure events.

## 3.6 Conclusions

Hybrid thermoplastic composites of waste cellulose and vermiculite have been effectively manufactured by high-shear thermokinetic mixing. Such a process was shown to create WC fiber clusters with heavily entangled randomly oriented WC fibers after 20 wt. % fiber loading. The presence of these clusters dominated the failure behavior of PPWC composites under tension and created a strength barrier due to enforced shear deformation, especially in 30WC. On the other hand, when WC content remained low (10 wt. %) the stiffness of PPWC composites remained limited.  When used along with WC fibers, results showed that VC platelets have trend into small platelets situated in between WC fibers while significantly increasing the thermal durability and crystallinity of PPWC composites. From a mechanical point of view, when used in the presence of high fiber content (20WC10VC) such platelets contributed significantly to tensile strength by making PP more brittle and allowing for an effective stress transfer during WC cluster debonding events. When used in the presence of low WC fiber content (10WC10VC) they mainly contributed to the stiffness of the samples and made it comparable to that of

30WC. In light of rheological measurements, it was also shown that such competitive hybrid composites also provide ease of processing when compared with WC-only composites.

# CHAPTER 4: Morphological adaptation of expanded vermiculite in polylactic acid and polypropylene matrices for superior thermoplastic composites

## 4.1 Abstract

The morphological transformation of expanded vermiculite (VC) during injection molding with brittle PLA and ductile PP polymers along with its positive and negative contribution to mechanical response is investigated. Polymer/VC mixtures with 30 wt. % VC are prepared by thermokinetic high shear mixing at 4000 rpm without any ex-situ exfoliation agents or compatibilizers. Obtained composite mixtures are then injection molded onto three-point bending and tensile test specimens. Performed mechanical tests suggested a significant increase in tensile (110 %) and flexural modulus (112%) of PP30VC samples. Presented fractographic and morphological investigations suggested that the root cause of measured improved tensile (36%) and bending strength (26%) of PP is the fibrillation of VC associated with PP/VC interactions under high shear. A similarly increasing trend for tensile (147 %) and bending modulus (137 %) was observed for PLA30VC samples. Contrary to PP30VC, a decreasing pattern was present in the case of tensile (-40%) and bending strength (-13 %) of PLA30VC. The root cause for such reduction is determined to be i) In-situ exfoliation of VC inside PLA matrix and transformation of VC into micron-sized platelets ii) Evaporation of trapped water/crystalline water in the interlayer region of VC which caused in-situ degradation of PLA during manufacturing.

## 4.2 Introduction

In recent years, various nanoscale reinforcing fillers inserted in polymers to create nanocomposites have been regarded as one of the most attractive study fields in both academic and commercial sectors. Clays, graphene, talc, and other nanofillers are examples of these materials [112]. Clays are employed in industrial, technical, and scientific applications as an affordable inorganic material [39].

Vermiculite represents a clay variety employed for enhancing the strength of polymers. It belongs to the mica-type layered silicates [97]. Vermiculite, a naturally occurring inorganic mineral with layered spacing, expands significantly upon high-temperature calcination, resulting in one of the world's lightest minerals—expanded vermiculite. Expanded vermiculite is a type of commercially available natural clay that has been used in thermoplastic matrices for various property improvements. With a layered structure and crystallization water between its layers, expanded vermiculite exhibits low density and thermal conductivity. Introducing polymer chains into its interlayer spaces enhances its properties, contributing to improved thermal stability, mechanical strength, and flame-retardant characteristics when integrated into polymer [113], [114].

The presence of an exceptionally large interlayer region containing crystalline water that loosely adheres to rather stiffer silicate layers [4], provides ease of ex-foliation down to well-structured 2D silicate platelets [115], [116]. This loose interlayer bonding enables for size reduction of VC down to micro -nano scale 2D silicate platelets [115], [116] by the means of intercalation [117] and exfoliation. [118] Adaptation of these 2D platelets to thermoplastic polymers through melt compounding can provide significant thermal [119] and mechanical [41], [120] property improvements to host polymers with relatively lower cost when compared to other 2D nanomaterials (i.e. graphene). A major point of attention hereby is the host polymer/organo-clay interactions which are mainly governed by polymer polarity. [121] The aim to achieve nano-scale dispersion also enforces the use of organoclays at relatively low weight fractions. [122] Another approach to obtain a homogeneous polymer/particle mixture is the implementation of compatibilizers or modification and use of adaptable polymer mixtures [117], [123], [124] or co-polymerization [125], [126] strategies. Even though previously proposed methodologies provided significant Young's modulus improvements 17.6% [45], 40.4% [126], 23.6%[3], 25.4% [127], tensile strength-wise, limited enhancements -10% [45], 3% [126], same[3], 8% [127] are reported. One fundamental reason for such a situation may be identified as the use of VC in the from platelets and in low volume fractions. Deriving from this point and implementing our previous experience on the efficiency of high shear thermokinetic mixing in melt compounding [128], [129], this short article aims to demonstrate morphological changes and associated mechanical property improvements that could be achieved by the integration of 30 wt. % expanded VC without any compatibilizers or any ex-situ clay modification strategies. Polylactic acid (PLA) was chosen as the polar host polymer whereas polypropylene (PP) was chosen as the non-polar host polymer. Polymeric composite samples were prepared by high shear thermokinetic mixing at 4000 RPM. Obtained PLA30VC and PP30VC samples are then cast into tensile and bending test specimens via injection molding. Thermogravimetric analysis along with the morphological investigations suggested that expanded VC went through in-situ exfoliation in PLA whereas it completely fibrillated in PP. Mechanical testing efforts suggested that in both cases a homogeneous distribution was obtained resulting in significant improvements in tensile (110%, 112%) and bending (147%, 137%) modulus values for PP and PLA respectively. Both bending and tensile strength of PLA30VC samples decreased, which is revealed to be water vapor/PLA interaction during high shear mixing. Contrarily, significant improvements in tensile (36%) and bending strength (26%) of PP30VC samples were measured due to VC fibrillation. In overall, the presented work forms a basis for the failure mechanisms associated with the changes in strength due to varying inclusion shapes and polymer types for VC reinforced polymeric composites.

Overall, the presented work forms an example study on the effect of chemistry driven polar/nonpolar matrix selection on the mechanical and rheological properties of PP and PLA composites containing VC. Moreover, the connection between process induced morphologic adaptation of VC to failure mechanisms associated with the changes in strength are revealed.

## 4.3 Materials and experimental

### 4.3.1 Materials

Vermiculite (Superfine Vermiculite) consisting of various particle sizes (The abundances based on the dimensions of vermiculite: size of 1.4 mm constitutes 46.3%, 1.0 mm represents 35%, 0.7 mm accounts for 12.5%, 0.5 mm makes up 4.3%, and smaller than 0.5 mm contributes to 1.9% of the total) was purchased from Serakulit, Canakkale, Turkey. The material data sheet indicates that vermiculite is composed of 39.2% $SiO_2$, 16.2% $Al_2O_3$, 15.4% MgO, 15.0% $Fe_2O_3$, 5.6% $K_2O$, 4.8% CaO, and minor quantities of various other compounds. An injection grade of PLA (Total Corbion, Luminy L130) with a melt flow rate of 23g/10min (210°C/2.16kg) was purchased from Kumru Kimya, Istanbul, Turkey. Homopolymer PP (Borealis HE125MO) with a melt flow rate of 12 g/10min (230°C/2.16kg) was purchased from Efa Kauçuk, Kocaeli, Turkey.

### 4.3.2 Processing and Sample Manufacturing

30 wt.% vermiculite containing PP and PLA were mixed by a custom-made thermokinetic mixer, Gelimat GI (Draiswerke). The high mixing speed of the thermokinetic mixer generates shear, allowing even incompatible materials to be processed homogeneously without the need for any external additives. Therefore, no compatibilizer has been used. All materials have been used as received.

Since there is no screw system in gelimat mixing, there is no need for a pre-drying process. With the help of the high shaft speed of the mixer, formulations were prepared in less than a minute. At around 4000 RPM, the temperature of the mixing chamber reaches 220$^{o}$ C and 240$^{o}$C for VC loaded PP and PLA, respectively. The composites, granulated with the help of a crusher, were prepared for injection molding. Neat PLA and PLA30VC were dehumidified at 60$^{o}$ C for 8 hours to remove moisture before the injection molding process. Test samples were molded by using an Xplore 12 mL micro-injection molding machine. (XPlore, Sittard, Holland) with a pressure of 12 bar to perform the reported mechanical tests.

## 4.4 Material Characterization

### 4.4.1 Thermogravimetric analysis

Thermal analyses were completed with TA Q 500 TGA by using Universal Analysis 2000 software. Analyzes were conducted at a heating rate of 20°C per minute from room temperature to 950°C under a nitrogen atmosphere for polymer and polymeric composite measurements and to 1500°C for vermiculite tests.

### 4.4.2 Mechanical Testing

Tensile and three-point bending tests were performed to obtain mechanical properties by using a 5982 Static Universal Test Machine in Sabancı University (UTM, Instron, Norwood, MA, USA) with a rate of 2.0mm/min and 5 kN load cell for ISO 527-2 and ISO 178 standards.

### 4.4.3 Electron Microscopy

Surface topography and composite morphologies were analyzed by using Leo Supra 35VP Field Emission Scanning Electron Microscope (FESEM, Carl Zeiss AG, Jena, Germany) followed by Au/Pd coating.

### 4.4.4 Rheology

Rheological analyses, frequency sweep, and viscosity sweep were conducted by MCR 702 TwinDrive Rheometer (Anton Paar, Graz, Austria). The complex viscosity of samples was measured under a constant shear strain of 10% at 1 Hz.

## 4.5 Results and discussions

### 4.5.1 Thermogravimetric Analysis

The mass loss percent versus temperature curve for purchased VC pellets is portrayed in Figure 22a. The initial temperature region for VC was observed between 100°C -150°C for 1.75 wt. % loss which belonged to moisture evaporation. A connected secondary event between 180°C -200°C corresponds to crystalline water in the interlayer region with a % weight loss of another 0.25wt%. It is vital to underline that this temperature range is in the same range as achieved manufacturing temperatures for PLA (240°C) and PP (220°C) during high shear mixing. The remaining decomposition events (500°C - 1400°C) in Figure 22a corresponded to hydroxyl groups present in the octahedral layer of VC that continued until only metal oxides remained.

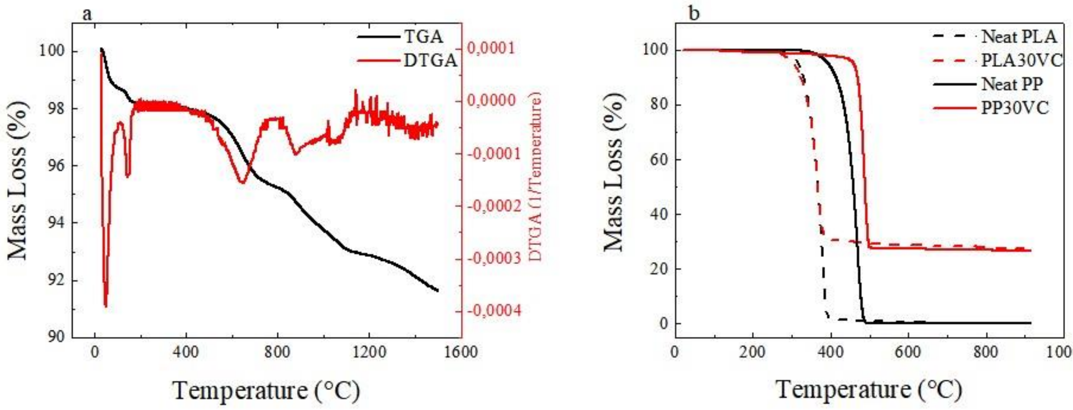

**Figure 22** TGA analysis performed on nitrogen environment to a) as purchased VC and b) neat and VC containing composites.

Thermogravimetric analysis performed on PP30VC and PLA30VC samples (Figure 22b) suggested that the onset temperature of decomposition ($T_{onset}$) has decreased from 264°C to 247°C for PLA30VC whereas it increased significantly from 318°C to 420°C for PP30VC case. This suggested that the presence of VC negatively affected the pristine molecular structure due to the effect of high-pressure water evaporation in hydrophilic PLA matrix during high shear mixing which will later be seen on fracture surfaces. An exact contrary situation was present in the case of a hydrophobic PP matrix where the presence of highly heat deflecting PP-VC fibrils significantly delayed molecular decomposition temperature onset and offset temperatures.

### 4.5.2 Constituent interactions in the absence of high shear

Constituent interactions were explored by i) determination of internal structure of expanded VC by heat application for potential particulate size ii) rotational rheometer temperature scan of neat polymers and polymeric composites to assess the melt viscosity which determines matrix/particulate wetting during manufacturing, iii) melt film casting experiments for morphological investigations. The following facts are reduced:

i) Considered expanded VC contains silicate layers with thicknesses varying from 40 microns (Figure 23a) to 100nm (Figure 23b) with inter-platelet porosities.

ii) With low melt viscosity (Figure 24a) and higher polarity PLA tends to fill interplatelet porosities (Figure 23c) and causes further platelet exfoliation. Surface interaction between resulting VC platelets and PLA is high (the yellow region in Figure 23d with polymer deformation due to interfacial tension). Positive interaction may be due to the presence of carbonyl groups available in PLA. [130]

iii) With high melt viscosity (Figure 24a) and low polarity PP tends to bind VC platelets (Figure 23e) with no signs of in-situ exfoliation. Smaller VC platelets can align with the PP matrix even under significantly low shear exerted on samples during film casting (Figure 23f).

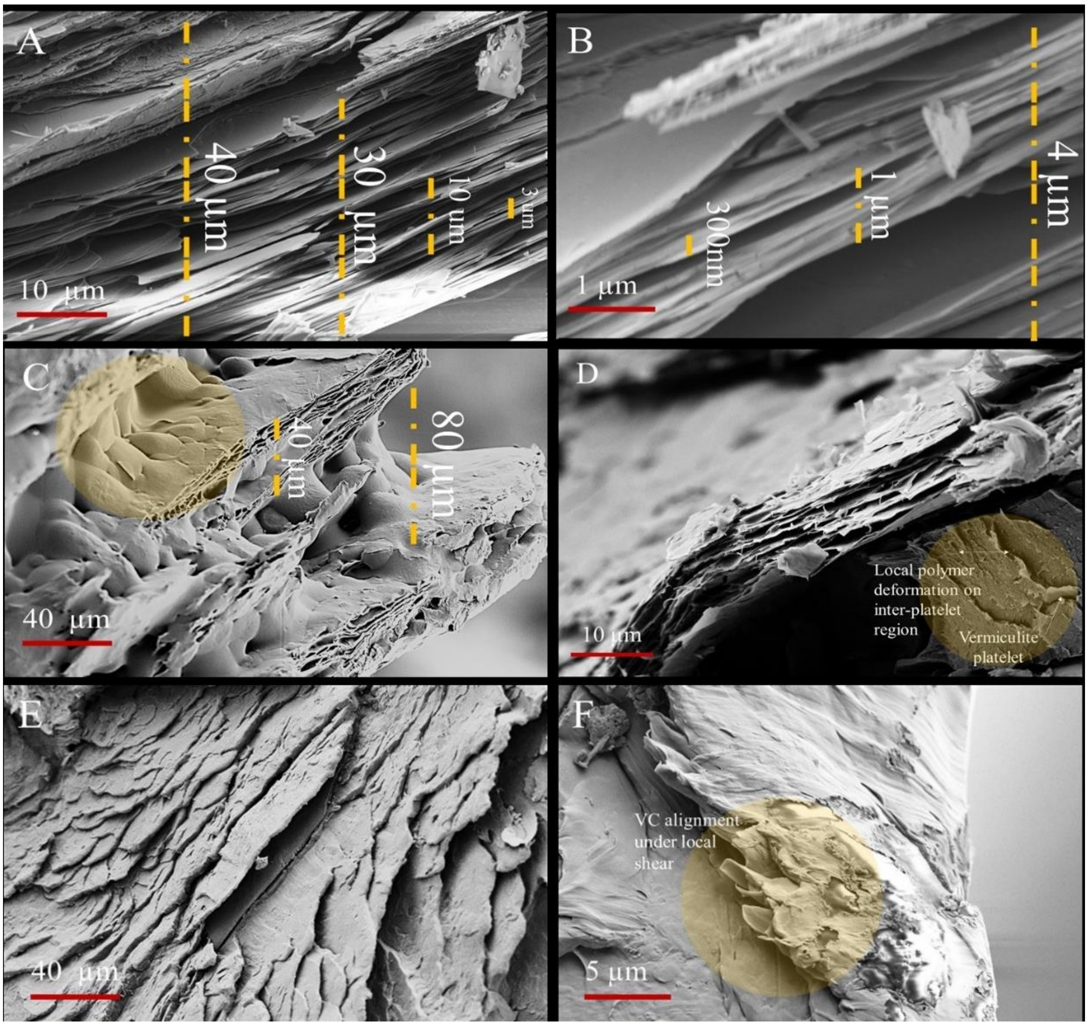

**Figure 23** a) A cross-sectional view from heat treated (1100°C) expanded VC b) A zoomed in cross-sectional view with nanometric VC layers c) Several VC layers wetted with PLA (yellow region showing the favorable PLA/VC interaction) d) A smaller VC platelet and PLA e) A view from PP/VC films. f) A closer view of PP/VC films with local VC rotation/alignment under shear due to film casting

### 3.3 Mechanical testing and fractography

Stress-strain curves obtained from tensile testing of neat polymer and VC composites are portrayed in Figure 24b and tensile fracture surfaces of tested samples are shown in Figure 25 a-b and Figure 25c-d-e respectively for PLA30VC and PP30VC cases. As a host polymer PLA portrayed a linear elastic behavior with a brittle fracture with $\sigma_{ult}$ =66.9 (±0.1) MPa (Table 13). When reinforced with homogeneously dispersed partially exfoliated VC platelets (Figure 24a), a steeper elastic region (increase in $E_{tens}$) with a lower tensile strength (58.0 (±0.2) MPa) was observed suggesting a pre-mature failure of composite samples.

**Table 13** Tensile test results of PLA, PP, and their VC-composites

| **Name** | **$E_{tens}$ (MPa)** | **Improvement %** | ***$\sigma_{yield}$ (MPa)** | **Improvement %** | **$\varepsilon_{yield}$ (%)** |
|---|---|---|---|---|---|
| **Neat PP** | 1880 (±51) | | 28.2 (±6.8) | | 3.6 (± 0.3) |
| **PP30VC** | 3957 (±158) | 110 | 38.4 (±0.1) | 36 | 2.1 (±0.2) |
| **Neat PLA** | 3236 (±30) | | 66.9 (±0.1) | | 2.5(±0.0) |
| **PLA30VC** | 8008 (±531) | 147 | 58.0 (±0.2) | -13 | 1.1 (±0.1) |

*$\sigma_{yield} = \sigma_{ult}$ for PLA and PLA30VC samples.

**Table 14** Flexural test results of PLA, PP, and their VC-composites

| **Name** | **$\sigma_{flex}$ (MPa)** | **Improvement %** | **$E_{flex}$ (MPa)** | **Improvement %** |
|---|---|---|---|---|
| **Neat PP** | 46.9 (±0.5) | | 1690 (±28) | |
| **PP30VC** | 59.3 (±2.2) | 26 | 3580 (±120) | 112 |
| **Neat PLA** | 105 (±7.7) | | 3230 (±65) | |
| **PLA30VC** | 64.0 (±8.2) | -39 | 7680 (±152) | 138 |

A closer view of a 5 micrometers thick multi-layered VC platelet is presented in Figure 25b where the surrounding porous structure of PLA that was not present in previously discussed film casting experiments is visible. The porous microstructure is hence attributed to water evaporation event during in-situ VC exfoliation and resulting partial dissolution of PLA matrix that caused the pre-mature failure. The same phenomena caused a more drastic drop (Figure 24c) in the flexural strength ($\sigma_{flex}$) of PLA30VC (64.0 (±8.2) MPa) when compared with the neat PLA samples (105 (±7.7) MPa).

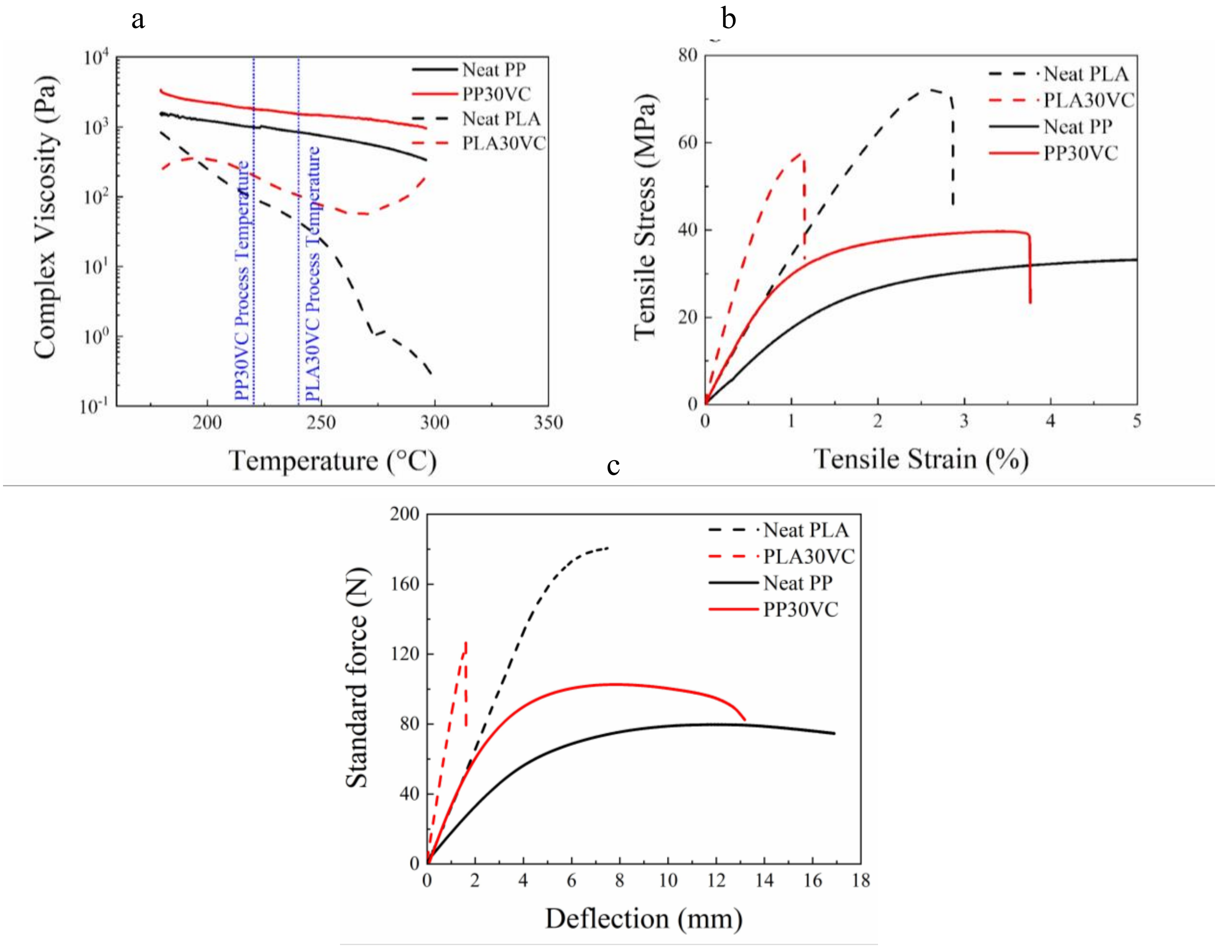

**Figure 24** a) Complex viscosity vs. temperature measurements at constant angular velocity b) Tensile stress-strain curves and c) Force–deflection curves of bending test

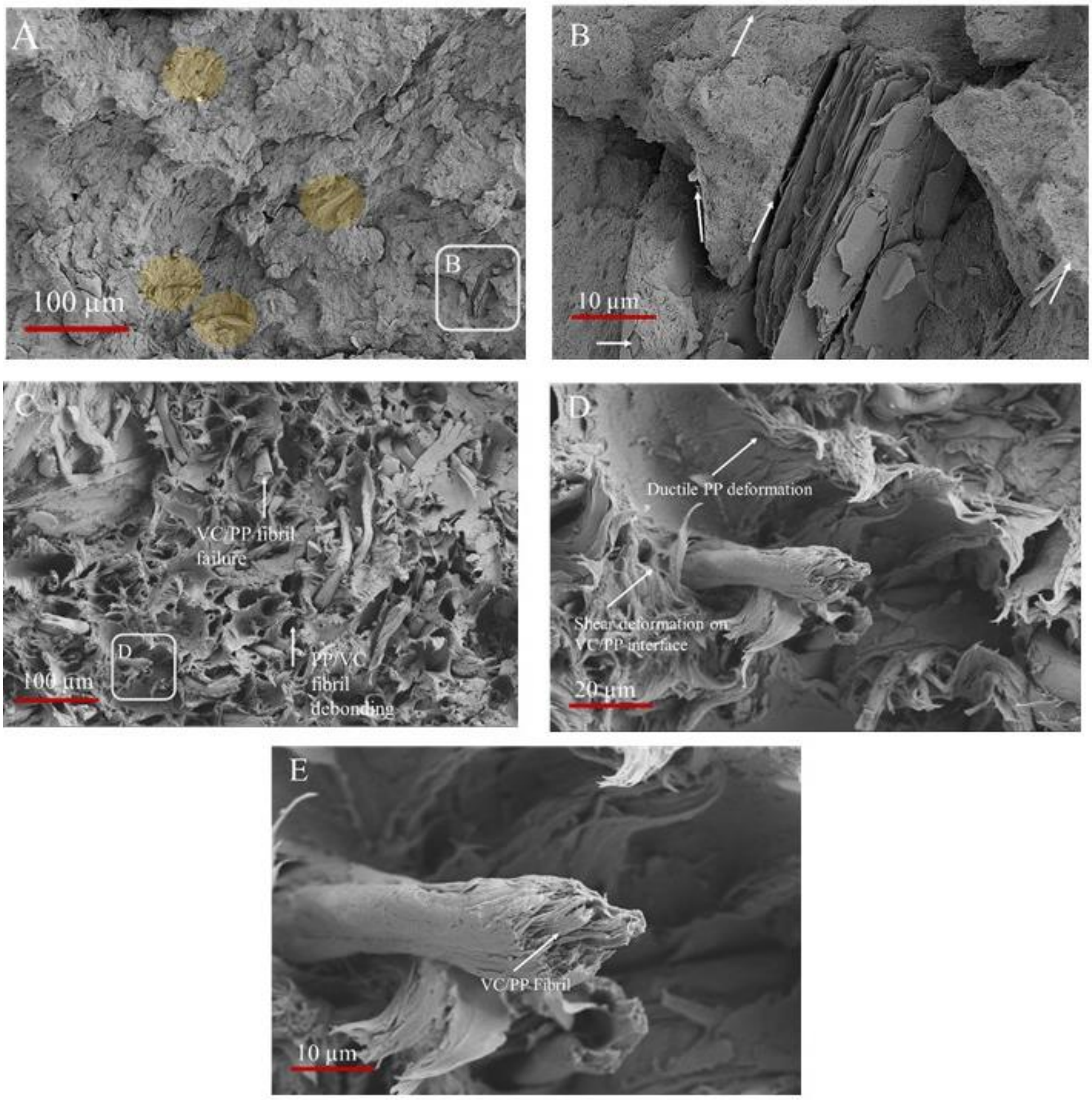

**Figure 25** a) Tensile fracture surface of PLA30VC with brittle fracture (yellow regions indicate dispersed VC platelets) b) A single partially exfoliated VC platelet inside porous PLA matrix (arrows indicate interplatelet placement of PLA c)Tensile fracture fracture surface of PP30VC with ductile polymer deformation and PP/VC fracture/debonding regions d) A zoomed in view of a single PP/VC fibril with polymer shear deformation e)A single PP/VC (diameter ~10 microns) fibril with layered micro-structure

The closeness of $\sigma_{yield}$ and $\sigma_{flex}$ values of PLA30VC samples suggested a tensile failure of samples during bending loading.

Contrary to PLA, the PP matrix was rather ductile with a well-defined yield point (28.2 (±6.8) MPa) followed by a chain elongation region up to strain values of 560% (this region is not portrayed in Figure 24b. Increases of up to 110% in $E_{tens}$ and 112% in $E_{flex}$

values are recorded for PP30VC when compared with neat PP samples. Most importantly, this increase in stiffness did not subsequently result in a decrease but rather an increase of up to 36% in $\sigma_{yield}$ and 26% in $\sigma_{flex}$ characteristics. A major point of attention was the ability of PP30VC samples to strain-harden during tensile testing. Along with morphological investigations (Figure 23e and Figure 23f), this situation suggested that VC fibrils portrayed in Figure 25c-d-e were composite fibrils consisting of aligned VC particulates with PP holding/binding them together. Fracture surface analysis also suggested that PP/VC composite fibril failure and fibril/matrix debonding events were the ultimate cause of failure at the end of plastic deformation (Figure 25c-d).

## 4.6 Conclusions

Composites with exceptional thermal stability and mechanical strength, capable of processing without the need for any compatibilizers, form the cornerstone of our findings. The thermogravimetric analysis of PP30VC and PLA30VC samples indicated a decrease in decomposition onset temperature for PLA30VC and a significant increase for PP30VC. The presence of VC negatively affected the molecular structure in the hydrophilic PLA matrix, while in the hydrophobic PP matrix, VC fibrils delayed molecular decomposition temperatures. When processed under high shear mixing (4000RPM) and in the absence of any compatibilizers, polar and less viscous PLA matrix tend to exfoliate already multi-layered VC platelets. Whereas nonpolar and more viscous PP matrices tend to bind those layers. Upon high shear mixing where processing temperatures reach up to water evaporation and crystalline water decomposition temperatures (200°C-240°C), exfoliation in PLA further intensifies and the resulting PLA30VC composite is platelet reinforced brittle composite with significantly high tensile (~8GPa) and bending stiffness :(~7.5GPa). This in situ exfoliation assisted with water evaporation degrades the PLA matrix by reducing its strength. On the other hand, high shear mixing transforms individual VC platelets to VC/PP composite fibrils. The resulting PP30VC composite is then a short fiber reinforced ductile composite with improved strength, stiffness, and resistance to degradation.

# CHAPTER 5: General Conclusions

The demand for polymer-based materials with enhanced performance and environmental compatibility has prompted researchers to pursue more sustainable and eco-friendly composite material designs. The fundamental approach in such designs is the incorporation of natural or recyclable material types that facilitate a more sustainable product lifecycle while offering comparable material performance to conventional alternatives. Meeting these demands necessitates a rigorous material selection process that prioritizes enhanced component interactions and effective manufacturing strategies. The application of these processes allows the discovery of new reinforcements adaptable to traditional thermoplastic polymers. The primary objective of this thesis is to present the results of a composite hybridization effort in which multiple reinforcement phases were incorporated into a biodegradable (PLA) and recyclable (PP) polymer matrix. The reinforcement types considered were cellulose fibers (WC), a textile industry waste, and expanded vermiculite (VC), a naturally abundant clay. The rationale behind the choice of reinforcement was based on the fibrous morphology of WC and the layered morphology of VC. The objective was to investigate the synergistic effect of these reinforcement types with two different properties when produced by high shear thermodynamic mixing and injection molding. This thesis reveals the constitutive interactions between WC/VC and the host matrices, resulting in improved mechanical response and ease of processing. The principal materials and findings of this thesis are presented in summary form in Figure 26.

## Integration of Waste cellulose and Vermiculite in polymer matrices

### WC and VC in Bio-polymer Matrix

- The production of bio-based composites via valorization of textile waste and eco-friendly clay.
- Achieve superior characteristics for hybrid case (127 % and 137 % increase for $E_{flex}$ and $E_{Youngs}$ respectively).
- 68 % increase in conductivity for PLA30VC.
- WC is responsible for debonding events that cause strength reduction, while VC generates brittle fractures.
- In the synergistic composition of PLA7.5VC22.5WC (highest strength), no de-bonding and no in-situ failure.
- In this particular composite, VC platelets introducing transverse cracking in the PLA matrix are observed t intensify with the debonding of the main filler (WC).
- PLA30WC lead to enormous improvements such as 141% of storage modulus for the rubbery state.

### WC and VC in Petroleum Matrix

- This study comprises the preparation of hybrid composites of PP via the incorporation of waste cellulose (WC) and vermiculite (V) as natural reinforcing agents
- With a hybrid approach, producing hybrid PP composites that are manufacturable by injection molding more crystallization, and better resistance against shear deformation during failure without suffering fro inherent fiber entanglement causing insufficient polymer/fiber wetting.
- the presence of high fiber content such platelets contributed significantly to tensile strength by making I more brittle and allowing for an effective stress transfer during WC cluster debonding events. . The enhancements in the PP hybrid composite were 118% for Young's modulus and 115% for flexural modulus. Furthermore, the strength of PP was increased by the hybridization of WC and VC. The flexura strength and tensile strength exhibited increases of up to 42% and 56%, respectively
- When used in the presence of low WC fiber content (10WC10VC) they mainly contributed to the stiffness of the samples and made it comparable to that of 30WC

### VC in both Bio-based and Petroleum Matrices

- The presence of VC negatively affected the molecular structure in the hydrophilic PLA matrix
- In the hydrophobic PP matrix, VC fibrils delayed molecular decomposition temperatures
- Polar and less viscous PLA matrix tend to exfoliate already multi-layered VC platelets. Whereas nonpolar and more viscous PP matrices tend to bind those layers.
- PLA30VC composite is platelet reinforced brittle composite with significantly high tensile (8 GPa) and bending stiffness: (7.5 GPa).

**Figure 26** Findings of the study

In the initial chapter, the study is introduced and motivated. In the subsequent chapter, a hybridization technique is employed, whereby vermiculite and waste cellulose fibers are incorporated into a bio-based PLA. This approach was intended to create eco-friendly composites with enhanced properties, including better thermal conductivity, improved processability, and increased mechanical strength. Composite samples containing waste cellulose fibers (WC) with an average diameter of 15 micrometers and vermiculite platelets (VC) with an average size of 1.4 millimeters were targeted. In this context, hybrid green composites of PLA were developed by incorporating waste cellulose (WC) and vermiculite (VC) as natural reinforcing agents at varying levels. The use of high shear mixing at 5000 rpm was a key innovation, allowing PLA, cellulose, and vermiculite to be processed without any modifications or compatibilizers. The PLA/WC and PLA/WC-VC blends were created to produce fully biobased and durable polymer compounds with enhanced mechanical and thermal properties. The results indicated that a combination of 7.5 wt.% vermiculite and 22.5 wt.% waste cellulose yielded the best mechanical performance. Compared to earlier research on cellulose-based PLA composites, this study found that the improvements in Young's modulus for the hybrid formulation were substantially higher (137%) without a notable loss in strength, which surpasses the results reported in similar studies in the literature. Generally, WC fillers cause de-bonding events that reduce strength, while VC fillers lead to brittle fractures. However, in the hybrid filler strategy, synergistic formulation shows the highest tensile strength. In this specific composite, VC platelets induce transverse cracking in the PLA matrix, which is intensified by the debonding of the primary filler, WC. Overall, combining waste cellulose and vermiculite together in a PLA matrix creates promising a stronger, more easily processable, and thermally conductive yet stable superior biopolymers that serve as an eco-friendly alternative to petroleum-based polymers due to their superior mechanical properties.

The third chapter focused on preparing hybrid PP composites by incorporating waste cellulose and vermiculite as natural reinforcing agents at various loading levels, aiming to create mechanically superior, easily processable hybrid green composite materials. Discontinuous fiber reinforcements were found to be less effective due to fiber entanglement, which compromised mechanical performance. However, using a hybrid approach, it was possible to manufacture hybrid PP composites suitable for injection molding. These composites exhibited increased crystallization and improved resistance to shear deformation during failure, without experiencing the fiber entanglement issues that lead to inadequate polymer/fiber wetting.

In the fourth chapter, the behavior of VC clay when incorporated solely to two different polymer matrices has been investigated. For this purpose, both bio-based PLA and petroleum-based PP were chosen. New composites were fabricated by incorporating 30% vermiculite into these two distinct matrices. These composites, along with the neat polymers, were subjected to thorough analysis in terms of their thermal, mechanical, rheological, and morphological properties. The results of mechanical testing indicated that the tensile modulus (110%) and flexural modulus (112%) of 30 wt% reinforced PP composite had significantly increased. According to the morphological and fractographic studies, VC-PP fibrillation related to PP/VC interactions under high shear is the primary reason for the observed increased tensile (36%) and bending strength (26%) of PP. For 30 wt.% VC reinforced PLA samples, a similar increase was noted for tensile (147%) and bending modulus (137%). In contrast to PP30VC, PLA30VC exhibited a declining pattern in both tensile (about 40%) and bending strength (about 13%). The primary reasons for this decrease have been shown to be the in-situ exfoliation of VC within the PLA matrix, resulting in the transformation of VC into micrometer-sized platelets, and the evaporation of trapped water or crystalline water in the VC interlayer region, leading to the in-situ degradation of PLA during the manufacturing process.

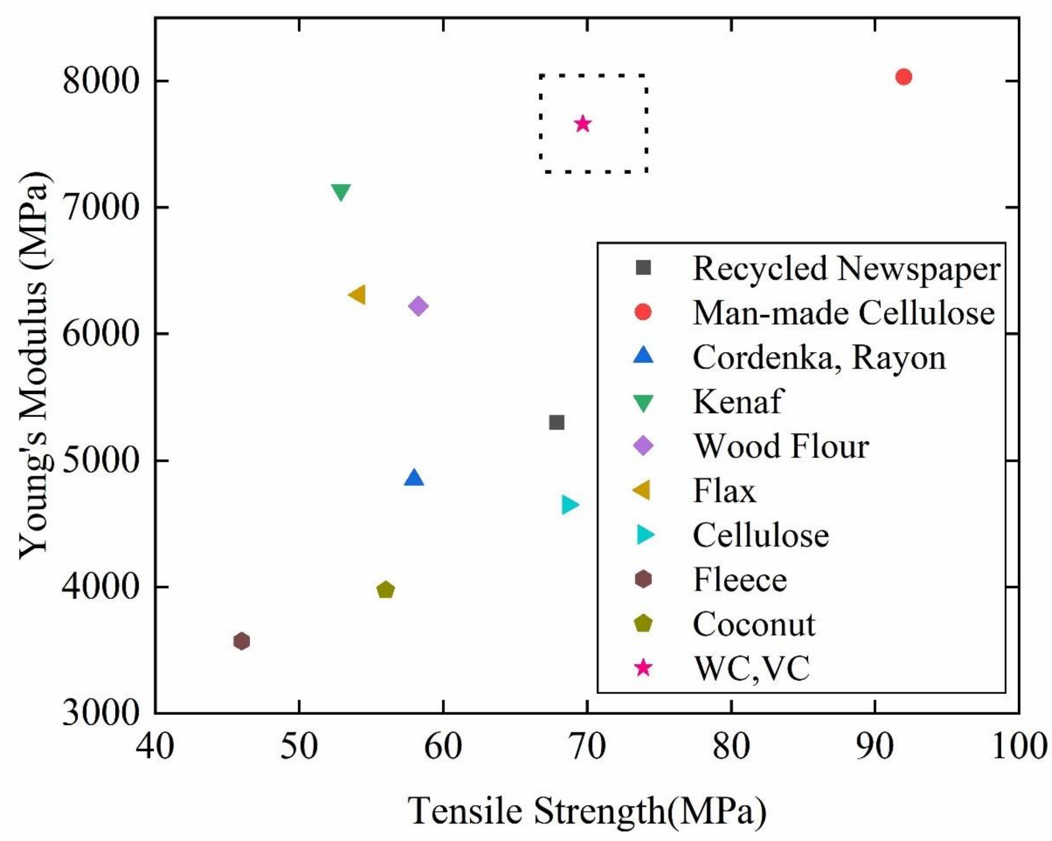

**Figure 27** Comparison of 30 % natural fiber loaded PLA composites considering Young’s modulus and tensile strength

The tensile strength and Young's modulus of PLA composites with 30% natural fiber additives are presented in Figure 27. When the results are compared with the hybrid formula (22.5WC_7.5VC), it is observed that the composite produced makes a significant difference in both tensile strength and Young's modulus compared to many studies in the literature. Furthermore, the majority of the values reported in the literature research contain compatibilizers, which is contrary to the thesis study. In this context, state of the art compounds include recycled newspapers[131], man-made cellulose[132], cordenka-rayon [133], kenaf fiber [94], wood flour[134], flax fiber [133], cellulose [135], fleece [136], and coconut fiber [136] reinforcements.

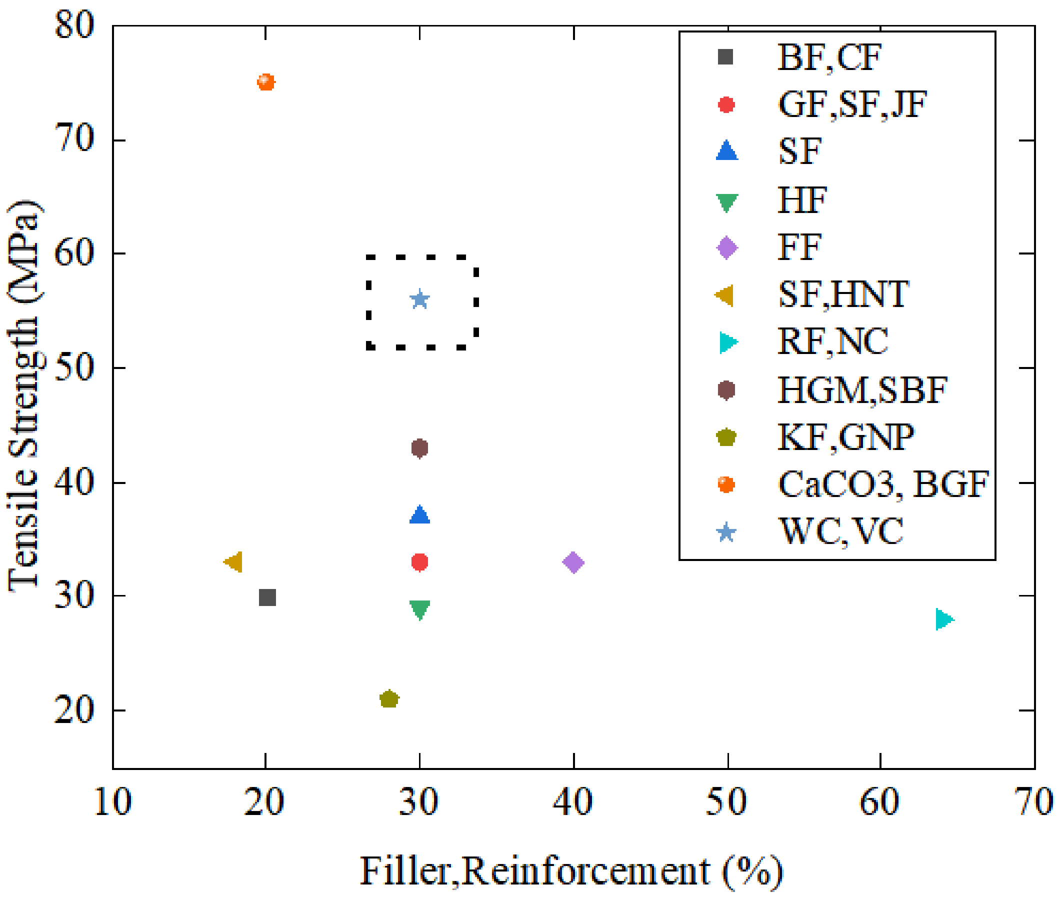

**Figure 28** Comparison of PP-fiber and PP-hybrid composites

Figure 28 presents a compilation of studies that have employed both fiber addition to PP and hybrid reinforcements. In the case of PP hybrid reinforcement, a significant increase in strength was reported (20WC_10VC), and thus, only tensile strength was interpreted in response to loading rate. It is noteworthy that the MAPP compatibilizer was utilized in numerous instances across these literature research results. Nevertheless, it was observed that the PP hybrid exhibited superior tensile strength values compared to numerous studies at both low and high additive ratios. In this context, state of the art compounds include banana fiber-coconut fiber [137] ,glass fiber-sisal fiber-jute fiber [138], sisal fiber [139],hemp fiber [140], flax fiber [141], sisal-HNT[142], reed flour-nano clay [143], hallow glass microspheres-bamboo fiber [144], exfoliated graphene nanoplate-kenaf fiber [145], bagasse fiber-$CaCO_3$ [146] reinforcement and mostly with addition of compatibilizer.

**Table 15** Cost Analysis

| Raw Material | €/kg | Compound | €/kg | Cost Down (%) | €/tons |
|---|---|---|---|---|---|
| **PLA** | 4.50 | **22.5WC-7.5VC** | 3.19 | 29 | 3190.00 |
| **PP** | 1.20 | **20WC-10VC** | 0.89 | 35 | 890.00 |

VC:0,5 €/kg

Furthermore, a rough cost analysis shows that hybrid formulations offer cost advantages. This analysis excludes transportation, compounding, and the price difference that would arise from the purchase of high tonnages. As shared in Table 15, PLA hybrid provides a cost advantage of 1170 €/ton while PP hybrid provides an advantage of 120 €/ton.

The final section of the study identifies promising avenues for further research on two types of composites: PLA and PP hybrids, which are reinforced with waste cellulosic fiber and vermiculite. Both materials exhibit considerable potential for a wide range of applications but require further investigation to fully realize their potential.

The promising results of the PLA-hybrid study indicate that further investigations could unlock the full potential of these bio-based composites. Firstly, investigating the printability of the developed hybrid composites using 3D printing techniques could open doors for complex and customized designs. It is possible that this printability would allow for the creation of intricate structures not achievable with traditional methods. Secondly, assessing water absorption and biodegradability is crucial for verifying their "green" credentials. Furthermore, investigating their potential for applications such as acoustic insulation and electromagnetic interference shielding can expand their range of uses. Finally, a life cycle assessment will provide valuable information on the environmental impact of the entire production process, allowing further optimization towards sustainability. By studying these areas, hybrid reinforcement strategies can be developed, thereby unlocking the full potential of these bio-based composites for diverse and environmentally friendly applications.

The use of waste cellulose (WC) fibers and expanded vermiculite (VC) to develop polypropylene (PP) composites presents a multitude of promising avenues for future research. One crucial area of investigation pertains to the optimization of WC/VC ratios. Current research indicates the existence of a strength threshold due to WC entanglement.

Future research could explore the fine-tuning of these ratios to achieve an optimal balance between stiffness and strength. This could entail the utilization of finer WC fibers or the modification of the surface treatment of the WC to enhance adhesion with the PP matrix. In addition to the optimization of the material itself, future research could investigate promising applications for these improved composites. Their stiffer and potentially more durable nature renders them suitable candidates for construction materials such as panels or pipes. The automotive industry could also benefit from these lightweight composites for car parts that require good stiffness. However, current research is primarily focused on the initial properties. Future research should investigate the long-term durability of these composites, examining their performance over time under various environmental conditions. Additionally, the research is likely to involve small-scale production. Future work could investigate how production processes can be scaled up for commercial applications.

Although the existing research provides valuable insights, further investigation is required to gain a comprehensive understanding of the interaction between VC and diverse polymer types, such as PLA and PP. Future research could examine the impact of varying VC content on mechanical properties and morphology. This could entail an investigation of the effects of varying VC loadings (higher or lower) on the properties and morphology of the composites. It would be beneficial to investigate alternative processing methods and compatibilizers in order to optimize the interaction between VC, and the polymers. This could entail investigating alternative mixing techniques, injection molding parameters, or the use of compatibilizers to enhance the adhesion and dispersion of VC particles. The impact of VC morphology on each polymer could be isolated to gain a deeper understanding of the underlying mechanisms. This could entail differentiating the impact of fibrillation (PP) and exfoliation (PLA) on the characteristics of the composites. To gain a more comprehensive understanding of the composites' performance, it would be beneficial to conduct tests on other mechanical properties, beyond tensile and flexural strength. This could include evaluating impact strength, thermal stability, and other relevant properties. To bridge the gap between fundamental research and practical utilization, it would be advantageous to evaluate the composites in real-world applications and assess their long-term performance under various conditions. This could involve testing the composites in relevant applications and assessing their durability under different environmental conditions.

## REFERENCES

[1] M. Kalkancı, ‘VERMICULITE FILLED POLYMER COMPOSITES’, in *Theory and Research in Engineering II* , vol. 1, 2020, pp. 125–144.

[2] M. Valkov and G. Simha, ‘Vermiculite: Structural Properties and Examples of the Use’, *Clay Miner. Nat. - Their Charact. Modif. Appl.*, Sep. 2012, doi: 10.5772/51237.

[3] R. B. L. Hanken *et al.*, ‘Effect of natural and expanded vermiculite clays on the properties of eco-friendly biopolyethylene-vermiculite clay biocomposites’, *Compos. Part B Eng.*, vol. 175, Oct. 2019, doi: 10.1016/J.COMPOSITESB.2019.107184.

[4] A. Wang and W. Wang, *Vermiculite nanomaterials: Structure, properties, and potential applications*. Elsevier Inc., 2019.

[5] L. P. Ogorodova, I. A. Kiseleva, L. V. Melchakova, M. F. Vigasina, and N. V. Vladykin, ‘Calorimetric measurement of the enthalpy of formation, dehydration, and dehydroxylation of vermiculite’, *Geochemistry Int.*, vol. 50, no. 10, pp. 878–883, 2012, doi: 10.1134/S001670291208006X.

[6] S. C. Tjong, Y. Z. Meng, and A. S. Hay, ‘Novel Preparation and Properties of Polypropylene-Vermiculite Nanocomposites’, 2002, doi: 10.1021/cm010061b.

[7] A. Awal, M. Rana, and M. Sain, ‘Thermorheological and mechanical properties of cellulose reinforced PLA bio-composites’, *Mech. Mater.*, vol. 80, no. Part A, pp. 87–95, Jan. 2015, doi: 10.1016/J.MECHMAT.2014.09.009.

[8] A. Abdulkhani, J. Hosseinzadeh, S. Dadashi, and M. Mousavi, ‘A study of morphological, thermal, mechanical and barrier properties of pla based biocomposites prepared with micro and nano sized cellulosic fibers’, *Cellul. Chem. Technol.*, vol. 49, no. 7–8, pp. 597–605, 2015.

[9] M. K. Bakri, A. Omoregie, and M. R. Rahman, ‘Environmental Sustainability of Biopolymers’, *Acad. Lett.*, no. August, 2021, doi: 10.20935/al2924.

[10] R. Balart, N. Montanes, F. Dominici, T. Boronat, and S. Torres-Giner, ‘Environmentally friendly polymers and polymer composites’, *Materials*

*(Basel).*, vol. 13, no. 21, pp. 1–6, 2020, doi: 10.3390/ma13214892.

[11] M. Zubair and A. Ullah, *Biopolymers in environmental applications*. Elsevier Inc., 2021.

[12] K. K. Sadasivuni, P. Saha, J. Adhikari, K. Deshmukh, M. B. Ahamed, and J. J. Cabibihan, ‘Recent advances in mechanical properties of biopolymer composites: a review’, *Polym. Compos.*, vol. 41, no. 1, pp. 32–59, 2020, doi: 10.1002/pc.25356.

[13] K. M. Zia, N. Akram, S. Tabasum, A. Noreen, and M. U. Akbar, ‘Future trends in the bio-based polymer processing industry’, *Process. Technol. Bio-Based Polym.*, pp. 267–279, 2021, doi: 10.1016/b978-0-323-85772-7.00001-x.

[14] R. Scaffaro, E. F. Gulino, M. C. Citarrella, and A. Maio, ‘Green Composites Based on Hedysarum coronarium with Outstanding FDM Printability and Mechanical Performance’, *Polymers (Basel).*, vol. 14, no. 6, 2022, doi: 10.3390/polym14061198.

[15] R. Scaffaro, M. C. Citarrella, and M. Morreale, ‘Green Composites Based on Mater-Bi&reg; and Solanum lycopersicum Plant Waste for 3D Printing Applications’, *Polymers (Basel).*, vol. 15, no. 2, 2023, doi: 10.3390/polym15020325.

[16] Y.-L. Cheng *et al.*, ‘We are IntechOpen , the world ’ s leading publisher of Open Access books Built by scientists , for scientists TOP 1 %’, *Intech*, vol. 11, no. tourism, p. 13, 2016, [Online]. Available: https://www.intechopen.com/books/advanced-biometric-technologies/liveness-detection-in-biometrics.

[17] J. P. Greene, ‘Bio-Based and Biodegradable Plastics’, *Automot. Plast. Compos.*, pp. 149–174, Jan. 2021, doi: 10.1016/B978-0-12-818008-2.00020-9.

[18] M. Asgher, S. A. Qamar, M. Bilal, and H. M. N. Iqbal, ‘Bio-based active food packaging materials: Sustainable alternative to conventional petrochemical-based packaging materials’, *Food Res. Int.*, vol. 137, no. August, 2020, doi: 10.1016/j.foodres.2020.109625.

[19] R. A. Ilyas *et al.*, *Properties and Characterization of PLA, PHA, and Other Types of Biopolymer Composites*. Elsevier Inc., 2020.

[20] A. Meraldo, *Introduction to Bio-Based Polymers*. Elsevier Inc., 2016.

[21] P. A. Kothavade and K. Shanmuganathan, ‘Mechanical Properties of

PLA/Nanocellulose Composites', *Polylactic Acid-Based Nanocellulose Cellul. Compos.*, no. January, pp. 181–206, 2022, doi: 10.1201/9781003160458-9.

[22] M. Murariu and P. Dubois, 'PLA composites: From production to properties', *Adv. Drug Deliv. Rev.*, vol. 107, pp. 17–46, 2016, doi: 10.1016/j.addr.2016.04.003.

[23] K. Hashima, S. Nishitsuji, and T. Inoue, 'Structure-properties of super-tough PLA alloy with excellent heat resistance', *Polymer (Guildf).*, vol. 51, no. 17, pp. 3934–3939, 2010, doi: 10.1016/j.polymer.2010.06.045.

[24] Y. Gao, O. T. Picot, E. Bilotti, and T. Peijs, 'Influence of filler size on the properties of poly(lactic acid) (PLA)/graphene nanoplatelet (GNP) nanocomposites', *Eur. Polym. J.*, vol. 86, pp. 117–131, Jan. 2017, doi: 10.1016/J.EURPOLYMJ.2016.10.045.

[25] S. Farah, D. G. Anderson, and R. Langer, 'Physical and mechanical properties of PLA, and their functions in widespread applications — A comprehensive review', *Adv. Drug Deliv. Rev.*, vol. 107, pp. 367–392, 2016, doi: 10.1016/j.addr.2016.06.012.

[26] S. Hazer and A. Aytac, 'The influence of various/different ratios synthetic fiber mixture on the mechanical, thermal, morphological and flammability properties of poly (lactic acid)/polycarbonate blend', *J. Compos. Mater.*, vol. 55, no. 8, pp. 1027–1038, 2021, doi: 10.1177/0021998320963533.

[27] T. Klaser, L. Balen, Ž. Skoko, L. Pavić, and A. Šantić, 'Polylactic Acid–Glass Fiber Composites: Structural, Thermal, and Electrical Properties', *Polymers (Basel).*, vol. 14, no. 19, Oct. 2022, doi: 10.3390/POLYM14194012.

[28] M. Ferdinánd, R. Várdai, J. Móczó, and B. Pukánszky, 'Poly(lactic acid) reinforced with synthetic polymer fibers: interactions, structure and properties', *Compos. Part A Appl. Sci. Manuf.*, vol. 164, no. October 2022, 2023, doi: 10.1016/j.compositesa.2022.107318.

[29] X. Zhao *et al.*, 'High-Strength Polylactic Acid (PLA) Biocomposites Reinforced by Epoxy-Modified Pine Fibers', *ACS Sustain. Chem. Eng.*, vol. 8, no. 35, pp. 13236–13247, 2020, doi: 10.1021/acssuschemeng.0c03463.

[30] K. Oksman, M. Skrifvars, and J. F. Selin, 'Natural fibres as reinforcement in polylactic acid (PLA) composites', *Compos. Sci. Technol.*, vol. 63, no. 9, pp. 1317–1324, 2003, doi: 10.1016/S0266-3538(03)00103-9.

[31] A. A. Yussuf, I. Massoumi, and A. Hassan, ‘Comparison of polylactic Acid/Kenaf and polylactic Acid/Rise husk composites: The influence of the natural fibers on the mechanical, thermal and biodegradability properties’, *J. Polym. Environ.*, vol. 18, no. 3, pp. 422–429, 2010, doi: 10.1007/s10924-010-0185-0.

[32] R. Scaffaro, A. Maio, E. F. Gulino, and G. Pitarresi, ‘Lignocellulosic fillers and graphene nanoplatelets as hybrid reinforcement for polylactic acid: Effect on mechanical properties and degradability’, *Compos. Sci. Technol.*, vol. 190, no. November 2019, p. 108008, 2020, doi: 10.1016/j.compscitech.2020.108008.

[33] S. Venkatarajan and A. Athijayamani, ‘An overview on natural cellulose fiber reinforced polymer composites’, *Mater. Today Proc.*, vol. 37, no. Part 2, pp. 3620–3624, 2020, doi: 10.1016/j.matpr.2020.09.773.

[34] S. Venkatarajan, C. Subbu, A. Athijayamani, and R. Muthuraja, ‘Mechanical properties of natural cellulose fibers reinforced polymer composites - 2015-2020: A review’, *Mater. Today Proc.*, vol. 47, pp. 1017–1024, 2021, doi: 10.1016/j.matpr.2021.05.547.

[35] A. Wattanakornsiri and S. Tongnunui, ‘Sustainable green composites of thermoplastic starch and cellulose fibers’, *Songklanakarin J. Sci. Technol.*, vol. 36, no. 2, pp. 149–161, 2014.

[36] F. Yetiş, X. Liu, W. W. Sampson, and R. H. Gong, ‘Acetylation of lignin containing microfibrillated cellulose and its reinforcing effect for polylactic acid’, *Eur. Polym. J.*, vol. 134, p. 109803, 2020, doi: https://doi.org/10.1016/j.eurpolymj.2020.109803.

[37] D. A. Ertek, N. O. Sanli, Y. Z. Menceloglu, and S. Avaz Seven, ‘Environmentally friendly, antibacterial materials from recycled keratin incorporated electrospun PLA films with tunable properties’, *Eur. Polym. J.*, vol. 185, no. October 2022, p. 111804, 2023, doi: 10.1016/j.eurpolymj.2022.111804.

[38] O. Oguz, N. Candau, M. K. Citak, F. N. Cetin, S. Avaz Seven, and Y. Z. Menceloglu, ‘A Sustainable Approach to Produce Stiff, Super-Tough, and Heat-Resistant Poly(lactic acid)-Based Green Materials’, *ACS Sustain. Chem. Eng.*, vol. 7, no. 8, pp. 7869–7877, 2019, doi: 10.1021/acssuschemeng.9b00319.

[39] M. Kotal and A. K. Bhowmick, ‘Polymer nanocomposites from modified clays: Recent advances and challenges’, *Prog. Polym. Sci.*, vol. 51, pp. 127–187, 2015,

doi: 10.1016/j.progpolymsci.2015.10.001.

[40] R. U. Rao, B. Venkatanarayana, and K. N. S. Suman, ‘Enhancement of mechanical properties of PLA/PCL (80/20) blend by reinforcing with MMT nanoclay’, *Mater. Today Proc.*, vol. 18, pp. 85–97, 2019, doi: 10.1016/j.matpr.2019.06.280.

[41] S. C. Tjong, Y. Z. Meng, and A. S. Hay, ‘Novel preparation and properties of polypropylene-vermiculite nanocomposites’, *Chem. Mater.*, vol. 14, no. 1, pp. 44–51, 2002, doi: 10.1021/cm010061b.

[42] K. Li, S. Bian, W. Zhen, H. Li, and L. Zhao, ‘Performance, crystallization and rheological behavior of poly(lactic acid)/N-(2-hydroxyl) propyl-3-trimethyl ammonium chitosan chloride intercalated vermiculite grafted poly(acrylamide) nanocomposites’, *React. Funct. Polym.*, vol. 158, no. June 2020, 2021, doi: 10.1016/j.reactfunctpolym.2020.104791.

[43] S. Y. Lee, I. A. Kang, G. H. Doh, H. G. Yoon, B. D. Park, and Q. Wu, ‘Thermal and mechanical properties of wood flour/talc-filled polylactic acid composites: Effect of filler content and coupling treatment’, *J. Thermoplast. Compos. Mater.*, vol. 21, no. 3, pp. 209–223, 2008, doi: 10.1177/0892705708089473.

[44] D. A. Neto *et al.*, ‘Expanded Vermiculite: A Short Review about Its Production, Characteristics, and Effects on the Properties of Lightweight Mortars’, *Build. Rev.*, 2023.

[45] H. mu Ye, K. Hou, and Q. Zhou, ‘Improve the thermal and mechanical properties of poly(L-lactide) by forming nanocomposites with pristine vermiculite’, *Chinese J. Polym. Sci. (English Ed.*, vol. 34, no. 1, pp. 1–12, 2016, doi: 10.1007/s10118-016-1724-5.

[46] J. H. Zhang, Z. Wei, and Q. Zhang, ‘Novel Polylactide/Vermiculite Nanocomposites by In Situ Intercalative Polymerization. I. Preparation, Characterization, and Properties’, *Polym. Compos.*, 2007, doi: 10.1002/pc.

[47] J. Shojaeiarani, D. S. Bajwa, N. M. Stark, and S. G. Bajwa, ‘Rheological properties of cellulose nanocrystals engineered polylactic acid nanocomposites’, *Compos. Part B Eng.*, vol. 161, no. May 2018, pp. 483–489, 2019, doi: 10.1016/j.compositesb.2018.12.128.

[48] P. Agrawal *et al.*, ‘Rheological and Mechanical Properties of Poly(lactic acid)/Bio-Based Polyethylene/Clay Biocomposites Containing Montmorillonite

and Vermiculite Clays’, *J. Polym. Environ.*, vol. 29, no. 6, pp. 1777–1788, Jun. 2021, doi: 10.1007/s10924-020-02015-z.

[49] T. Zhu *et al.*, ‘Preparation of methacrylic acid modified microcrystalline cellulose and their applications in polylactic acid: flame retardancy, mechanical properties, thermal stability and crystallization behavior’, *Cellulose*, vol. 27, no. 4, pp. 2309–2323, 2020, doi: 10.1007/s10570-019-02931-x.

[50] W. min Guan, J. hong Li, T. ting Qian, X. Wang, and Y. Deng, ‘Preparation of paraffin/expanded vermiculite with enhanced thermal conductivity by implanting network carbon in vermiculite layers’, *Chem. Eng. J.*, vol. 277, pp. 56–63, 2015, doi: 10.1016/j.cej.2015.04.077.

[51] Y. Huang *et al.*, ‘Conductive Polymer Composites from Renewable Resources: An Overview of Preparation, Properties, and Applications’, *Polymers (Basel).*, vol. 11, no. 2, 2019, doi: 10.3390/polym11020187.

[52] W. Shen, W. Wu, C. Liu, Z. Wang, and Z. Huang, ‘Achieving a high thermal conductivity for segregated BN/PLA composites via hydrogen bonding regulation through cellulose network’, *Polym. Adv. Technol.*, vol. 31, no. 9, pp. 1911–1920, 2020, doi: 10.1002/pat.4916.

[53] C. Zhang, Q. Lan, T. Zhai, S. Nie, J. Luo, and W. Yan, ‘Melt Crystallization Behavior and Crystalline Morphology of Polylactide/Poly(ε-caprolactone) Blends Compatibilized by Lactide-Caprolactone Copolymer’, doi: 10.3390/polym10111181.

[54] J.-M. Chen *et al.*, ‘A Robust Experimental Model to Explore the Three-Dimensional Printing of Polylactide Parts: Solution versus Melt Extrusion’, 2020, doi: 10.3390/app10020509.

[55] M. A. Cuiffo *et al.*, ‘Impact of the Fused Deposition (FDM) Printing Process on Polylactic Acid (PLA) Chemistry and Structure’, doi: 10.3390/app7060579.

[56] P. Krishnamachari, J. Zhang, J. Lou, J. Yan, and L. Uitenham, ‘Biodegradable Poly(Lactic Acid)/Clay Nanocomposites by Melt Intercalation: A Study of Morphological, Thermal, and Mechanical Properties’, *Int. J. Polym. Anal. Charact.*, vol. 14, no. 4, pp. 336–350, 2009, doi: 10.1080/10236660902871843.

[57] A. A. Sapalidis, F. K. Katsaros, T. A. Steriotis, and N. K. Kanellopoulos, ‘Properties of Poly(vinyl alcohol)-Bentonite Clay Nanocomposite Films in Relation to Polymer-Clay Interactions’, *J Appl Polym Sci*, vol. 123, pp. 1812–

1821, 2011, doi: 10.1002/app.34651.

[58] A. P. Mathew, K. Oksman, and M. Sain, ‘Mechanical Properties of Biodegradable Composites from Poly Lactic Acid (PLA) and Microcrystalline Cellulose (MCC)’, 2005, doi: 10.1002/app.21779.

[59] A. N. Frone, S. Berlioz, J. F. Chailan, and D. M. Panaitescu, ‘Morphology and thermal properties of PLA-cellulose nanofibers composites’, *Carbohydr. Polym.*, vol. 91, no. 1, pp. 377–384, Jan. 2013, doi: 10.1016/J.CARBPOL.2012.08.054.

[60] S. Sinha Ray and M. Okamoto, ‘Polymer/layered silicate nanocomposites: A review from preparation to processing’, *Prog. Polym. Sci.*, vol. 28, no. 11, pp. 1539–1641, Nov. 2003, doi: 10.1016/J.PROGPOLYMSCI.2003.08.002.

[61] P. B. Messersmith and E. P. Giannelist, ‘Synthesis and Barrier Properties of Poly(e-Capro1actone)-Layered Silicate Nanocomposites’, doi: 10.1002/pola.1995.080330707.

[62] V. Krikorian and D. J. Pochan, ‘Unusual Crystallization Behavior of Organoclay Reinforced Poly(L-lactic acid) Nanocomposites’, 2004, doi: 10.1021/ma049283w.

[63] M. J. Fernández, M. D. Fernández, and I. Aranburu, ‘Poly(l-lactic acid)/organically modified vermiculite nanocomposites prepared by melt compounding: Effect of clay modification on microstructure and thermal properties’, *Eur. Polym. J.*, vol. 49, no. 6, pp. 1257–1267, Jun. 2013, doi: 10.1016/J.EURPOLYMJ.2013.02.031.

[64] K. E. Strawhecker and E. Manias, ‘Structure and Properties of Poly(vinyl alcohol)/Na+ Montmorillonite Nanocomposites’, *Chem. Mater.*, vol. 12, no. 10, pp. 2943–2949, Sep. 2000, doi: 10.1021/cm000506g.

[65] C. Huang, X. Qian, and R. Yang, ‘Thermal conductivity of polymers and polymer nanocomposites’, *Mater. Sci. Eng. R Reports*, vol. 132, pp. 1–22, Oct. 2018, doi: 10.1016/J.MSER.2018.06.002.

[66] N. Murugarren *et al.*, ‘Highly Aligned Bacterial Nanocellulose Films Obtained During Static Biosynthesis in a Reproducible and Straightforward Approach’, *Adv. Sci.*, vol. 9, no. 26, p. 2201947, Sep. 2022, doi: 10.1002/ADVS.202201947.

[67] A. Salazar, ‘On thermal diffusivity’, *Eur. J. Phys.*, vol. 24, no. 4, p. 351, May 2003, doi: 10.1088/0143-0807/24/4/353.

[68] A. Sethurajaperumal, A. Manohar, A. Banerjee, E. Varrla, H. Wang, and K.

Ostrikov, 'A thermally insulating vermiculite nanosheet-epoxy nanocomposite paint as a fire-resistant wood coating †', 2021, doi: 10.1039/d1na00207d.

[69] S. Spinella *et al.*, 'Polylactide/cellulose nanocrystal nanocomposites: Efficient routes for nanofiber modification and effects of nanofiber chemistry on PLA reinforcement', *Polymer (Guildf).*, vol. 65, pp. 9–17, May 2015, doi: 10.1016/J.POLYMER.2015.02.048.

[70] M. Sadia *et al.*, 'Adaptation of pharmaceutical excipients to FDM 3D printing for the fabrication of patient-tailored immediate release tablets', *Int. J. Pharm.*, vol. 513, no. 1–2, pp. 659–668, Nov. 2016, doi: 10.1016/J.IJPHARM.2016.09.050.

[71] B. G. Compton, J. A. Lewis, B. G. Compton, and A. Lewis, '3D-Printing of Lightweight Cellular Composites', 2014, doi: 10.1002/adma.201401804.

[72] Y. X. Yang, L. Haurie, J. Zhang, X. Zhang, R. Wang, and D. Wang, 'Effect of bio-based phytate ( PA-THAM ) on the flame retardant and mechanical properties of polylactide ( PLA )', vol. 14, no. 8, pp. 705–716, 2020.

[73] A. Meena, T. Parikh, S. S. Gupta, and A. T. M. Serajuddin, 'Investigation of thermal and viscoelastic properties of polymers relevant to hot melt extrusion - II: Cellulosic polymers', *J. Excipients Food Chem.*, vol. 5, no. 1, pp. 46–55, 2014.

[74] M. D. Hayes, D. B. Edwards, and A. R. Shah, *Fractography in Failure Analysis of Polymers: A volume in Plastics Design Library*. Elsevier, 2015.

[75] E. S. Greenhalgh, *Failure analysis and fractography of polymer composites*. Elsevier Ltd, 2009.

[76] R. M. Bajracharya, D. S. Bajwa, and S. G. Bajwa, 'Mechanical properties of polylactic acid composites reinforced with cotton gin waste and flax fibers', *Procedia Eng.*, vol. 200, pp. 370–376, 2017, doi: https://doi.org/10.1016/j.proeng.2017.07.052.

[77] S. M. Rangappa, S. Siengchin, and H. N. Dhakal, 'Green-composites: Ecofriendly and Sustainability', *Appl. Sci. Eng. Prog.*, vol. 13, no. 3, Jun. 2020, doi: 10.14416/j.asep.2020.06.001.

[78] F. P. La Mantia and M. Morreale, 'Green composites: A brief review', *Compos. Part A Appl. Sci. Manuf.*, vol. 42, no. 6, pp. 579–588, Jun. 2011, doi: 10.1016/j.compositesa.2011.01.017.

[79] E. Zini and M. Scandola, 'Green composites: An overview', *Polym. Compos.*,

vol. 32, no. 12, pp. 1905–1915, Dec. 2011, doi: 10.1002/pc.21224.

[80] P. Jagadeesh *et al.*, ‘Sustainable recycling technologies for thermoplastic polymers and their composites: A review of the state of the art’, *Polym. Compos.*, vol. 43, no. 9, pp. 5831–5862, Sep. 2022, doi: 10.1002/pc.27000.

[81] R. Stewart, ‘Thermoplastic composites — recyclable and fast to process’, *Reinf. Plast.*, vol. 55, no. 3, pp. 22–28, May 2011, doi: 10.1016/S0034-3617(11)70073-X.

[82] P. Ramesh and S. Vinodh, ‘State of art review on Life Cycle Assessment of polymers’, *Int. J. Sustain. Eng.*, vol. 13, no. 6, pp. 411–422, Nov. 2020, doi: 10.1080/19397038.2020.1802623.

[83] M. R. Mansor, M. S. Salit, E. S. Zainudin, N. A. Aziz, and H. Ariff, ‘Life Cycle Assessment of Natural Fiber Polymer Composites’, in *Agricultural Biomass Based Potential Materials*, Cham: Springer International Publishing, 2015, pp. 121–141.

[84] A. Gholampour and T. Ozbakkaloglu, ‘A review of natural fiber composites: properties, modification and processing techniques, characterization, applications’, *J. Mater. Sci.*, vol. 55, no. 3, pp. 829–892, Jan. 2020, doi: 10.1007/s10853-019-03990-y.

[85] S. . Joshi, L. . Drzal, A. . Mohanty, and S. Arora, ‘Are natural fiber composites environmentally superior to glass fiber reinforced composites?’, *Compos. Part A Appl. Sci. Manuf.*, vol. 35, no. 3, pp. 371–376, Mar. 2004, doi: 10.1016/j.compositesa.2003.09.016.

[86] P. Wambua, J. Ivens, and I. Verpoest, ‘Natural fibres: can they replace glass in fibre reinforced plastics?’, *Compos. Sci. Technol.*, vol. 63, no. 9, pp. 1259–1264, Jul. 2003, doi: 10.1016/S0266-3538(03)00096-4.

[87] R. Yadav and Z. Kamble, ‘Textile waste-based cellulose composites: a review’, *J. Mater. Sci.*, vol. 59, no. 17, pp. 7147–7168, May 2024, doi: 10.1007/s10853-024-09585-6.

[88] S. Venkatarajan and A. Athijayamani, ‘An overview on natural cellulose fiber reinforced polymer composites’, *Mater. Today Proc.*, vol. 37, pp. 3620–3624, 2021, doi: 10.1016/j.matpr.2020.09.773.

[89] J. Proy, F. Massa, D. Notta-Cuvier, F. Lauro, T. Tison, and G. Spingler, ‘Integrating fibers and injection molding process variability in short-natural-

fiber-reinforced thermoplastics behavior: A review’, *Mater. Today Commun.*, vol. 29, p. 102785, Dec. 2021, doi: 10.1016/j.mtcomm.2021.102785.

[90] X. Bi and R. Huang, ‘3D printing of natural fiber and composites: A state-of-the-art review’, *Mater. Des.*, vol. 222, p. 111065, Oct. 2022, doi: 10.1016/j.matdes.2022.111065.

[91] V. S. Sangawar and S. S. Deshmukh, ‘A Short Overview on Development of the Plastic Waste Management: Environmental Issues and Challenges’, *Sci. Revs. Chem. Commun*, vol. 2, no. 3, pp. 349–354, 2012.

[92] D. W. Jones, ‘How urbanization affects energy-use in developing countries’, *Energy Policy*, vol. 19, no. 7, pp. 621–630, 1991, doi: https://doi.org/10.1016/0301-4215(91)90094-5.

[93] M. Bengtsson, M. Le Baillif, and K. Oksman, ‘Extrusion and mechanical properties of highly filled cellulose fibre–polypropylene composites’, *Compos. Part A Appl. Sci. Manuf.*, vol. 38, no. 8, pp. 1922–1931, Aug. 2007, doi: 10.1016/j.compositesa.2007.03.004.

[94] N. Graupner, A. S. Herrmann, and J. Müssig, ‘Natural and man-made cellulose fibre-reinforced poly(lactic acid) (PLA) composites: An overview about mechanical characteristics and application areas’, *Compos. Part A Appl. Sci. Manuf.*, vol. 40, no. 6–7, pp. 810–821, Jul. 2009, doi: 10.1016/j.compositesa.2009.04.003.

[95] E. V. D. Gomes, L. L. Y. Visconte, and E. B. A. V Pacheco, ‘Morphological, thermal and mechanical properties of polypropylene and vermiculite blends’, *Int. J. Polym. Mater.*, vol. 57, no. 10, pp. 957–968, 2008.

[96] S. Venkatarajan, C. Subbu, A. Athijayamani, and R. Muthuraja, ‘Mechanical properties of natural cellulose fibers reinforced polymer composites – 2015–2020: A review’, *Mater. Today Proc.*, vol. 47, pp. 1017–1024, 2021, doi: https://doi.org/10.1016/j.matpr.2021.05.547.

[97] S. Khammassi, M. Tarfaoui, K. Škrlová, D. Mě\vr\'\inská, D. Plachá, and F. Erchiqui, ‘Poly (Lactic acid)(PLA)-Based nanocomposites: impact of vermiculite, silver, and graphene oxide on thermal stability, isothermal crystallization, and local mechanical behavior’, *J. Compos. Sci.*, vol. 6, no. 4, p. 112, 2022.

[98] P. V. Joseph, G. Mathew, K. Joseph, G. Groeninckx, and S. Thomas, ‘Dynamic

mechanical properties of short sisal fibre reinforced polypropylene composites', *Compos. Part A Appl. Sci. Manuf.*, vol. 34, no. 3, pp. 275–290, Mar. 2003, doi: 10.1016/S1359-835X(02)00020-9.

[99] Y. Borja, G. Rieß, and K. Lederer, 'Synthesis and characterization of polypropylene reinforced with cellulose I and II fibers', *J. Appl. Polym. Sci.*, vol. 101, no. 1, pp. 364–369, Jul. 2006, doi: 10.1002/app.23847.

[100] P. Bataille, L. Ricard, and S. Sapieha, 'Effects of cellulose fibers in polypropylene composites', *Polym. Compos.*, vol. 10, no. 2, pp. 103–108, Apr. 1989, doi: 10.1002/pc.750100207.

[101] I. Risnasari, E. Herawati, and E. N. Sirait, 'Characterization of Polypropylene Composite Reinforced with Wood Flour or Cellulose Fiber', *IOP Conf. Ser. Earth Environ. Sci.*, vol. 166, p. 012002, Jun. 2018, doi: 10.1088/1755-1315/166/1/012002.

[102] X. Li, B. Lei, Z. Lin, L. Huang, S. Tan, and X. Cai, 'The utilization of organic vermiculite to reinforce wood–plastic composites with higher flexural and tensile properties', *Ind. Crops Prod.*, vol. 51, pp. 310–316, Nov. 2013, doi: 10.1016/j.indcrop.2013.09.019.

[103] Y. Zhang, W. Han, and C.-F. Wu, 'Preparation and Properties of Polypropylene/Organo-Vermiculite Nanocomposites', *J. Macromol. Sci. Part B*, vol. 48, no. 5, pp. 967–978, Aug. 2009, doi: 10.1080/00222340903038323.

[104] G. Ariturk, K. Bilge, S. A. Seven, and Y. Z. Menceloglu, 'Morphological adaptation of expanded vermiculite in polylactic acid and polypropylene matrices for superior thermoplastic composites', *Polym. Compos.*, vol. 45, no. 6, pp. 5043–5050, Apr. 2024, doi: 10.1002/pc.28108.

[105] G. Ariturk, C. Girisken, K. Bilge, C. Yargici Kovanci, Y. Z. Menceloglu, and S. Avaz Seven, 'Hybrid green composites of PLA incorporated with upcycled waste cellulose and vermiculite', *Eur. Polym. J.*, vol. 203, p. 112667, 2024, doi: https://doi.org/10.1016/j.eurpolymj.2023.112667.

[106] S. Mustapha, J. Lease, K. Eksiler, S. T. Sim, H. Ariffin, and Y. Andou, 'Facile Preparation of Cellulose Fiber Reinforced Polypropylene Using Hybrid Filler Method', *Polymers (Basel).*, vol. 14, no. 8, p. 1630, Apr. 2022, doi: 10.3390/polym14081630.

[107] J. Gao, H. Ju, Z. Yao, G. Zhang, Y. Liu, and J. Niu, 'Effect of silicon dioxide and

organized montmorillonite on the crystalline morphology and dielectric properties of polypropylene-based composites', *Polym. Compos.*, vol. 44, no. 5, pp. 2804–2815, May 2023, doi: 10.1002/pc.27281.

[108] D. T. Quillin, D. F. Caulfield, and J. A. Koutsky, 'Crystallinity in the polypropylene/cellulose system. I. Nucleation and crystalline morphology', *J. Appl. Polym. Sci.*, vol. 50, no. 7, pp. 1187–1194, Nov. 1993, doi: 10.1002/app.1993.070500709.

[109] T. Kuboki, 'Foaming behavior of cellulose fiber-reinforced polypropylene composites in extrusion', *J. Cell. Plast.*, vol. 50, no. 2, pp. 113–128, Mar. 2014, doi: 10.1177/0021955X13504775.

[110] M. Le Baillif and K. Oksman, 'The Effect of Processing on Fiber Dispersion, Fiber Length, and Thermal Degradation of Bleached Sulfite Cellulose Fiber Polypropylene Composites', *J. Thermoplast. Compos. Mater.*, vol. 22, no. 2, pp. 115–133, Mar. 2009, doi: 10.1177/0892705708091608.

[111] K.-J. Kim, S. Bumm, R. K. Gupta, and J. L. White, 'Interfacial adhesion of cellulose fiber and natural fiber filled polypropylene compounds and their effects on rheological and mechanical properties', *Compos. Interfaces*, vol. 15, no. 2–3, pp. 301–319, Jan. 2008, doi: 10.1163/156855408783810939.

[112] S. Kumar Ghosh *et al.*, 'Silane functionalization of sodium montmorillonite and halloysite (HNT) nanoclays by "grafting to" method to improve physico-mechanical and barrier properties of LLDPE/clay nanocomposites', vol. 80, pp. 4307–4335, 2023, doi: 10.1007/s00289-022-04281-4.

[113] W. Xiong, J. Wu, H. Tian, A. Xiang, C. Wang, and Q. Wu, 'Enhanced mechanical and thermal properties of polyurethane-imide foams with the addition of expended vermiculite', *Polym. Compos.*, vol. 41, no. 3, pp. 886–892, 2020.

[114] A. Auliawan and E. M. Woo, 'Nanocomposites based on vermiculite clay and ternary blend of poly(L-lactic acid), poly(methyl methacrylate), and poly(ethylene oxide)', *Polym. Compos.*, vol. 32, no. 12, pp. 1916–1926, Dec. 2011, doi: https://doi.org/10.1002/pc.21194.

[115] E. Ruiz-Hitzky and A. Van Meerbeek, 'Clay mineral--and organoclay--polymer nanocomposite', *Dev. Clay Sci.*, vol. 1, pp. 583–621, 2006.

[116] J. Dan *et al.*, 'Two-dimensional porous silica nanomesh from expanded multilayered vermiculite via mixed acid leaching', *Nanosci. Nanotechnol. Lett.*,

vol. 8, no. 11, pp. 1028–1032, 2016.

[117] J. Xu, R. K. Y. Li, Y. Xu, L. Li, and Y. Z. Meng, ‘Preparation of poly (propylene carbonate)/organo-vermiculite nanocomposites via direct melt intercalation’, *Eur. Polym. J.*, vol. 41, no. 4, pp. 881–888, 2005.

[118] M. Li, Y. Zhao, Z. Ai, H. Bai, T. Zhang, and S. Song, ‘Preparation and application of expanded and exfoliated vermiculite: A critical review’, *Chem. Phys.*, vol. 550, p. 111313, 2021.

[119] E. V.D. Gomes, L. L. Y. Visconte, and E. B. A. V. Pacheco, ‘Thermal characterization of polypropylene/vermiculite composites’, *J. Therm. Anal. Calorim.*, vol. 97, no. 2, pp. 571–575, 2009, doi: 10.1007/s10973-009-0331-x.

[120] J. H. Zhang *et al.*, ‘Novel polylactide/vermiculite nanocomposites by in situ intercalative polymerization. I. Preparation, characterization, and properties’, *Polym. Compos.*, vol. 28, no. 4, pp. 545–550, 2007.

[121] S. C. Tjong and Y. Z. Meng, ‘Impact-modified polypropylene/vermiculite nanocomposites’, *J. Polym. Sci. Part B Polym. Phys.*, vol. 41, no. 19, pp. 2332–2341, 2003.

[122] P. Svoboda, C. Zeng, H. Wang, L. J. Lee, and D. L. Tomasko, ‘Morphology and mechanical properties of polypropylene/organoclay nanocomposites’, *J. Appl. Polym. Sci.*, vol. 85, no. 7, pp. 1562–1570, 2002.

[123] W. Shang, D. L. Li, W. C. Xu, and X. M. Yu, ‘Preparation and Properties of Polypropylene/Expended Vermiculite Micro-nano Composite’, *Adv. Mater. Res.*, vol. 602, pp. 265–272, 2013.

[124] J. V. Amador-Noya *et al.*, ‘Graphene Oxide and Vermiculite Clay Combinations to Produce Enhanced Flame Retardant Polypropylene Composite with Low Magnesium Hydroxide Loading’, *J. Vinyl Addit. Technol.*, vol. 26, no. 4, pp. 586–600, 2020, doi: 10.1002/vnl.21773.

[125] E. V.D. Gomes, L. L. Y. Visconte, and E. B. A. V. Pacheco, ‘Morphological, thermal and mechanical properties of polypropylene and vermiculite blends’, *Int. J. Polym. Mater. Polym. Biomater.*, vol. 57, no. 10, pp. 957–968, 2008, doi: 10.1080/00914030802153488.

[126] S. C. Tjong, Y. Z. Meng, and Y. Xu, ‘Preparation and properties of polyamide 6/polypropylene-vermiculite nanocomposite/polyamide 6 alloys’, *J. Appl. Polym. Sci.*, vol. 86, no. 9, pp. 2330–2337, 2002, doi: 10.1002/app.11253.

[127] W. Shao, Q. Wang, Y. Chen, and Y. Gu, ‘Preparation and properties of polypropylene/vermiculite nanocomposite through solid-state shear compounding (S3C) method using pan-mill equipment’, *Mater. Manuf. Process.*, vol. 21, no. 2, pp. 173–179, 2006.

[128] O. Oguz *et al.*, ‘High-Performance Green Composites of Poly(lactic acid) and Waste Cellulose Fibers Prepared by High-Shear Thermokinetic Mixing’, *Ind. Eng. Chem. Res.*, vol. 56, no. 30, pp. 8568–8579, 2017, doi: 10.1021/acs.iecr.7b02037.

[129] O. Oguz, E. Simsek, K. Bilge, and Y. Z. Menceloglu, ‘Low density polypropylene/waste cellulose fiber composites by High-Shear Thermo-Kinetic mixer’, *Int. Polym. Process.*, vol. 32, no. 5, pp. 562–567, 2017, doi: 10.3139/217.3426.

[130] M. Gelfer *et al.*, ‘Manipulating the microstructure and rheology in polymer-organoclay composites’, *Polym. Eng. \& Sci.*, vol. 42, no. 9, pp. 1841–1851, 2002.

[131] M. S. Huda, L. T. Drzal, A. K. Mohanty, and M. Misra, ‘Chopped glass and recycled newspaper as reinforcement fibers in injection molded poly(lactic acid) (PLA) composites: A comparative study’, *Compos. Sci. Technol.*, vol. 66, no. 11, pp. 1813–1824, 2006, doi: https://doi.org/10.1016/j.compscitech.2005.10.015.

[132] A. K. Bledzki, A. Jaszkiewicz, and D. Scherzer, ‘Mechanical properties of PLA composites with man-made cellulose and abaca fibres’, *Compos. Part A Appl. Sci. Manuf.*, vol. 40, no. 4, pp. 404–412, 2009, doi: https://doi.org/10.1016/j.compositesa.2009.01.002.

[133] B. Bax and J. Müssig, ‘Impact and tensile properties of PLA/Cordenka and PLA/flax composites’, *Compos. Sci. Technol.*, vol. 68, no. 7, pp. 1601–1607, 2008, doi: https://doi.org/10.1016/j.compscitech.2008.01.004.

[134] E. Petinakis, L. Yu, G. Edward, K. Dean, H. Liu, and A. Scully, ‘Effect of Matrix–Particle Interfacial Adhesion on the Mechanical Properties of Poly(lactic acid)/Wood-Flour Micro-Composites’, *J. Polym. Environ.*, vol. 17, pp. 83–94, Jun. 2009, doi: 10.1007/s10924-009-0124-0.

[135] M. Huda, A. Mohanty, L. Drzal, M. Misra, and E. Schut, ‘Physico-mechanical properties of “green” composites from polylactic acid (PLA) and cellulose fibers’, *Glob. Plast. Environ. Conf. 2004 - Plast. Help. Grow a Greener Environ.*

*GPEC 2004*, pp. 75–87, Jan. 2004.

[136] L. Běhálek, P. Lenfeld, M. Seidl, J. Bobek, and A. Ausperger, 'Friction properties of composites with natural fibres, synthetic and biodegradable polymer matrix', *NANOCON 2010 - 2nd Int. Conf. Conf. Proc.*, pp. 634–639, Jan. 2010.

[137] G. Bujjibabu, V. C. Das, M. Ramakrishna, and K. Nagarjuna, 'Mechanical And Water Absorption Behavior Of Natural Fibers Reinforced Polypropylene Hybrid Composites', *Mater. Today Proc.*, vol. 5, no. 5, pp. 12249–12256, 2018, doi: 10.1016/j.matpr.2018.02.202.

[138] K. Ray *et al.*, 'Glass/jute/sisal fiber reinforced hybrid polypropylene polymer composites: Fabrication and analysis of mechanical and water absorption properties', *Mater. Today Proc.*, vol. 33, pp. 5273–5278, 2020, doi: 10.1016/j.matpr.2020.02.964.

[139] A. K. Maurya, R. Gogoi, and G. Manik, 'Study of the Moisture Mitigation and Toughening Effect of Fly-ash Particles on Sisal Fiber-Reinforced Hybrid Polypropylene Composites', *J. Polym. Environ.*, vol. 29, no. 7, pp. 2321–2336, Jul. 2021, doi: 10.1007/s10924-021-02043-3.

[140] D. M. Panaitescu, Z. Vuluga, C. G. Sanporean, C. A. Nicolae, A. R. Gabor, and R. Trusca, 'High flow polypropylene/SEBS composites reinforced with differently treated hemp fibers for injection molded parts', *Compos. Part B Eng.*, vol. 174, p. 107062, Oct. 2019, doi: 10.1016/j.compositesb.2019.107062.

[141] F. Puch and C. Hopmann, 'Experimental investigation of the influence of the compounding process and the composite composition on the mechanical properties of a short flax fiber–reinforced polypropylene composite', *Polym. Compos.*, vol. 36, no. 12, pp. 2282–2290, Dec. 2015, doi: 10.1002/pc.23141.

[142] P. Krishnaiah *et al.*, 'Surface-treated short sisal fibers and halloysite nanotubes for synergistically enhanced performance of polypropylene hybrid composites', *J. Thermoplast. Compos. Mater.*, vol. 35, no. 11, pp. 2089–2104, Nov. 2022, doi: 10.1177/0892705720946063.

[143] A. Najafi, B. Kord, A. Abdi, and S. Ranaee, 'The impact of the nature of nanoclay on physical and mechanical properties of polypropylene/reed flour nanocomposites', *J. Thermoplast. Compos. Mater.*, vol. 25, no. 6, pp. 717–727, Sep. 2012, doi: 10.1177/0892705711412813.

[144] R. Gogoi, N. Kumar, S. Mireja, S. S. Ravindranath, G. Manik, and S. Sinha,

‘Effect of Hollow Glass Microspheres on the Morphology, Rheology and Crystallinity of Short Bamboo Fiber-Reinforced Hybrid Polypropylene Composite’, *JOM*, vol. 71, no. 2, pp. 548–558, Feb. 2019, doi: 10.1007/s11837-018-3268-3.

[145] C. I. Idumah and A. Hassan, ‘Characterization and preparation of conductive exfoliated graphene nanoplatelets kenaf fibre hybrid polypropylene composites’, *Synth. Met.*, vol. 212, pp. 91–104, Feb. 2016, doi: 10.1016/j.synthmet.2015.12.011.

[146] I. O. Oladele, I. O. Ibrahim, A. D. Akinwekomi, and S. I. Talabi, ‘Effect of mercerization on the mechanical and thermal response of hybrid bagasse fiber/CaCO3 reinforced polypropylene composites’, *Polym. Test.*, vol. 76, pp. 192–198, Jul. 2019, doi: 10.1016/j.polymertesting.2019.03.021.